**TABLE OF CONTENTS**

Page

## LIST OF TABLES

Page

## LIST OF FIGURES

Page

## LIST OF ABBREVIATIONS

| | |
|---|---|
| AAA | Abdominal Aortic Aneurysm |
| ANOVA | Analysis of variance |
| AVM | ArterioVenous Malformation |
| BGP | β-Glycerol Phosphate |
| CH | Chitosan |
| CHRU | Centre Hospitalier Regional Universitaire |
| CIPA | CHUM institutional animal care committee |
| CRCHUM | Centre de Recherche du Centre Hospitalier de l'Université de Montréal |
| DDA | Degree of Deacetylation |
| DMSO | Dimethyl Sulfoxide |
| DNA | Deoxyribonucleic acid |
| DOX | Doxycycline |
| DSA | Digital Subtraction Angiogram |
| ETS | École de Technologie Supérieure |
| EVAR | Endovascular Aneurysm Repair |
| EVOH | Ethylenevinyl-Alcohol |
| FTIR | Fourier-Transform Tnfrared Spectroscop |
| GAG | Glycosaminoglycane |
| GIT | Gastrointestinal Tract |
| LCST | Lower Critical Solution Temperature |
| LMEM | Linear Mixed Effect Model |
| LMs | Lymphatic Malformations |
| MMP | Matrix Metalloproteinase |
| MW | Molecular Weight |
| NBCA | N-Butyl-Cyanoacrylate |

| | |
|---|---|
| NSERC | Natural Sciences and Engineering Research Council of Canada |
| PB | Phosphate Buffer |
| PEG | Poly Ethylene Glycol |
| RNA | Ribonucleic Acid |
| RPMI | Roswell Park Memorial Institute |
| SEM | Scanning Electron Microscopy |
| SG | Stent Graft |
| SHC | Sodium Hydrogen Carbonate |
| SMC | Smooth Muscle Cells |
| SPD | Sodium Phosphate Dibasic |
| SPM | Sodium Phosphate Monobasic |
| STS | Sodium Tetradecyl Sulphate |
| VIS | Visipaque |
| VSMC | Vascular Smooth Muscle Cells |

# INTRODUCTION

Today, both diagnostic and treatment of vascular diseases remain challenging. These diseases include the well-known stenosis of blood vessels due to atherosclerosis but also localized dilatation of arteries (called aneurysms) (Moxon et al., 2010), abnormal connection between arteries and veins (called arteriovenous malformations, AVM) (Cho et al., 2006) and abnormally formed blood vessels such as venous or lymphatic malformations (Bloom et al., 2004). A possible treatment of the aforementioned diseases is blood vessel embolization, which involves the injection by catheter of an embolic agent to stop the flow of blood.

In this Ph.D. project, the main focus is on abdominal aortic aneurysm (AAA), a permanent dilatation of the abdominal aorta due to the weakened vessel wall, which can cause vessel bursts and lead to death within minutes. This chronic disease can be treated via open surgery or, a minimally-invasive alternative to open repair, endovascular repair (EVAR). The long-term success of EVAR remains limited in part due to the development of endoleaks, i.e. the perfusion of the aneurysm outside of the stent graft, which can be treated by sac embolization (Siracuse et al., 2016a).

However, the efficacy of the presently commercialized embolic agents is limited by several drawbacks such as cost, difficulty of handling and the frequent and repeated occurrence of endoleaks (Stavropoulos, Kim, et al., 2005). Therefore clinicians seek for new embolic agents which could address the present gap in the market. The main hypothesis of this thesis is that endoleak recurrence are due to the fact that the current embolic agents used for AAA have not been developed to address the underlying pathophysiology of the disease, but only as basic occlusive agents thanks to their mechanical properties.

The development of AAAs has been linked to persistent, localized inflammation associated with excessive activity of matrix metallopeptidases (MMPs), resulting in the progressive destruction of the vessel's extracellular matrix (Grzela et al., 2011). Additionally, as previously shown by our team (Fatimi et al., 2012), the presence of the endothelial layer has been implicated in the development and persistence of endoleaks. Therefore, the general aim of this work is to develop an embolization agent that is occlusive, able to inhibit MMP and promote

endothelial sclerosis, these being numerous potential approaches for AAA/endoleak prevention and treatment.

In chapter 1, the literature review presents the basic knowledge regarding the pathophysiology of aneurysms and their risk factors, as well as the current available treatment options. Moreover the advantages and disadvantages of various commercialized embolic agents have been reviewed and the design criteria of an ideal embolic agent are presented.

The objectives and hypothesis of the project are established in the Chapter 2. Chapters 3, 4 and 5 present the three papers published during this Ph.D, related to these objectives. The first article reports the superiority of an embolizing/sclerosing agent (CH-STS hydrogel), compared with an embolizing but non sclerosing agent (CH hydrogels) to treat endoleaks in a canine model of endovascular aneurysm repair. The second article presents the integration of a well-known sclerosing agent (Ethanol) to a currently commercialized embolic agent (Onyx) and investigates its potential as an embolizing sclerosing agent. The third and final article is about designing and developing a new MMP inhibitor/sclerosing embolizing agent by integration of Doxycycline (DOX) in chitosan hydrogel, a well know MMP inhibitor and sclerosing agent, in order to address all the gaps present in the current embolic agents.

Finally in Chapter 6, a general discussion to compare the entire developed agent based on some unpublished results, literature data and design criteria with some recommendations for future steps will be presented, followed by a general conclusion.

# CHAPTER 1

# LITERATURE REVIEW

## 1.1. Clinical problematic

### 1.1.1. Structure of the arteries

Arteries are large and elastic vessels, which carry blood away from the heart to the organs to provide tissues with oxygen, nutrients and hormones essential for their proper function. The closer the arteries are to the heart, the higher their diameter and the thicker they are, the largest artery being the aorta. The structure of their walls gives them the mechanical strength and elasticity necessary to support blood flow.

On the contrary, the capillaries which infiltrate the tissues have thin walls which allow nutrient exchanges with surrounding cells (Nicpon-Marieb et al., 1998).
The arterial wall is composed of three layers: the tunica intima, tunica media and tunica adventitia (Figure 1.1).

The tunica intima is the thinnest layer and consists of endothelium, a simple epithelium squamous covering the inside of all blood vessels. In a healthy organism, the endothelium has a smooth surface to reduce friction with blood. The endothelium is a monolayer of endothelial cells arranged longitudinally resting on a layer of connective tissue called basement membrane. It forms a semi-permeable and thromboresistant membrane controlling activation, adhesion and aggregation of platelets, leukocyte adhesion and migration and the proliferation of smooth muscle cells (Nicpon-Marieb et al., 1998).

The tunica media is composed of elastin fibres and vascular smooth muscle cells (VSMC) and gives its mechanical strength and elasticity to the vessel.

Tunica adventitia is the thickest and outermost layer of a blood vessel. It is mainly made of a network of collagen and elastin but fibroblast cells are also found. The collagen serves to anchor the blood vessel to nearby organs, giving it stability. It also contains nerve fibres, lymphatic vessels and in the case of large vessels, it has many tiny blood vessels to irrigate the

outer vessel wall, called vasa vasorum. The vessel provides the external elasticity and resistance to deformation (Nicpon-Marieb et al., 1998).

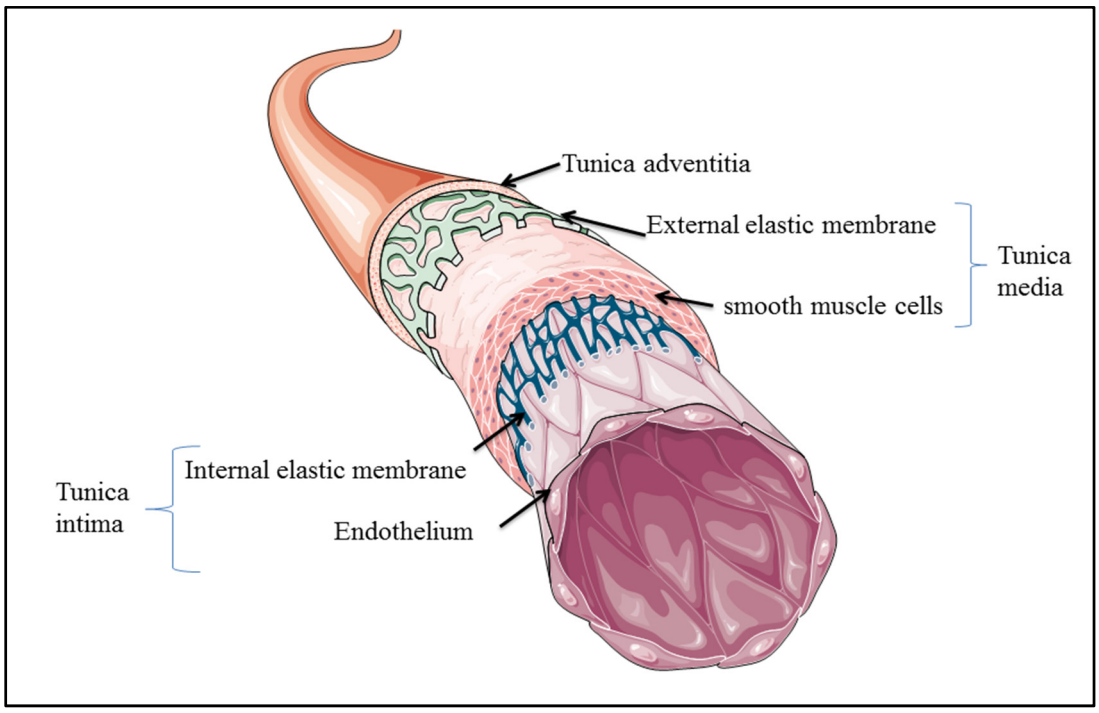


Figure 1.1 Structure of the arterial wall. Image from (Servier-Medical-Art)

Several vascular diseases can affect the vascular system. This thesis will mainly focus on abdominal aortic aneurysms, an abnormal dilation of the aorta which will be presented in more details in the next section. Other diseases which interest us include arteriovenous malformations (AVM) and lymphatic malformations. AVM is an abnormal connection between arteries and veins, bypassing the capillary system (abnormal communications). Normally, arteries supply oxygen-rich blood from the heart to the body, and veins carry oxygen-depleted blood away back to the heart. While in an AVM, a tangle of blood vessels bypasses normal tissue and directly diverts blood from the arteries to the veins (Crotty et al., 1993) (Figure 1.2).

Furthermore a localized abnormality of lymphatic vessels could lead to a mass in the head or neck named lymphatic malformation. Lymphangioma and Cystic hygroma are two main types

of lymphatic malformations. Lymphangioma are malformations which are sometimes found in the mouth, cheek, and tissues surrounding the ear, as well as other parts of the body consisting of a collection of blood vessels and greatly enlarged lymphatic vessels that are overgrown and clumped together. Cystic hygroma are large cyst or pocket of lymphatic fluid that result from blocked lymphatic vessels and usually occur in the neck (Bloom et al., 2004).

One of the treatment options for all these diseases is embolization with an embolic agent although there are some differences in the details of the embolotherapy. AVM and lymphatic malformation and their treatment options will be explained in greater details in the discussion section. In the next section, we explain the definitions, causes and risk factors and treatment options of abdominal aortic aneurysm.

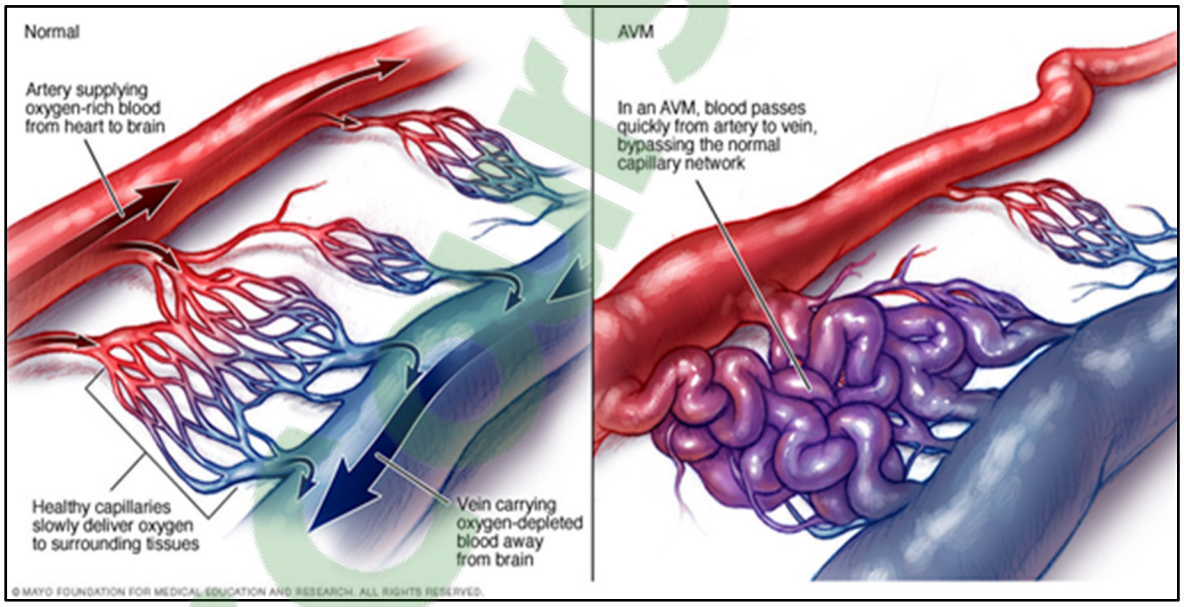


Figure 1.2 Difference between normal blood vessels and AVM (© 2015 Medical Foxx)

### 1.1.2. The abdominal aortic aneurysm (AAA)

#### 1.1.2.1. Definition

An aneurysm is a localized dilatation, more than 50% of the normal diameter, permanent and irreversible of a vessel caused by weakening of the wall (Fievez, 1989). The locations of

aneurysms are mainly the abdominal aorta and arteries of the brain. AAA, which is the main interest of this PhD project, is a dilatation of the infrarenal aorta, the main blood vessel that carries blood from the heart to the rest of the body (Figure 1.3).

If the aneurysm is not detected and managed preventively, it may rupture suddenly when the vessel wall can no longer resist pulsatile blood flow. The patient then undergoes massive hemorrhage which can cause death in minutes. Rupture of AAA is the 10th leading cause of death in men over the age of 55 (Guidebook, 2012). When an AAA is diagnosed in a patient, follow-up is done by imaging to allow the physician to assess the risk of rupture and the risk of complications in an intervention based on the patient's state of health. Generally, when the diameter of the AAA exceeds 5 cm or the increase exceeds 0.5 cm / year the doctors recommend surgery or endovascular therapy, as developed in the next section (Thompson et al., 2012). Approximately 36 of every 100,000 surgical operation performed in the U.S. is for treating AAA.

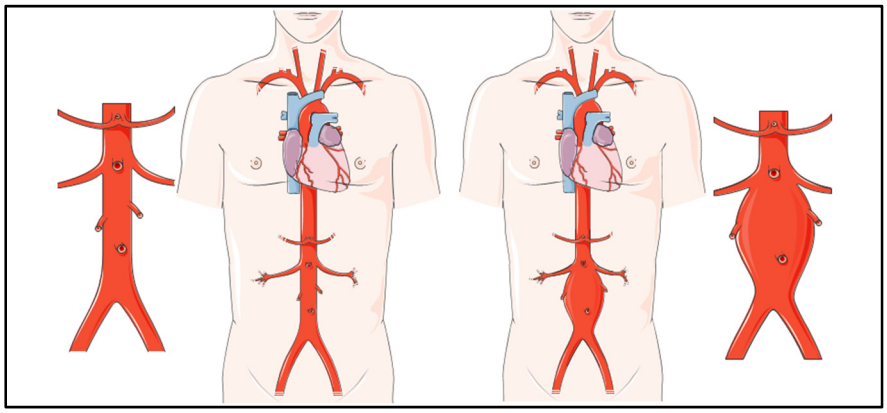

Figure 1.3 Normal aorta versus abdominal aortic aneurysm.
Image from (Servier-Medical-Art)

**1.1.2.2. Risk factors**

The origin of the AAA remains unclear, although several risk factors for the disease have been identified. Indeed, risk factors commonly associated with AAA are male gender, age, hypertension, environmental factors (smoking) or family history (Vardulaki et al., 2000). Male sex is the greatest risk factor for AAA and the risk of having AAA increases with age, such

that women between 65 and 79 years are six times less likely to develop an AAA than men of the same age (Vardulaki et al., 2000). Also smoking is the largest avoidable risk factor for AAA, such that male smokers are 2.5 times more likely to develop an AAA than non-smokers. Hypertension may be a factor predisposing to AAA by increasing the growth rate or risk of rupture of an existing AAA. Overall, the most effective parameter on AAA is male sex following by smoking and age, also effects of hypertension may be involved (Vardulaki et al., 2000).

**1.1.2.3. Pathophysiology of AAA**

Based on the researches, various genetic risk factors and biological processes have been recognized that contribute to AAA pathogenesis. Although there are a number of visible signs of AAA pathogenesis such as inflammation, vascular smooth muscle cell (VSMC) apoptosis, extracellular matrix degradation, and oxidative stress on the histological level, the order of the pathological events and their direct contribution to AAA, are not yet understood (Kuivaniemi, Ryer, Elmore, et al., 2015) (Figure 1.4).

In an AAA, alterations in the aortic wall are believed to be based on three main mechanisms: (i) the presence of inflammatory cells, (ii) cellular apoptosis, and (iii) proteolysis of structural proteins.

The wall of the aneurysms plays the role of infiltration of inflammatory cells, macrophages and T and B lymphocytes, which release cytotoxic mediators such as cytokines, perforin and Fas ligand (FasL), which in turn can trigger apoptosis of VSMCs (Choke et al., 2005; Henderson et al., 1999).

Due to the dual role of VSMCs, protection against inflammation and proteolysis, and maintenance of the vascular wall through the production of elastin and collagen, the reduction of the density of smooth muscle cells will play an important role in the development of AAA (Sakalihasan et al., 2005). The depletion of VSMCs in the media is explained by a high rate of apoptosis observed in aneurysms (Henderson et al., 1999). Apoptosis is a programmed cell death mechanism that allows tissue homeostasis in a healthy context. The death of cells by apoptosis involves caspase activation whose role is to cleave important cellular proteins (for

example cytoskeletal proteins) and to trigger fragmentation of the chromosomal DNA (Durdu et al., 2012; Rowe et al., 2000). It can be triggered extrinsically (such as presence of oxidizing agents or proapoptotic cytokines) or intrinsic (such as hypoxia or serum deprivation). However, when these stimuli are pathologically present, such as in the case of aneurysms, smooth muscle cells begin to produce markers of apoptosis leading to a phenomenon of successive deaths of smooth muscle cells of the tunica media which can lead to cell depletion that affects tissue function (Henderson et al., 1999).

In a healthy vessel, the structural proteins of the arterial wall provide a uniform distribution of the pulsatile mechanical stresses exerted by the blood (Wills et al., 1996) while in the case of an aneurysmal aorta, there is a fragmentation of the elastin and collagen fibres and approximately 60% of Glycosaminoglycane (GAG) deficiency (Ailawadi et al., 2003; Theocharis et al., 1999). The expansion and contraction of vessels caused by blood flow, and also the lack of smooth muscle cells (as a mechanical support of vessels) can lead to growth of small aneurysms.

An important part of the decomposition of the protein structure is related to an amplified activity of proteolytic enzymes, a family of zinc endopeptidases, which are called matrix metalloproteinases (MMP). In a healthy vessel, the action of MMPs is countered by inhibitors in order to maintain a balance between fibre fragmentation and regeneration. In the case of an AAA, because of the imbalance between these enzymes and their inhibitors, the phenomenon becomes excessive and compromises the mechanical strength of the walls.

MMP-2 and MMP-9 are two of identified MMPs in AAA tissue, and expressed principally by infiltrating macrophages, vascular smooth muscle cells (SMCs) and endothelial cells and they have destructive effect on the basement membrane collagen (collagen IV) (Sho et al., 2004). MMP-2 is able to degrade elastin and fibrillar collagen which are two major macromolecules of aortic extracellular matrix. Increased MMP-2 protein and messenger RNA levels have been reported in AAAs, which suggests a role in pathogenesis or progression of aneurysms (Liu et al., 2003). MMP-9, produced mainly by macrophages, plays an important role in the early stages of aortic aneurysm formation; MMP-9 degrades elastin and other extracellular matrix components to result in progressive expansion of aneurysms.

It was demonstrated that MMP-9 was the dominant MMP in large aneurysms, while elastolytic MMP-2 was predominant MMP type in the small aneurysms. In view of this conclusion, it is suggested that MMP-2 participates in initiation of aneurysm formation, while MMP-9 has a significant role in the dilation of larger aneurysms (Kaito et al., 2003).

Although the mechanism is not well understood, autoimmunity may also contribute in AAA initiation and progression. There are also hypotheses that suggest the possibility of a breakdown of the immunoregulatory mechanisms or some type of a molecular mimicry following a bacterial or viral infection (Hinterseher et al., 2012; Kuivaniemi, Ryer, Elmore, et al., 2015).

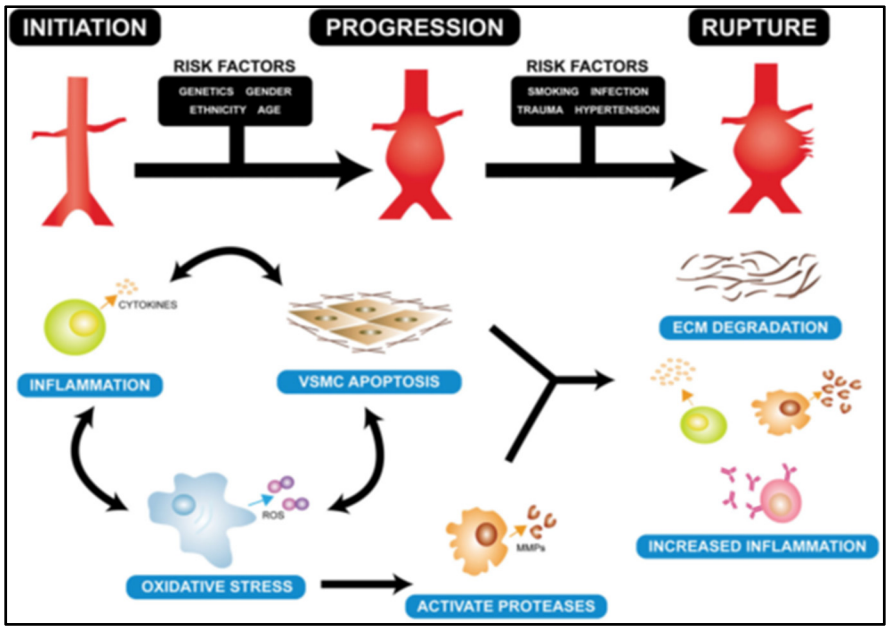


Figure 1.4 Summary of the pathogenesis of AAA. Several biological processes and risk factors have been identified that contribute to AAA pathogenesis such as inflammation, vascular smooth muscle cell (VSMC) apoptosis, extracellular matrix degradation, and oxidative stress (from (Kuivaniemi, Ryer, Richard Yoon, et al., 2015).

### 1.1.3. Treatments of AAA

There are presently two ways to prevent AAA rupture: Open surgery and Endovascular aneurysm repair (EVAR) (Figure 1.5).

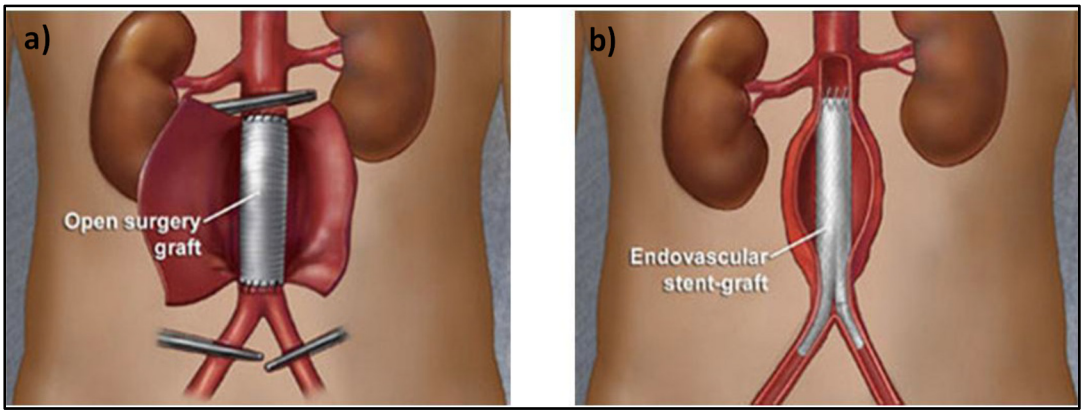


Figure 1.5 Treatment of AAA by open surgery (a) and endovascular treatment (b) (adapted from http://www.mayoclinic.org/aortic-aneurysm/)

The standard procedure for the treatment of aneurysms is open surgery. The operation involves making a large incision along the abdomen, locate the neck of the aneurysm and its extent, clamp the aorta and the iliac arteries, opening the aneurismal sac in length, then a woven vascular graft is sutured to the distal and proximal ends. Finally, the aneurismal sac is wrapped around the implant and sutured to protect it and the incision site is closed with sutures and/or staples (Creech, 1966; Schermerhorn, 2009). The most important complication of this treatment is operation risks, which are high in some patients with comorbidities (van Zeeland et al.). Therefore, although excellent results for open surgery have been reported, EVAR has been proposed as an appealing, less invasive, alternative to open surgery, especially in elderly patients due to reduced patient operating risks and time of recovery (Geisbusch et al., 2011).

#### 1.1.3.1. Endovascular aneurysm repair (EVAR)

EVAR is an endovascular procedure, used to treat pathology of the aorta, most commonly an AAA. In the EVAR method, a tubular implant, called stent-graft (SG) (Figure 1.6) is inserted through an artery and serves as a blood flow conduit through the aneurysm sac. The SG excludes the aneurysm and acts as a barrier occluding blood flow at systemic pressures from coming in contact with the weakened wall of aneurysm, thereby preventing continued aneurysm expansion and rupture (Figure 1.5b) (S. W. Stavropoulos et al., 2007).

The EVAR was introduced in humans for the first time in 1991 by Parodi (Parodi et al., 1991). Endovascular treatment is mainly used today on fragile patients (age, vascular or respiratory diseases, etc.) for whom surgery is high risk because of possible postoperative complications. However, this technique cannot be used in patients whose iliac arteries form does not allow access catheter or for those who do not have a healthy portion of infrarenal aorta to allow attachment of the stent (Sakalihasan et al., 2005; Schermerhorn, 2009).

Moreover, on average, 3.7%/year of patients from the US population who underwent EVAR require secondary intervention (Nordon et al., 2010). Reoperation may range from additional stent placement to surgical conversion (Moulakakis et al., 2010). These secondary interventions are mostly due to complications such as endoleak and stent-graft migration or stenosis or thrombosis inside the implant.

Figure 1.6 Stent-graft (from http://www.cookmedical.com/zenithflex/)

#### 1.1.3.2. Endoleak

Endoleak, the persistent or recurrence of blood flow inside the aneurismal sac is one of the most significant challenges related to EVAR. There are various classifications for endoleak. Anatomic factors and patient selection are some reasons for certain of the leaks, others are

device related like an equipment failure or poor integration of the implant into the surrounding tissue and some others are intrinsic (Hobo et al., 2006).

Type I endoleak: In this type of endoleak, blood flow into the aneurysm sac because of inadequate or ineffective seal at the proximal (type IA) or distal (type IB) end of the graft. it mostly appears in the early course of treatment, but may also appear later (Figure 1.7 Various types of endoleak: type I, leak at the attachment site; type II, leak from a branch artery; type III, graft defect; and type IV, graft porosity (Bastos et al., 2011); (Golzarian et al., 2005).

Type II endoleaks: In this type of endoleak, retrograded blood flow from collateral vessels fills the aneurysm sac. Collateral vessels are the ones which connect portions of the same artery or link two different arteries (Figure 1.7) (Golzarian et al., 2005).

Type III endoleak: Blood flows into the aneurysm sac due to incomplete or ineffective sealing between two component of the stent graft (SG) or rupturing of the grafted fabric, which can lead to direct connection between the aorta and aneurysm sac (Figure 1.7)(Golzarian et al., 2005).

Type IV endoleak: In this type, blood can pass from the graft into the aneurysm sac due to the porosity of the graft fabric (Figure 1.7) (Golzarian et al., 2005).

Type V endoleaks (ie, endotension): This type of endoleaks have been defined as a continuous enlargement of the aneurysmal sac without evidence of endoleak on imaging.

Certain endoleaks have to be treated as soon as possible, since the aneurysm sac is under the continuous pressurization. The majority of these complications can be resolved to a great extent by applying endovascular techniques, without using open surgery (Rosen et al., 2008).

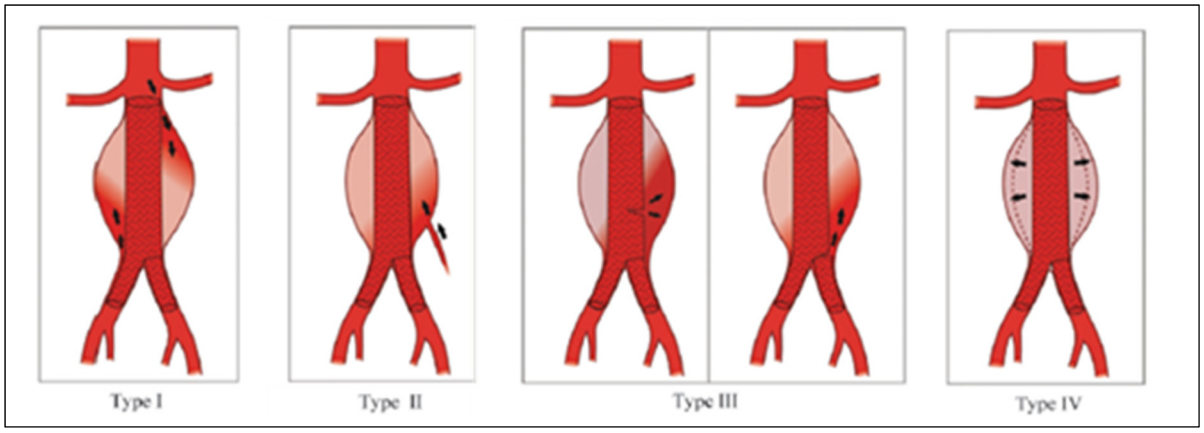


Figure 1.7 Various types of endoleak: type I, leak at the attachment site; type II, leak from a branch artery; type III, graft defect; and type IV, graft porosity (Bastos et al., 2011)

**1.1.3.3. Sac embolization procedure**

To treat or prevent endoleaks (especially type II and some of type I leaks) (Golzarian et al., 2005) sac embolization is increasingly performed by injection of an embolic agent to block the blood flow. In this method, an embolic agent is used to fill the aneurysmal sac (Bosman et al., 2010).

For type II endoleaks, the key to success is to disrupt the communications between the vessels involved in the leak and the perigraft space inside the AAA. Since type II endoleak can resolve itself, sac embolization is now generally used when aneurysm sac continues to grow (Gandhi et al., 2016). For a successful embolization of type II endoleaks, the inflow vessels and the leak area inside the aneurysm sac need to be embolized (Golzarian et al., 2005).

In type IA and IB endoleak, this technique is used when there are no other treatment options (Golzarian et al., 1997; Sheehan et al., 2004).

Treatment of type II endoleaks via embolization might be performed by transarterial (TA) approach: embolization of the dominant feeding artery (either the inferior mesenteric artery (IMA) or the lumbar artery), or translumbar (TL) approach: embolization of entire endoleaks cavity. Previous study showed that the TL thechnique might be more durable than TA because

in this method endoleak cavity in addition to feeding artery would be embolized which would potentially address the weakness of the TA technique and result in a more durable embolization (Stavropoulos et al., 2009).

The embolizing agent (in our study, mixing precursor solutions of the hydrogel outside of the catheter to form a mixed hydrogel) would be injected using catheter in the implantation site.

Off-target embolization does remains problematic of all embolic agents, particularly those that are liquid based (Vaidya et al., 2008). As a fail-safe, transcatheter embolization could be performed through a balloon catheter. This will prevent not only off target embolization but reflux as well.

**1.1.3.4. Cons and pros of current embolic agents**

Presently there are just few commercialized embolizing materials, namely 1) Coils (made from platinum or stainless Steel) or 2) liquid embolic agents like Onyx (ethylenevinyl-alcohol (EVOH))® (Micro Therapeutics Inc, Irvine, USA), NBCA (n-butyl-cyanoacrylate) and fibrin glue combined or not with coils (Martin et al., 2001). However each of them have some drawbacks such as high cost, hard to handle, high toxicity, and extensive medical comorbidities and also they do not fully prevent endoleak recurrence (Stavropoulos, Kim, et al., 2005).

Coils are commonly used to embolize intracranial aneurysms and are sometimes used to occlude collateral arteries leading to type II endoleaks. However in some cases, embolizing some endoleak sac and arteries by coil is impossible because it is hard to control (Stavropoulos, Kim, et al., 2005). The main drawback of using coils to treat endoleaks is the high cost of coils, increased procedure time, and risk of backing the access catheter out of endoleak when deploying the coils (Stavropoulos, Kim, et al., 2005) and the high radiopacity which impair future CT scan examination. Also effectiveness and durability of coil is limited because of recanalization of blood flow within the interstices of coils and coil compaction. For this reason, it is increasingly replaced or used in combination with a liquid embolic agent.

Unlike coils (Bonvini et al., 2003; Golzarian et al., 2002), liquid embolic agent can fill the endoleak sac completely, including all inflow and outflow vessels, without selective

catheterization of each parent vessel. Besides owning to structure of the solid cast formed by a liquid embolic agent in the aneurysm sac, the possibility of recanalization is reduced and finally more durable repair is achieved (Martin et al., 2001).

One of the available liquid embolic agent is n-butyl-cyanoacrylate (NBCA) (Cordis Neurovascular, Miami Lakes, USA), which is approved by the U.S. Food and Drug Administration for presurgical embolization of cerebral arteriovenous malformations. The most important advantage of this liquid embolic agent over other current embolic agents is the variety of its viscosity and hardening time.

By cons, one of the most significant drawbacks of NBCA is the possibility of gluing at the time of embolization; therefore injection of NBCA needs a remarkable skill (Stavropoulos, Kim, et al., 2005).

**- Onyx**

Onyx is a nonviscous biocompatible liquid embolic agent of ethylenevinyl-alcohol (EVOH) copolymer dissolved in dimethyl sulfoxide (DMSO) that can be injected through DMSO-compatible microcatheters and due to its content of tantalum powder is very well visualized under fluoroscopy (Martin et al., 2001). Once injected, when Onyx is exposed to blood or saline solution, the solidification process starts, DMSO dissipates and the EVOH precipitates (Ayad et al., 2006). Two formulations of Onyx can be used: Onyx 18 (6% EVOH) and Onyx 34 (8% EVOH). Onyx 18 is less viscous and may flow further in the endoleak cavity. Both formulas solidify within 5 minutes of injection (Abularrage et al., 2012). This is presently the only liquid embolic agent approved by the FDA for the treatment of endoleaks in AAA.

Unlike NBCA (n-butyl-cyanoacrylate), catheter occlusion with Onyx is uncommon, provided that the delivery catheter has been flushed with DMSO before Onyx delivery. The risk of ischemic complications, which may result from inadvertent occlusion of downstream vessels, decreases by using Onyx. This is because it can be delivered in a slower, more controlled manner than other available liquid embolic agents (Martin et al., 2001).

However Onyx has its own particular difficulties. First of all, Onyx is highly radiopaque so it is possible, when the endoleak cavity is filled, that the micro catheter tip becomes hidden. Therefore using Onyx as an embolic agent can increase the risk of non-target embolization, unless the accurate location of the microcatheter tip is known. Second, embolisation by Onyx is time consuming because it must be injected slowly. Third disadvantage of Onyx is its cost and this may be the determining factor in using alternative embolic agents. Fourth, the tantalum which is added to Onyx as a contrast agent causes long term radiopacity which would interfere with follow-up imaging (Chun et al., 2013).

Studies by Chaloupka et al. demonstrated that injection of DMSO into a porcine rete mirabile exhibited high toxicity with vascular failure, bleeding, and vascular necrosis (Chaloupka et al., 1999). These effects in an animal test have been reduced by decreasing the dosage and injection speed of DMSO. Generally, those embolic agents that used organic solvents as a vehicle cause some undesirable effects in vivo. Because the organic solvents spread into the blood flow and dissolved the polymers precipitate (Stavropoulos, Kim, et al., 2005).

Both Onyx and NBCA have some difficulties during the injection, are non-biodegradable and non porous and prevent tissue healing in the cast. Also their long term biocompatibility is a concern. Injection of fibrin glues in aneurysm sac, reduce the rate but cannot entirely prevent type II endoleak. In general, while embolic agents have shown the potential to minimize endoleak occurrence, embolization failures (recurrence and recanalization) was reported with all of tested agents (S Lerouge et al., 2011).

Due to the inconvenience of these agents, clinicians seek for new liquid embolic agents that do not require high levels of injection skill or solvents with harmful effects in vivo. Over the last decades, multiple variations of new embolic materials have been evaluated. While each agent has its own benefits and limitations, no single embolic agent is suitable for all indications. Therefore, for each case, the most appropriate agent among the available agents should be chosen based on some factors: the pathovascular nature, site and hemodynamic status of the lesion to be embolized, systematic and local effects of embolization and some potential complications like the availability and cost of embolic material and practicability of injection (Dondelinger et al., 1990).

#### 1.1.3.5. Design criteria of an ideal embolizing agent

In order to develop better embolizing agents, it is important to understand the main design criteria of an ideal embolic agent, as briefly summarized below:

- Deliverability under control is one of the most important design criteria of an embolic agent. First, the product must be injectable and compatible with microcatheters. Moreover it should present an adequate solidification kinetic. If the solidification speed is too fast, the catheter might be blocked or lead to limited control during injection because of the great injection force required. And if solidification speed is too slow, the embolic agent might not be able to fill the cavity properly and migrate into distal vessels that may occlude.

- Radiopacity of the embolic agent is indispensable to visualize the injection of embolic agent under fluoroscopy.

- Occlusive properties of the embolic agent have a significant impact on its functions. It should have a reliable occlusion of both the primary and collateral vessels with a low failure and recurrence rate. This feature is explained in detail in the next section.

- Should address the underlying pathophysiology of aneurysm formation and progression. As explained in detail in the next section, the embolization agent should ideally not only occlude flow in the short term, but also stop the pathophysiological mechanism leading to aneurysm progression and formation. As discussed above, inducing endothelial denudation can help for preventing recanalisation processes and promoting fibrosis and healing (Fatimi et al., 2012), Besides inhibiting aneurysmal wall degradation may also prevent aneurysm progression.

- Biocompatibility is another important factor that should be considered when designing an embolic agent. An embolic agent should have a low toxicity and no adverse reaction on the adjacent tissues and promote fibrous healing

- Biodegradability: while not obligatory, the biodegradability and porous structure of the embolizing agent is very important to favor replacement by fibrous tissue, resulting in the aneurysm shrinking and healing completely after degradation.

- Universal availability at reasonable cost (Stavropoulos, Kim, et al., 2005).

#### 1.1.3.5.1. Occlusive properties

Embolization consists of occluding the aneurysmal sac (type I endoleak) or the collateral artery feeding the aneurysmal sac (type II endoleak). In both cases, it is sought to prevent the flow of blood to the aneurysmal sac. The main force applied to hydrogel after implantation is due to the blood flow. The mechanical properties can be measured with a rheometer and make it possible, inter alia, to compare the different gels from one to another and to be able to measure the effect of the modification of the composition or components of the hydrogel. Moreover, it is essential to evaluate their ability to block blood flow. This cannot be extrapolated from the rheometry data. For that reason, in this study, an in vitro embolization bench test was designed to evaluate embolization properties by measuring the maximal pressure sustained by the gel before breaking (Fatimi et al., 2016). The mechanical force applied to the gel is a function of the blood pressure and vessel diameter. The *in vitro* mechanical test was performed using a tube with a diameter equivalent to a segmental renal artery (3 mm) with a liquid having viscosity similar to blood. Despite the limitation of *in vitro* models such as excluding blood-biomaterials interactions from the study and the absence of circulating fluid, rheometry results along with *in vitro* embolization results could suggest that if their mechanical properties are sufficient to occlude aneurysm *in vivo* or not. 800 Pa was previously demonstrated as an *in vitro* threshold that correlates to *in vivo* embolization success (Fatimi et al., 2016). However, the real ability to occlude the blood flow should be confirmed by the *in vivo* experiments.

#### 1.1.3.5.2. Endothelial ablation

Endoleaks are endothelialized neochannels between the aneurysm wall and the stent-graft. They are connecting the residual aneurysm with the parent vessel or a collateral branch. The formation of such neovascular channels is believed to play a significant role in EVAR failures

due to limitations in thrombosis of circulating blood into the aneurysm (Soulez et al., 2008). Moreover endoleaks cause formation of an active self-perpetuating endothelialized space which can provide the essential conditions to maintain abnormal flows, aneurysm persistence, ongoing vessel wall disease, and, sometimes, aneurysm growth (Soulez et al., 2008). Raymond et al., studied the role of the endothelial lining in persistence or recurrence of endoleak after embolization of intracranial aneurysms (Raymond et al., 2004; Raymond et al., 2002) According to their results, endothelial ablation can inhibit recanalization after coil occlusion of arteries (Raymond et al., 2004; Raymond et al., 2002). Our team also previously showed that endothelial lining, which lines the interior surface of blood vessels and exhibits anti-thrombotic properties, plays an important role in endoleak persistence or recurrence in AAA. *In vivo* studies suggested that the combination of occlusive properties and endothelial denudation of the aneurysm could provide a new strategy for improving the long-term results of stent-graft repair of abdominal aortic aneurysms. Therefore one additional criterion should be the ability to remove the endothelial layer to avoid recanalization process. This can be achieved by Sclerotherapy.

**Sclerotherapy** is a technique to apply an agent with specific chemical, physical, and biological properties to disrupt target tissue which can lead to the formation of sclerosed or ‘‘hardened’’ by-products (Albanese et al., 2010). For instance, this procedure aims to restrict recurrence, proliferation, or collateralization by irreversibly destroying the endothelium layer of targeted vein (Albanese et al., 2010). Provoking a permanent endothelial injury in the target vascular structures is the fundamental basis of a successful sclerotherapy. It could be done by irritating, dehydrating, changing the surface tension of the endothelium with inducing a controlled acute inflammatory response without causing any chronic effects (Chu, 2006). This induced localized inflammatory reaction can produce small thrombosis that eventually leads to permanent fibrosis and elimination of the vein. It is used for instance for varicose veins. The procedure involves direct injection of a sclerosing agent into the varicose veins (Wiegand et al., 2011). After that, compression therapy may be applied to assist healing for a few days or as long as 8 weeks (Pollack et al., 1949). The most commonly used sclerosing agents are Ethanol, STS, Ethanolamine, Bleomycin, DOX, etc.

#### 1.1.3.5.3. Prevent aneurysm progression

Aneurysm progression has been shown to occur even after EVAR treatment and has been related to endoleak late occurrence of recurrence (Liu et al., 2003). This is believed to be due to continuous destruction of extracellular matrix components of the artery, leading to progression of the disease to the adjacent vessel segments.

Several drugs have been proposed to stop aneurysm progression. DOX is probably the most investigated drug in preclinical models of AAA (Kroon et al., 2015). Oral administration of DOX, in particular, had been proven effective in multiple animal models of AAA and short term human studies; these studies have consistently reported that doxycycline limit AAA growth by limiting the extracellular matrix remodelling and inflammation (Kroon et al., 2015; Prall et al., 2002; R. W. Thompson et al., 1999). However, in some studies, long-term DOX therapy neither reduce aneurysm growth nor influence the need for AAA repair or time to repair, supposedly due to the suboptimal dose of drug. High, long-term, systemic dosing may be avoided due to the risk of negative side-effects (Meijer et al., 2013).

Doxycycline inhibits MMP-2 and MMP-9 derived from human vascular cell types and from tissue explants from AAAs by binding to the active zinc sites and also by binding to an inactive calcium site, which causes conformational change and loss of enzymatic activity (Liu et al., 2003). Petrinec et al first demonstrated that doxycycline therapy preserved elastic lamellar structure, and reduced enlargement of experimental AAAs by inhibition of MMP-9 activity (Petrinec et al., 1996). In addition to these effects, doxycycline may influence connective tissue degradation within human aneurysms by reducing the monocyte/macrophage expression of MMP-9 mRNA and by suppressing the post-translocational processing (activation) of proMMP-2 (Kaito et al., 2003). Moreover, there might be other non-MMP dependent mechanisms involved in AAA formation that could be stopped by DOX (Kroon et al., 2015). Indeed, AAA can be considered an autoimmune disease given the observation that AAA tissue shows clonal expansion of T cells. Lindeman et al. proposed that doxycycline can also inhibit mitochondrial protein synthesis which will result in a proliferation arrest, especially of clonally expanding T cells (Lindeman et al., 2009).

According to this list of design criteria, hydrogels appear as interesting candidates to act as embolic matrices able to deliver drugs (such as sclerosing agent (STS) or MMP inhibitor such as DOX) locally due to their favourable features such as biocompatibility, biodegradability, injectability and tunable mechanical properties. Hydrogels and their properties are described in the hydrogel section.

### 1.2. HydrogelsDefinition

Hydrogels are crosslinked networks of 3D, hydrophilic polymers composed of copolymers or homopolymers. Chemical crosslinks (tie-points, junctions), or physical crosslinks, such as entanglements or crystallites provide the physical integrity and network structure and also make the hydrogel insoluble (Peppas, Bures, et al., 2000).

#### 1.2.2. Advantages and limitations of hydrogels

Hydrogels can absorb a huge amount of aqueous solution compared to other types of materials. Owning to their large water content, soft consistency and high flexibility, they have a certain similarity to living tissues. Moreover, their low polymer concentration limits their toxicity. Sensitive Hydrogels are called 'Intelligent' or smart' hydrogels and they have the ability to sense external physical and chemical stimuli and respond in different ways (Qiu et al., 2001). Moreover, some types of hydrogels are injectable exhibiting a sol–gel phase transition in respond to environmental stimuli, such as pH and/or temperature changes (Nguyen et al., 2010). Also, the properties of hydrogels are tunable and can be modified. Regarding to these properties, hydrogels find plenty of applications, ranging from hygiene products, to soil conditioner, to biomedical and pharmaceutical devices. Some specific examples of applications are biosensor membranes, contact lenses, artificial heart coating, synthetic vascular grafts, artificial skin, and drug delivery and release devices (Joseph D., 1976). However, these highly hydrated polymer networks have some limitations. Due to high water content in hydrogels, they generally have a low mechanical strength and need further modifications to reach the required mechanical features based on their applications (Mujumdar et al., 2008).

### 1.2.3. Types of Hydrogels

Hydrogels can be classified based on the polymer origin (natural, synthetic and synthetic/natural hybrid hydrogels) or the type of crosslinks between polymer chains (chemical crosslinks (tiepoints, junctions), or physical crosslinks, such as entanglements or crystallites) (Gulrez et al., 2011).

### 1.2.4. Natural polymers versus Synthetic hydrogels

Polymers of natural origin are one of the most attractive options for biomedical applications, mainly owing to their similarities with the extracellular matrix and other polymers found in the human body, their biocompatibility, critical biological functions and inherent biodegradability. Such systems are also chemically versatile, may be modified by well-established chemical methods and mostly show a rather good biological performance (Reis et al., 2008).

Natural polymers are present in, or created by, living organisms including polymers from renewable resources. There are three main types of natural polymers: 1) polymers derived from living organisms including carbohydrates (chains of sugar), 2) proteins (chains of amino acids), and 3) polynucleotides (chains of nucleotides) (DNA, RNA). Among them, most commonly used hydrogel of natural origin are: cellulose, chitosan, collagen etc.

Hydrogels can be prepared with synthetic polymer for using in various biomedical disciplines. They are still developing for new promising applications. These polymers have great versatility in structure, molecular weight and composition so they can be designed to meet specific needs. Using this kind of hydrogels has some advantages including precise control and mass produced, that can be tailored to give a wide range of properties, low immunogenicity and minimize risk of biological pathogens or contaminants. In contrast, they have some drawback such as low biodegradability and also they can contain toxic substances (Park et al., 2010).

Synthetic polymer hydrogels exhibit different characteristics due to various chemical structures, methods of preparation, water content and cross-linking degree. So by using synthetic hydrogels, it is possible to design a new desired hydrogel with specific functions for a specific application. These changes can be performed in chemical composition and

concentration of material or even in one of the synthesis factors (cross-linking method, cross-linking agent, method and conditions of the synthesis) which can lead to new functional intelligent biomaterials (Gibas et al., 2010). Among them, most commonly used synthetic hydrogel are: Poly (ethylene glycol) (PEG), poly (hydroxyethyl methacrylate) etc. Often, hydrogels synthesized from natural polymers are more biocompatible, more biodegradable and have less toxic byproducts compared to those synthesized from synthetic constituents (Piai et al., 2009). Natural hydrogels synthesised from natural polymers have a broad application range in tissue engineering due to their biocompatibility, intrinsic biodegradability and critical biological properties (Zhu et al., 2011).

### 1.2.5. Physical versus chemical hydrogel

Referring to the forces involved in the building up of networks, two main classes of hydrogels can be determined: (i) chemical hydrogels and (ii) physical hydrogels (Figure 1.8).

In chemical gels, polymer chains are covalently cross-linked and make three dimensional networks (Hennink et al., 2002). In this type of hydrogels the equilibrium swelling levels depends on crosslink density and the polymer-water interaction parameters like hydrophilicity of the polymer chains (Rosiak et al., 1999). In Physical or Reversible gels, the polymer chains bond together by physical crosslinks, such as entanglements or crystallites and/or other weak forces (van der Waals, hydrogen and ionic bonding). Existence of physical cross-links between diverse polymer strings, prevent dissolution of the hydrogels (Hennink et al., 2002). However applying stress or changing physical conditions can break all of these links. So this kind of hydrogels is called reversible hydrogels (Rosiak et al., 1999).

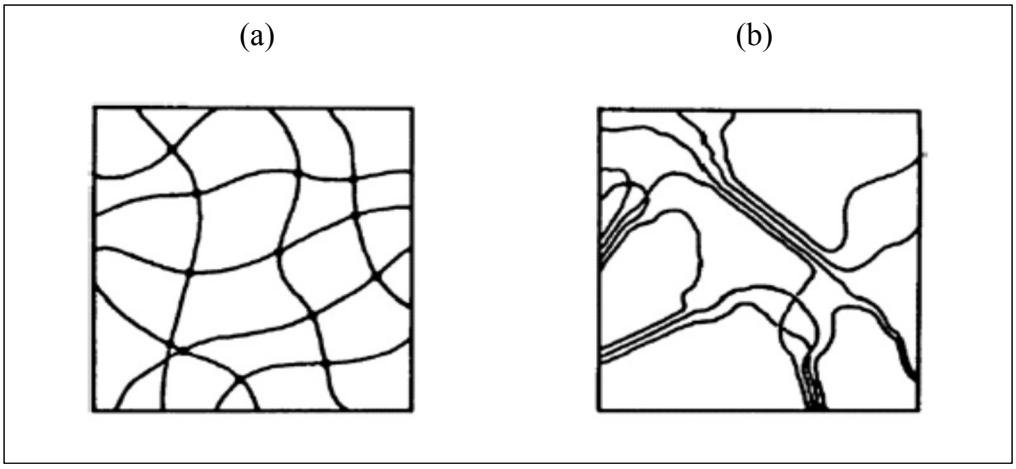


Figure 1.8 Schematic diagram of (a) a chemical hydrogel with point crosslinks and (b) a physical hydrogel with multiple-junction zones

### 1.2.6. Environmentally-sensitive hydrogels

Environmentally-sensitive hydrogels can sense external environment stimuli like changing in pH, temperature, ionic strength, surrounding biological fluid, etc. and also they can respond to them. These responses can be exhibited in various manners like changing in swelling behavior, network structure, permeability or mechanical strength.

These types of hydrogels are also called ‘smart’ or ‘Intelligent’ hydrogels and categorized based on the type of their stimuli. They have been used in diverse biomedical applications, such as in making artificial valves, inducing vascular angiogenesis and immobilization of enzymes cells (Qiu et al., 2001).

Temperature-sensitive hydrogels are part of the family of environmentally stimulus-sensitive hydrogels, which are able to respond to environmental temperature changes by changing their physical properties. Thermo-responsive hydrogels exhibit a change of the degree of swelling with temperature of the surrounding fluid. They are classified into three groups including negatively thermo-sensitive, positively thermo-sensitive, and thermally reversible gels. Negative temperature-sensitive hydrogels have a lower critical solution temperature (LCST) and swelling at low temperature (<LCST) and shrinking at high temperature (>LCST). Conversely, positively thermosensitive swell at high temperature and shrinking at low

temperature (Fang et al., 2008). Thermally reversible gels are copolymers made of different monomers with different LCST values.

### 1.2.7. Injectable hydrogels

For the purpose of AAA embolization, hydrogels must be injectable by small catheter but rapidly demonstrate enough mechanical properties to occlude blood flow. This limits the number of available materials. To that purpose, the hydrogel should be gel in response to an external stimulus such as calcium ions, light, chemical crosslinker, pH, temperature, etc. Injectable hydrogels have lots of applications in biomedical and pharmaceutical fields like drug delivery, cell growth, and tissue engineering. Solution of hydrogels can be mixed with drugs, proteins, or cells and then injected and formed in situ by chemical or physical crosslinking methods (Madan et al., 2009). Chemical crosslinked hydrogels are formed by photo polymerization, disulfide bond formation, or reaction between thiols and acrylate or sulfones methods. Physical crosslinked hydrogels are formed by the self-assembly in response to environmental stimuli (Nguyen et al., 2010). Therefore, physical hydrogels are more attractive for biomedical applications, because they do not use any organic solvents, crosslinking agents or photo irradiation. Moreover unlike chemical crosslinked hydrogels, they do not damage incorporated proteins, embedded cells and surrounding tissues by the heat of reaction (Nguyen et al., 2010).

Nowadays, only a few injectable hydrogels are proposed as embolic agents for blood vessels. These are EmboGel and UltraGel. EmboGel is a hydrogel embolic agent consisting of a mixture of Iohexol and alginate, with a calcium chloride solution used to initiate polymerization. UltraGel consists of irgacure, iohexol and polyethylene glycol diacrylate (Barnett et al., 2011). These materials show a rapid polymerization. Also when used in an AAA endoleak model, the agent is delivered in a strand-like form. Due to this form, EmboGel is able to effectively fill the aneurismal cavity and occlude it from the blood flow (Barnett et al., 2009). However EmboGel also has a problem in terms of insufficient inherent strength. Recently, new embolizing agents based on Chitosan thermogels have been proposed by Lerouge's team. These are detailed in the "Previous work by the team" section.

### 1.2.8. Drug delivery

Drug delivery is the approaches, formulations or technologies of applying a pharmaceutical compound to achieve a therapeutic effect in humans or animals (Tiwari et al., 2012). Targeted drug delivery systems with a controlled rate are very attractive approaches and have been pursued vigorously.

Some examples of controlled-release delivery systems are encapsulated cells, oral soft gels, iontophoretic devices to administer drugs through skin, and a variety of programmable, implanted drug-delivery devices. Using these systems of drug delivery have the potential to overcome the weaknesses of conventional drug administration methods (Tiwari et al., 2012).

Hydrogels, specially chitosan based hydrogels, are widely used as a delivery system and it was suggested that hydrogels as a delivery carrier could enhance efficacy and/or reduce toxicity of the delivered drug (Shanmuganathan et al., 2008). Due to porous structure of chitosan hydrogels, free water can diffuse through the hydrogel and drug could be released by diffusion or swelling. Indeed, the changes of mesh size of the hydrogel network directly depend on changes of the swelling ratio. This means that with increase or decrease of the swelling ratio the mesh size would increase or decrease and subsequent drug release would be modulated. Diffusion mainly depends on the crosslinking density, as the crosslinking density increases, water content, and the mesh size of the network would decrease considerably. Indeed, increasing the crosslinking density would reduce the hydrogen bonds between water molecules and chitosan chains, and also the swelling ability of chitosan hydrogels due to the slower relaxation time of the polymeric chains which leads to a decreased drug-release rate (Berger et al., 2004). The analysis of drug release kinetics allows to gain insight into the drug release behaviour from the network and it could be quantified using Korsemeyer-Peppas formula (Peppas, Huang, et al., 2000). This formula and description of its parameters are in the chapter 5. Given that in our third article (chapter 5) we used chitosan hydrogels as DOX delivery system, we briefly discuss the research done in this regard in the following paragraphs.

Bartoli et al. (Bartoli et al., 2006) demonstrated that local administration of DOX could achieve similar effect with systemic administration, while theoretically mitigating systemic toxicity

and side effect such as pulmonary fibrosis, hair loss and pigmentation (Albanese et al., 2010). Continuously or intervally delivering doxycycline or other active agents in AAA disease in the local area might help the wall stabilization and aneurysm exclusion maintenance (Sho et al., 2004).

One of the important challenges of this study is to find the appropriate concentration of the drug which can play both desired roles of endothelial ablation and MMP inhibition while becoming biocompatible after burst release. Chaudry et al. assess the safety and efficacy of percutaneous image-guided sclerotherapy with doxycycline as primary treatment of intra-abdominal lymphatic malformations (LMs) (Chaudry et al., 2011). They used DOX at concentration of 10 mg/mL. Although the amount of used doxycycline depends on the malformation size, Cahill et al. also used the same concentration (10 mg/mL) of DOX with 50 to 500 mg per session dose range routinely via catheter in 3 instillations for head and neck lymphatic malformations of infants and percutaneous sclerotherapy in neonates (Cahill et al., 2011).

Based on the Franklin et al. results, the concentration of tetracycline accumulated in the aneurysm wall varied, but the maximum achieved was 10 μg per g tissue wet weight (Franklin et al., 1999). *In vivo*, therapeutic serum concentrations of tetracycline lie in the range 3±10 μg/ml.

Based on the literature review and toxicological information of DOX available in the information sheet, we could define a good range of doxycycline with sclerosing properties (10 mg/ml) and MMPs inhibition (10-100 μg/ml).

Considering the difference in the magnitude of the two concentrations, the control of drug release can be very useful.

## 1.3. Previous work by the team

### 1.3.1. Chitosan radiopaque injectable gels

Recently chitosan has become a mostly used natural polymer in biomaterials studies and regenerative medicine such as orthopedics, wound healing applications, drug delivery systems, and tissue engineering (Heinemann et al., 2010).

Chitosan, a natural hetero polymer chain with β (1→4) linked D-glucosamine and N-acetyl-Dglucosamine residues, is obtained by alkaline deacetylation of chitin. Chitin, a tough, inelastic, nitrogenous polysaccharide, is the second most abundant polysaccharide, which can be degraded by chitinases. It is found in the cell walls of fungi and exoskeletons of crustaceans, insects and spiders. However, the principal source of chitin is shellfish waste. This material is highly insoluble with low chemical reactivity and in spite of the presence of nitrogen, it has a low immunogenicity (Ravi Kumar, 2000).

Deacetylation of chitin is the main source of production of chitosan (Figure 1.9). During the deacetylation process, strong alkali solutions are used to remove of N-acetyl groups, both at room and elevated temperatures. The term chitosan is used when the percentage of N-acetylglucosamine units is lower than 50%. The degree of deacetylation (DDA), which determines the content of free amino groups in the polysaccharides, is a significant factor to define some of chitosan properties such as the polymer's solubility. It is calculated as:

$$DD = 100 \frac{n_{GlcN}}{n_{GlcN} + n_{GlcNAc}}$$

Where, $n_{GlcN}$ – average number of D-glucosamine units, $n_{GlcNAc}$ - average number of Nacetylglucosamine units. Both the DDA and the molecular weight (MW) of chitosan have a strong influence on the rheological properties and degradation rate of chitosan.

Chitosan is considered as a valuable natural biocompatible polymer. It is nontoxic, biodegradable and mucoadhesive. Chitosan and its derivatives can be digested by lysozymal enzymes in the digestive tract (Bernkop-Schnürch et al., 1998; George et al., 2006). Because of its solubility in dilute acids, chitosan is accessible for various established processing

technologies (e.g., freeze-drying, freeze gelation) and has been used to produce films, gels, as well as porous sponge-like scaffolds.

More importantly it possesses gel-forming ability at body pH and temperature (Coutu et al., 2013). Indeed chitosan, a cationic polyelectrolyte, has a pKa of 6.5, so it is not soluble in water at a pH greater than 6.5. Thus, addition of a strong base leads to precipitation. But chitosan (CH) can form an injectable thermogel when combined with a weak base such as β-glycerol phosphate (BGP) (Figure 1.10) (Assaad et al., 2015). This system remained in solution at room temperature and physiological pH, but changed into gel upon heating at physiological temperature, undergoing therefore a heat-induced gelation (Coutu et al., 2013).

Though this thermogel has been considered for several biomedical applications, its mechanical properties are very poor and its biocompatibility is limited. Indeed, the concentration of BGP required to reach rapid gelation is cytotoxic to cells due to its hyperosmolality (R. Ahmadi et al., 2008). Our team has worked on the improvement of chitosan thermogels to adapt them to AAA embolization and to improve their intrinsic biocompatibility.

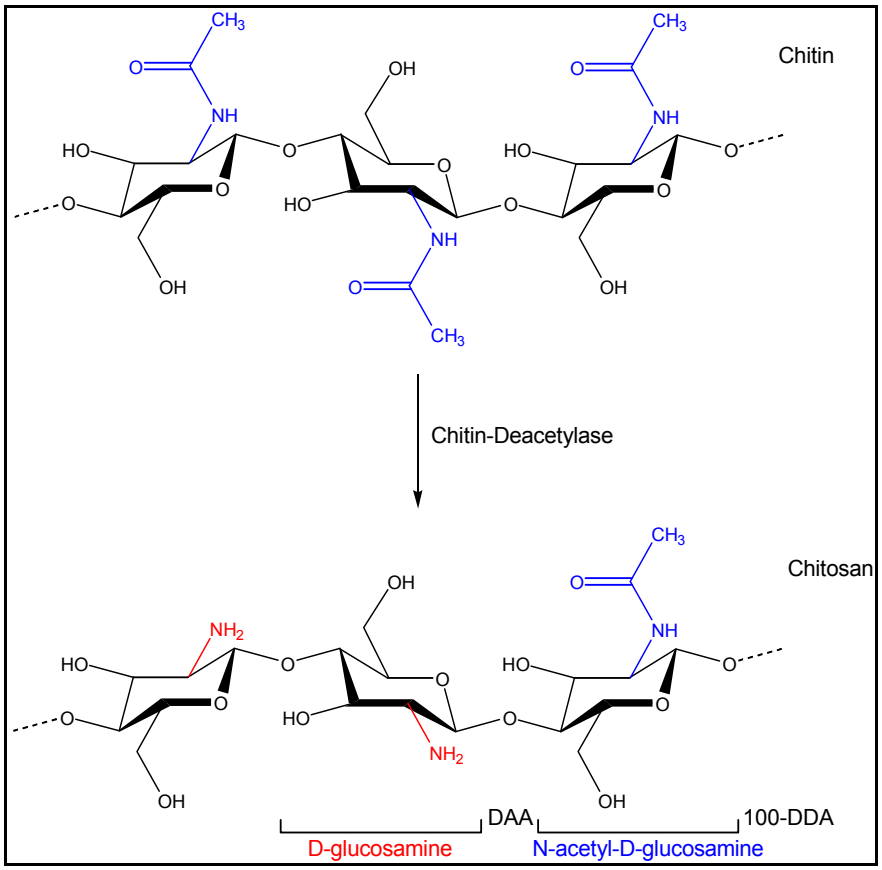


Figure 1.9 Typical structure of chitosan (D-glucosamine + N-acetyl-D-glucosamine) obtained by alkaline deacetylation of chitin (N-acetyl-D-glucosamine). DDA (degree of deacetylation) represents the average number of D-glucosamine units per 100 monomers

These limitations were overcome by our laboratory by replacing BGP with a combination of sodium hydrogen carbonate (NaHCO3, hereafter called SHC) and phosphate buffer (PB) (Assaad et al., 2015).

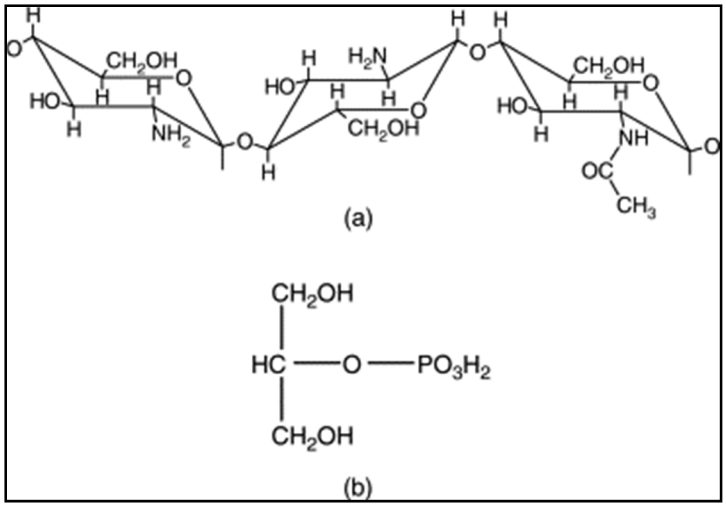


Figure 1.10 Chemical structure of (a) chitosan and
(b) βglycerophosphate (β-GP)

This combination has a strong synergic effect on both the gelation rate and mechanical properties. In contrast with BGP-CH gels, where BGP concentration is increased to achieve fast gelation, in this system the total salt concentration is reduced, thus allowing to keep osmolality in the hydrogels close to physiological values. These injectable hydrogels offer many benefits such as: i) a higher gelation rate and stronger mechanical properties (Young modulus reaching 50 kPa) compared to CH-BGP hydrogels; ii) thermosensitivity, which allows for easy injection and homogenous cell distribution inside the gel; iii) cell biocompatibility, thanks to a low salt concentration; iv) a porous structure with variable pore size depending on the salt composition and ratio; v) a controllable rate of degradation by modifying the molecular weight or degree of deacetylation of chitosan; vi) the possibility of making temporarily radiopaque hydrogels through the addition of an iodised contrast agent (i.e. Iodixanol). This can be useful to follow gel injection through catheter by fluoroscopy, when the injection site is in the blood vessels. These results strongly suggest that these new formulations might be ideal for cell/ drug encapsulation and delivery in AAA (Assaad et al., 2015; Ceccaldi et al., 2017).

### 1.3.2. Chitosan-sclerosing gels

Based on CH-BGP technology, the laboratoire de biomatériaux endovasculaires (LBeV) team has developed chitosan sclerosing gels based on the combination with Sodium tetradecyl sulfate (STS), a sclerosant drug. CH-STS hydrogel is made of 1) chitosan (CH) (polymer base), 2) glycerophosphate (β-GP) (gelation agent), 3) Iodixanol (contrast agent) and 4) Sodium tetradecyl sulphate (STS) (sclerosing agent) (Fatimi et al., 2012).

STS is an anionic surfactant, which occurs as a white, waxy solid and commonly used in the treatment of varicose and spider veins of the leg, during the procedure of sclerotherapy. STS damages the endothelium resulting in thrombosis and fibrosis (Figure 1.11). The addition of β-GP enables to add STS to chitosan without inducing its precipitation.

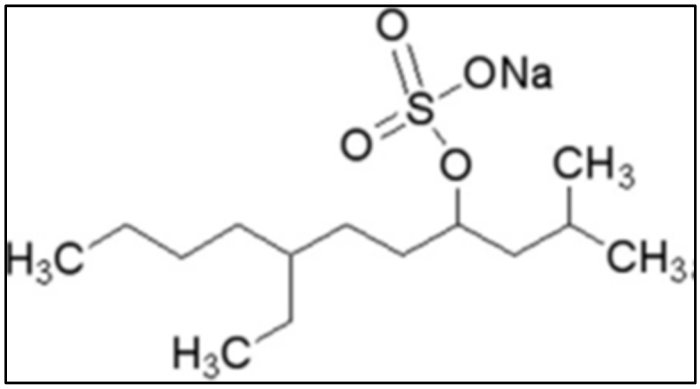


Figure 1.11 Chemical structure of sodium tetradecyl sulfate (C14H29NaO4S) (Fatimi et al., 2012)

The proposed hydrogel is believed to be the first product with sclerosing properties proposed to treat endoleaks or do prophylactic prevention of endoleaks in AAAs. So the two main roles of the chitosan/STS hydrogel are the embolization of aneurysm sacs or other structures (to block any blood flow entering the aneurysms) and to cause an irreversible endothelial injury in the aneurysm sac (or other structure) to prevent recanalization process by endothelial cells that could lead to recurrence of blood flow after a while, this process being thought to be a cause of failure of presently used embolic treatments (S Lerouge et al., 2011).

Chitosan/STS hydrogels were characterized and optimized using rheometry (viscoelastic properties such as gelation rate, and storage modulus), scanning electron microscopy (SEM), swelling and *ex vivo* embolization assay. Impact of STS, Iodixanol and β-GP on gelation kinetic, mechanical properties, radiopacity and cytotoxicity was tested. Increasing the amount of STS (1-3%) in hydrogel composition leads to better mechanical properties of hydrogel.

Previous positive results suggest that chitosan/STS hydrogels have great potential as embolizing and sclerosing agents for EVAR. But based on the preliminary results of histology, due to the presence of STS in the combination of hydrogels, despite of enough mechanical properties and endothelial removal, this embolic agent can lead to impair tissue healing because of high toxicity of STS. Therefore, further evaluation and optimization is needed.

# CHAPTER 2

## PROJECT OBJECTIVES

The literature data shows that there is a clear need for a new, more efficient embolization agent for endoleak treatment and prevention after EVAR. Recent work showed the importance of endothelial denudation to avoid recanalization after embolization. Moreover, late endoleak can appear due to aneurysm progression with time.

To address these gaps, ***the general objective*** *of this PhD consists in the optimization and characterization of new embolizing and sclerosing injectable agents as a* multi-faceted embolic agent for the prevention and treatment of endoleak and possible other vascular diseases.

The ***general hypothesis*** is that an embolic agent which can remove the endothelial lining and counteract biological mechanisms leading to aneurysm progression would potentially be more efficient than an only occlusive embolic agent.

A secondary hypothesis is that chitosan hydrogels have a great potential to be used as embolic agent matrix due to its unique properties such as the ability of integration of a sclerosing and/or MMP inhibitor drug such as STS and DOX in its structure, degradability, thermosensitivity and tunable mechanical properties.

**Objective 1:** The first objective of this thesis is to demonstrate in vivo the superiority of an embolizing/sclerosing agent, compared with an embolizing but non sclerosing agent (CH hydrogels) to treat endoleak in a canine model of endovascular aneurysm repair. This will be achieved by comparing the chitosan-STS gel (sclerosing and embolizing) previously developed by our team (Fatimi et al. 2012) with chitosan gels without STS (embolizing only). Prior to in vivo testing, in vitro characterization is requested to confirm that both gel present similar embolizing properties.

**Objective 2:** Since chitosan-STS gel may not easily be transferred to the clinics, the second objective of this thesis consists in studying the feasibility and preliminary assessment of a sclerosing embolizing agent based on the currently commercialized embolic agent (Onyx) and a famous sclerosing agent (Ethanol). The underlying hypothesis is that such product would have a better commercialization potential as an embolizing sclerosing agent, with interesting characteristics regarding visibility, injection control and penetration depth.

**Hypothesis 3:**

Combination of vascular occlusion, sclerosis effect and MMP inhibition could be a more efficient multifaceted approach to treat aneurysm/ endoleaks formation.

**Objective 3:** The third objective of this thesis is to develop and evaluate an embolizing agent that is able to stop recanalization and aneurysm progression at the same time by targeting their biological mechanisms. This could be achieved by developing an injectable and radiopaque chitosan-based embolization agent containing doxycycline (DOX) as an MMP inhibitor/sclerosing embolizing agent for the treatment of AAAs.

The next three chapters present the work done to meet these different objectives, in three different papers published in peer-review journals. In addition, some of the in vitro evaluation tools are presented in the Appendix, to give more methodological details.

# CHAPTER 3

# CHITOSAN-SODIUM TETRADECYL SULFATE HYDROGEL: CHARACTERIZATION AND PRECLINICAL EVALUATION OF A NOVEL SCLEROSING EMBOLIZING AGENT FOR THE TREATMENT OF ENDOLEAKS

Fatemeh Zehtabi[a,b], Vincent Dumont-Mackay[c], Ahmed Fatimi1[b,e], Antony Bertrand-Grenier[b,d], Hélène Héon[b], Gilles Soulez[b,d], Sophie Lerouge[a,b,d]

[a] Department of Mechanical Engineering, École de technologie supérieure, 1100 Notre-Dame Street West, Montréal, QC H3C 1K3, Canada
[b] Research Centre, Centre Hospitalier de l'Université de Montréal (CRCHUM), 900 St Denis, Tour Viger, Montréal, QC H2X 0A9, Canada
[c] Département de pathologie, Centre hospitalier de l'Université de Montréal, Montréal, Canada
[d] Department of Radiology, Université de Montréal, Montréal, QC H2L 4M1, Canada
[e] Faculté Polydisciplinaire, Department of Chemistry, Université Sultan Moulay Slimane, Mghila BP:592, 23000 Beni-Mellal, Morocco

This article has been published in "Cardiovascular Intervent Radiol (2017) 40:576-584"

## 3.1. Context

The aim of this first article, published in 2017 in the CardioVascular and Interventional Radiology (Volume 40, Issue 4, pp 576–584) (Zehtabi, Dumont-Mackay, et al., 2017), is to meet the first specific objective of this PhD: to demonstrate the advantage of an embolizing sclerosing agent (CH-STS hydrogels) compared with an only embolizing agent to treat endoleak in a canine model of endovascular aneurysm repair. The majority of this work has been done by F. Zehtabi (realization of in vitro experiments, treatment and analysis of results, preparation of figures and manuscript) and is a continuation of the post-doctoral work of Ahmed Fatimi (Fatimi et al., 2012).

These results were also presented at 15ème Congrès des étudiants, stagiaires et résidents du Centre de Recherche du CHUM (2012) Canadian Biomaterials society (2013) Society for Biomaterials Annual Meeting (2013 & 2015).

## 3.2. Abstract

Purpose: To compare the efficacy of an embolization agent with sclerosing properties (made of chitosan and sodium tetradecyl sulfate, CH–STS) with a similar embolization agent but without sclerosing properties (made of chitosan, CH) in treating endoleaks in a canine endovascular aneurysm repair model.

Methods: Two chitosan-based radiopaque hydrogels were prepared, one with STS and one without STS. Their rheological, injectability, and embolizing properties were assessed in vitro; afterwards, their efficacy in occluding endoleaks was compared in a canine bilateral aneurysm model reproducing type I endoleaks (n = 9 each). The primary endpoint was endoleak persistence at 3 or 6 months, assessed on a CT scan and macroscopic examination. Secondary endpoints were the occurrence of stentgraft (SG) thrombosis, the evolution of the aneurysm mean diameter, as well as aneurysm healing and inflammation scores in pathology examinations.

Results: In vitro experiments showed that both products gelled rapidly and presented initial storage moduli greater than 800 Pa, which increased with time. Both gels were compatible with microcatheter injection and occlude flow up to physiological pressure in vitro. In a type I endoleak model, the injection of CH–STS sclerosing gel tended to reduce the risk of occurrence of endoleaks, compared to CHnon-sclerosing agent (2/9 vs. 6/9, p = 0.069). No case of SG thrombosis was observed. Moderate inflammation was found around both gels, with a comparable intensity score in both CH and CH–STS groups (2.6 ± 0.9 and 2.7 ± 0.9, respectively; p = 0.789).

Conclusions: Flow occlusion combined with chemical endothelial denudation appears promising for the treatment of endoleaks.

**Keywords:** Sclerosing agent, Endovascular aneurysm repair, Chitosan, Hydrogels, Endoleak, Embolization

## 3.3. Introduction

The clinical outcomes of endovascular aneurysm repair (EVAR) are limited by the occurrence of endoleaks, observed in 10 to 36% of cases (Hiramoto et al., 2007; Nevala et al., 2010; Seriki et al., 2006). Type II endoleaks are more frequent and need to be treated if they are associated with aneurysm progression (Brewster et al., 2006; Chung et al., 2015). Presently, the most common treatment strategy consists in injecting a liquid embolization agent (ethylene vinyl alcohol copolymer (Onyx, Covidien, Irvine, CA), cyanoacrylate glue, or fibrin glue) in the sac, combined with coils or not, to occlude the leak inside the aneurysmal sac, and the collateral arteries (Khaja et al., 2014; Muller-Wille et al., 2013; Sarac et al., 2012). However, complete nidus embolization is observed in 55-85% of cases (Martin et al., 2001; Sarac et al., 2012; Stavropoulos, Kim, et al., 2005), and reintervention is needed in 15- 44% (Muller-Wille et al., 2013; Stavropoulos, Kim, et al., 2005). In the case of type I endoleaks, embolization by liquid agent is less common but remains one of the several treatment options (including SG extension, stents, mechanical anchorage by aptus staples, or snorkel-assisted extension technique (Cao et al., 2010; Ghouri et al., 2010), which choice depends of the appearance of the leak and the aneurysm morphology. In these cases, the use of Onyx leads to a recurrence in 20% of cases and frequent Onyx migration (Chun et al., 2013; Eberhardt et al., 2014; Henrikson et al., 2011). Recently, Soulez et al. demonstrated the role of the endothelium, which lines the endoleak areas and exhibits anti-thrombotic properties promoting endoleak persistence or recurrence (Soulez et al., 2008). Therefore, a new paradigm for the treatment of endoleaks, based on achieving flow occlusion combined with endothelial denudation was proposed. An embolization agent with occlusive and sclerosing properties was created by combining chitosan (CH)–β-glycerophosphate (BGP) thermosensitive hydrogels with sodium tetradecyl sulfate (STS) (Sotradecol®)(Fatimi et al., 2012), a sclerosing agent commonly used in sclerotherapy (Cabrera et al., 2003; Dubois et al., 2001). Chitosan is a natural biodegradable polymer increasingly used in the biomedical, cosmetic, and pharmaceutical fields due to its unique properties such as biocompatibility, hemostatic, antibacterial properties. This polysaccharide forms polycationic solutions in dilute acids, and can be processed to form films, porous sponge-like scaffolds or thermosensitive hydrogels(Ahmadi et al., 2015). This study aimed to compare the efficacy of the embolic sclerosing agent (CH-STS) with a similar

hydrogel without sclerosing properties (CH), in a bid to prevent persistence and recurrence of endoleaks in a canine EVAR model.

## 3.4. Methods

### 3.4.1. Hydrogels Preparation and In Vitro Characterization

CH and CH-STS hydrogels were formed (Fatimi et al., 2012) by mixing two solutions: On the one hand, chitosan (Marinard Biotech, Rivière-au-Renard, Canada) was dissolved in HCl 0.1M solution containing 30%v/v Visipaque 320® contrast agent (GE Healthcare, Rahway, USA). On the other hand, an aqueous solution containing β-glycerophosphate disodium salt hydrate (BGP, Sigma Aldrich, Oakville, Canada), with or without STS 3% w/v (NiaproofTM, Sigma-Aldrich, Oakville, Canada). To form hydrogels, the two solutions were loaded in separate syringes joined by a luer lock connector, and then mixed just prior to their use. In CH: BGP concentration was raised to 20 w/vol% (versus 12% in CH-STS gels) to accelerate gelation and increase the mechanical properties to levels close to those of CH-STS gels. Mechanical properties, injectability and absence of damage on the gel during passage through a microcatheter (internal diameter of 0.61 mm) were first verified (Online Resource). The efficacy of both formulations in occluding blood flow was then tested on a custom-made in vitro bench system (Fatimi et al., 2016) which applies a pressurized liquid on the gel (up to 220 mmHg).

Table 3.1 pH and concentration of each compound in CH and CH–STS hydrogels used in this study

| **Hydrogels** | **Chitosan** | **Iodixanol** | **βGP** | **STS** | **pH** |
|---|---|---|---|---|---|
| | (% w/v) | (% v/v) | (% w/v) | (% w/v) | At room temp. |
| CH-STS | 2 | 30 | 12 | 3 | 7.39 |
| CH | 2 | 30 | 20 | 0 | 7.38 |

### 3.4.2. In Vivo Embolization of Endoleaks

#### Aneurysm Construction and Stent-Graft (SG) Implantation

The feasibility and efficacy of both hydrogels (CH-STS versus CH) in embolizing endoleaks was compared in vivo in a bilateral iliac EVAR model with a type I endoleak (Lerouge et al., 2004; Soulez et al., 2007). This model was chosen since it is more challenging than a type II endoleak model in terms of risk of gel migration, SG thrombosis and endoleak persistence. All interventions were performed under general anesthesia, according to the guidelines of the Canadian Council on Animal Care, and were approved by the institutional animal committee. Bilateral iliac aneurysms were surgically constructed using a jugular vein patch and a collateral outflow was created by the reimplantation of the sacroiliac trunk in the middle of the aneurysm sac (Fatimi et al., 2012; Lerouge et al., 2004). After 8-week recovery, a covered stent (iCAST, Atrium, Hudson, NH) was inserted using the carotid approach, and type I endoleaks were created by inducing SG plastic deformation at its proximal end through a 3.5 mm Savy balloon catheter (Cordis, Warren, NJ) deployed alongside the SG (Figure 3.1). At this step, all aneurysms had a type I endoleak entering through the misfit created at the proximal neck and leaving through the caudal artery (collateral outflow).

#### Embolization

In each animal, one aneurysm (single-blind random assignation) was embolized with CH–STS hydrogel, while the contralateral side was embolized with CH. Embolization agents were slowly injected through a 4-French catheter (Glidecath, Terumo, Japan) located longside the SG into the aneurysm sac. During injection, a temporary occlusion of blood flow was achieved with a balloon catheter positioned proximal to the bifurcation. The injection was continued until complete angiographic occlusion of the endoleak, including the origin of the collateral vessel when possible, while avoiding gel migration into the common iliac artery (about 5 mL of gel was injected in each aneurysm, with no difference between groups). Blood was collected for hematological and biochemical analysis at regular time points before and after embolization to detect possible inflammation induced by the embolization products.

**Follow-up Imaging**

All operators involved in imaging acquisitions and postprocessing were blind to the gel group attribution. Angiography (Koordinat 3D II, Siemens, Erlengen, Germany) was performed at SG implantation/embolization and before sacrifice at 3 months (n = 6) or 6 months (n = 3) to assess the presence of endoleaks and assess SG patency. Doppler ultrasound (US, 7–10 MHz probe; Supersonic Imagine, France) was performed at 1 week, and 1, 3, and 6 months (n = 3) to detect endoleak and follow changes in aneurysm size over time, by recording the aneurysm area at the proximal, middle, and distal thirds of the aneurysms. Finally, contrast-enhanced CT scanning (Sensation 64, Siemens medical, Erlangen, Germany) was performed before sacrifice as the gold standard for endoleak detection, whereas angiography was only used to classify endoleaks. Type I endoleak was defined on angiography as residual opacification of the aneurysm through an antegrade flow coming from the proximal neck and exiting through the collateral vessel, while type II was defined as retrograde flow coming from the collateral vessel (Stavropoulos, Clark, et al., 2005).

**Histopathology**

The animals were sacrificed by barbiturate overdose, and their iliac arteries with SG were fixed in buffered formalin. Serial transverse sections of the aneurysms were photographed, and histological analysis was performed after careful SG removal. The intensity of inflammation was given a semi-quantitative numerical score ranging from 0 to 4 (0 = no; 1 = minimal; 2 = mild; 3 = moderate; 4 = severe inflammation) (Carter et al., 2004). The percentage of aneurysm area occluded by fibrosis, thrombus, residual embolization material, and the percentage of leak was determined. Endoleak was defined as the presence of a channel, generally endothelialized and circulating through the embolization agent or surrounding tissues (Lerouge et al., 2004).

The primary endpoint was the proportion of endoleaks in both groups at 3 or 6 months, based on CT scan findings confirmed on macroscopic tissue slides. Secondary endpoints were the occurrence of SG thrombosis, the evolution of the aneurysm mean diameter with time, and aneurysm healing and inflammation scores based on pathology examination. The technical success was defined by a complete nidus occlusion after embolization on angiography.

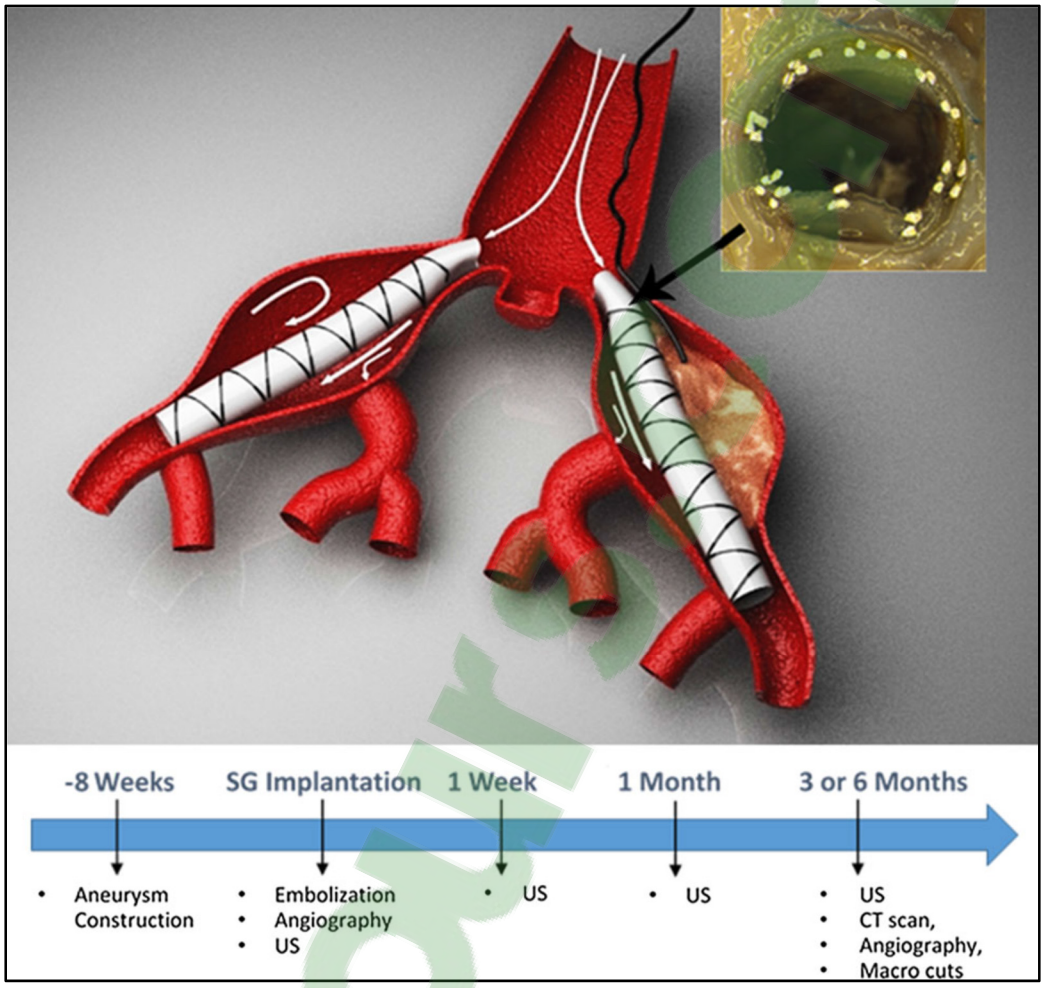


Figure 3.1 Schematic representation of the bilateral iliac aneurysm model with macroscopic image of the misfit created at the proximal neck using SG deformation. This led to type I endoleaks with large collateral outflow taking place through the reimplanted collateral outflow taking place through the reimplanted collateral in the center of the aneurysm. CH or CH–STS gel was then injected in the aneurysm to occlude the leak, through the lumen of a 4-French Glidecath catheter. The timeline of each experimental and imaging step is presented at the bottom

**Statistical Analysis**

Statistical analysis was performed using one-way ANOVA, followed by Fisher's post hoc tests with a minimum confidence level (p\0.05) for statistical significance. The effect of the embolization product (CH vs. CH–STS) on endoleak occurrence was estimated using a linear mixed effect model with logit link (LMEM), and with the product (fixed effect) and subject (random effect). The model is suited for correlated observations, i.e., it adjusts for patientlevel intra-correlation.

## 3.5. Results

### 3.5.1. In Vitro Characterization

Rheological measurements showed that both CH and CH–STS gelled immediately at body temperature. Their mechanical properties, assessed by the shear storage moduli, were above the threshold value identified for in vitro flow occlusion (G′≥800 pa) (Fatimi et al., 2016) and continued to increase with time (Figure 3.2a). In vitro embolization tests showed that both gels were immediately able to withstand pressurized liquid up to 220 mmHg without gel breakage. Both gels were injectable by hand through microcatheter using a 1-mL syringe, even after 1 h stagnation. Of interest, the gels formed a continuous and cohesive thread at injection (Figure 3.2b).

***Technical Success, Endoleak Occurrence, and Complications***

CH and CH–STS gels were successfully injected through a 4-French catheter in all aneurysms. Both gel formulations were visible during injection under fluoroscopy, allowing the monitoring of aneurysm sac filling with the gel and detection of gel migration when present. Technical success (immediate endoleak occlusion) was observed in 5/9 and 8/9 aneurysms in the CH and CH–STS groups, respectively (Table 3.2). CT scans performed before sacrifice detected 2 endoleaks out of 9 aneurysms treated with CH–STS, compared to 6 endoleaks out of 9 aneurysms treated with CH. The probability of observing a residual endoleak decreased by about 85% with the use of CH–STS, compared to CH (odds ratio = 0.1437; p value = 0.069). All were type I endoleaks, and no case of type II endoleaks was detected. In 4 cases of residual

endoleaks (3 in the CH group, one in the CH–STS group), no endoleak had been initially detected, suggesting possible cases of recurrence. SG remained patent in all cases, but one internal iliac artery (localized below a CH-embolized aneurysm) was thrombosed. Two animals suffered from tail necrosis and required partial amputation of the tail (Table 3.2). In two animals, hematological and biochemical analyses detected inflammation at weeks 2–4 after embolization (see details in Table 3.2), but everything was back to normal after 1 month. No other significant complication was observed.

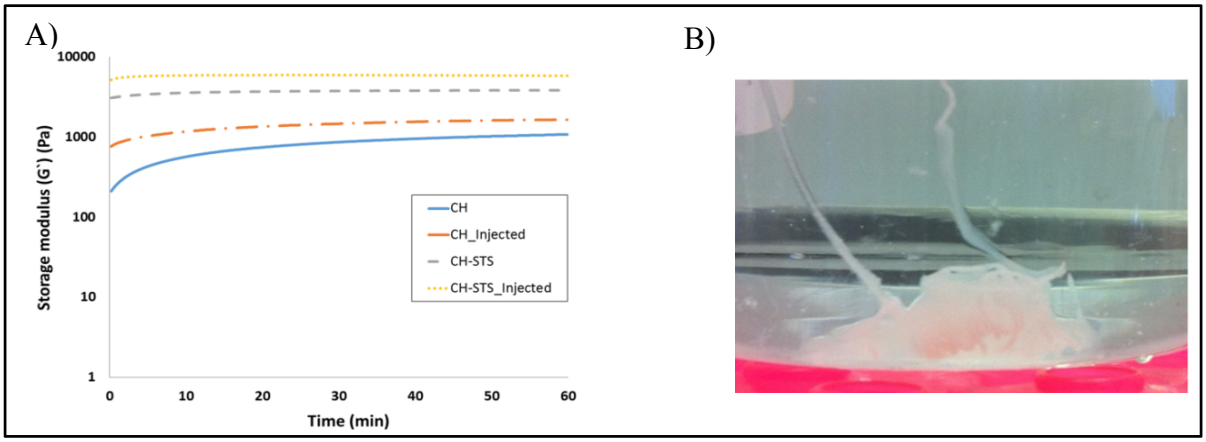


Figure 3.2 A) Rheological properties and injectability of the embolizing agents: The evolution of the storage modulus, G', B) CH-STS gel injected through a 0.61 mm microcatheter, showing the continuous thread and cohesive product obtained

**Evolution of Aneurysm Size**

Figure 3.4 presents the evolution of aneurysm size with time, expressed as mean aneurysm areas normalized to their initial value (before SG implantation). At the time of SG implantation, the mean aneurysm area was similar in both groups (1.92 and 1.85 cm2 for CH and CH–STS groups, respectively; p = 0.76). As expected, SG implantation led to increased aneurysm area (140% of the initial value at 1 week). After stabilization or a slight increase of aneurysm size at 4 weeks, it decreased with time, with the reduction tending to be more rapid in the CH group (109 vs. 130% at 3 months (p = 0.305) and 65 vs. 110% at 6 months (p = 0.216).

**Macroscopic Observations**

The mean percentage of aneurysm sac filling with embolization agent was slightly higher with CH–STS (42 ± 14%, vs. 30 ± 11% for CH; p = 0.120). CH gel was found in the vicinity of the SG, while the distribution of CH–STS was more peripheral, in contact with the aneurysmal wall (Figure 3.5).

In the CH–STS group, the two cases of endoleaks could be explained by poor initial embolization. In the first case (#4), the abnormal bilobal form of the aneurysm led to poor initial embolization (Figure 3.6). In the second case (#8), the collateral artery was not embolized, and retrograde flow almost entering the aneurysm was observed just after embolization. Six months later, a small type I endoleak was observed, with an endothelialized canal traveling through the regions without embolization agent. In contrast, in 5 out of the 6 endoleak cases observed in the CH group, the endoleak circulated throughout or in contact with the chitosan matrix (Figure 3.7) without correlation between the endoleak area and the percentage of embolized area (Figure 3.3).

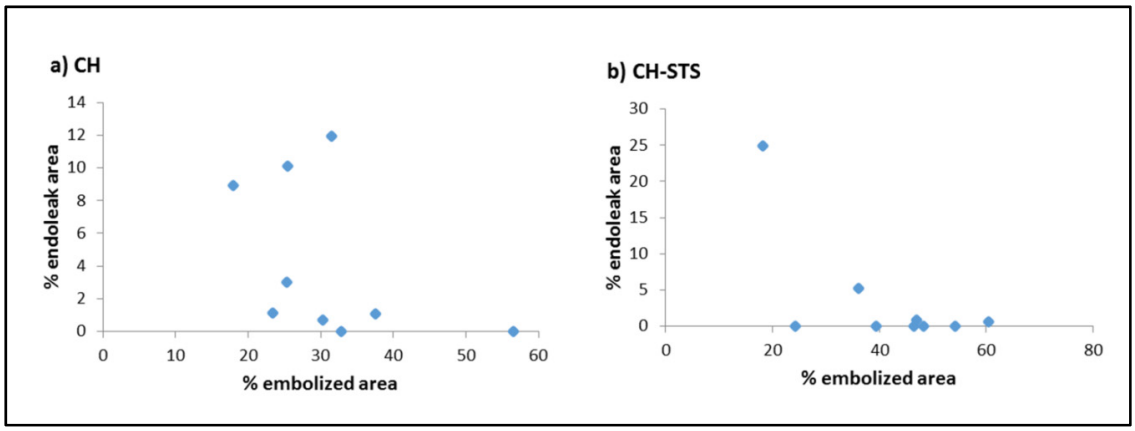


Figure 3.3 Percentage of endoleak area (%) as a function of percentage of aneurysm embolized for a) CH gel; b) CH-STS gels. In the case of CH-STS, endoleaks appeared in two poorly embolized aneurysms, while for CH, no relation could be observed between the two parameters

Table 3.2 The presence of residual endoleak immediately after embolization (based on angiography) and before sacrifice at 3 or 6 months (according to CT scan and confirmed by defect on macroscopic tissue slides). Complications are also indicated. No SG thrombosis was observed

| Dog # | Implanta-tion time (Months) | **Complication** | **Endoleak right after embolization** | | **Endoleak at sacrifice** | |
|---|---|---|---|---|---|---|
| | | | **CH** | **CH-STS** | **CH** | **CH-STS** |
| 1 | 3 | Distal embolization of internal iliac artery on CH side | Yes | - | Yes | - |
| 2 | 3 | Distal embolization of internal iliac and tail necrosis (surgery) on CH side | Yes | - | Yes | - |
| 3 | 3 | Distal embolization of internal iliac and tail necrosis (surgery) on CH side | Yes | - | - | - |
| 4 | 3 | | - | Yes | Yes * | Yes |
| 5 | 3 | Mild inflammation (eosinophilia) at 2-3 weeks.Normal at 1 month | Yes | - | Yes | - |
| 6 | 3 | Mild Inflammation at 2-4 weeks (high WBC, lymphocytosis, neutropenia) | - | - | Yes* | - |
| 7 | 6 | | - | - | - | - |
| 8 | 6 | | - | - | Yes * | - |
| 9 | 6 | | - | - | - | Yes* |
| **Total** | Endoleaks at sacrifice | | | | 6/9 | 2/9 |
| | Possible endoleak recurrence* (not observed at 1 week on US) | | | | 3/9 | 1/9 |
| | SG thrombosis | | | | 0/9 | 0/9 |

* Possible case of endoleak recurrence (endoleak detected at sacrifice after initial technical success)

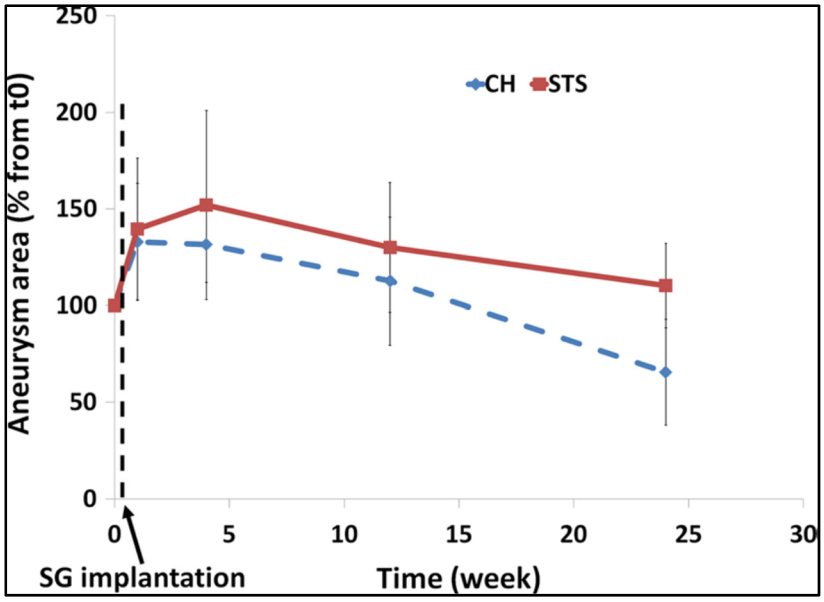


Figure 3.4 Evolution of aneurysm mean area in both groups normalized to the initial area (mean + SD)

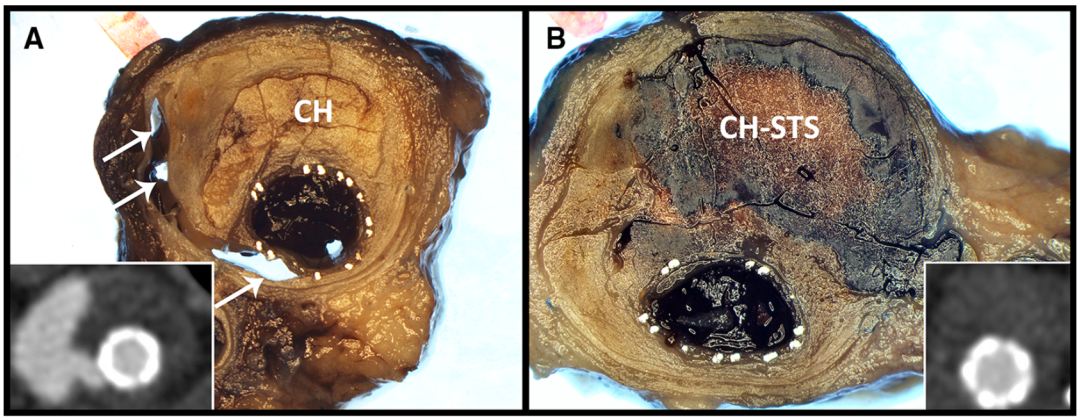


Figure 3.5 Macroscopic pictures of aneurysms treated by A CH and B CH–STS gels in the same animal (#5). A large endoleak can be seen in the CH-embolized aneurysm, which follows the aneurysm wall (single arrows) (insert CT scan)

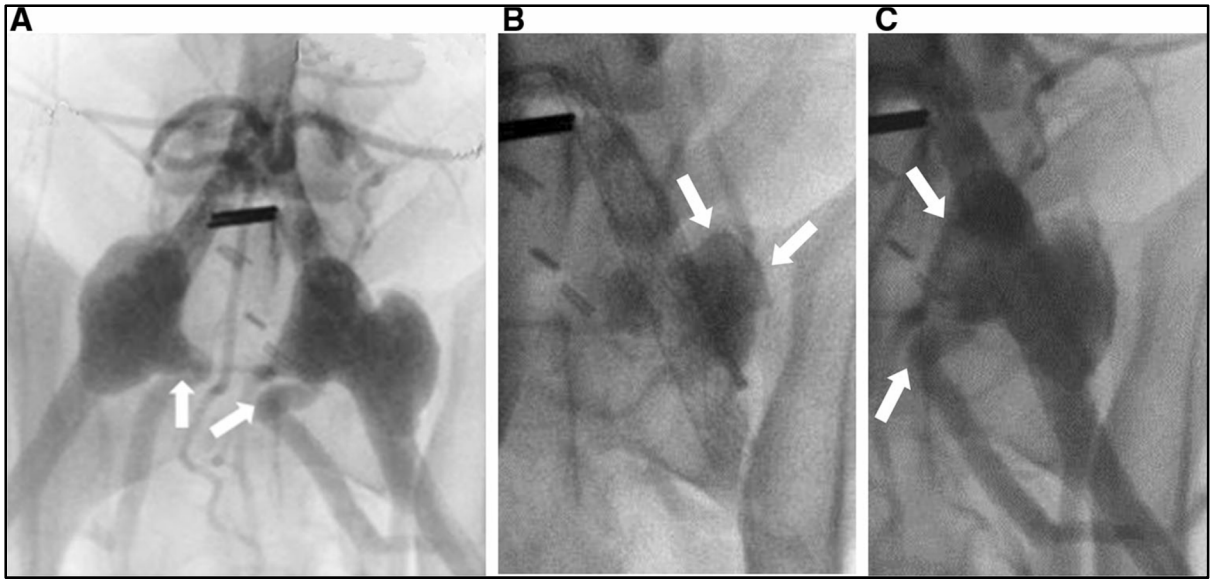


Figure 3.6 A Angiography of the bilateral aneurysm model, showing the bilobal form of the left aneurysm (Dog #4) (white arrows = outflow through the reimplanted caudal artery); B fluoroscopic image of the left aneurysm, showing incomplete embolization by CH–STS (ar rows = radiopaque gel filling only part of the aneurysm); C angiography post-embolization with residual type I endoleak (arrows)

**Histology**

Moderate inflammation was observed around both gels, with a comparable intensity score in both the CH and CH– STS groups (2.6 ± 0.9 and 2.7 ± 0.9, respectively; p = 0.789). It was overwhelmingly of granulomatous/resorptive type, with a predominance of macrophages admixed with polymorphonuclear neutrophils and some lymphocytes, mostly around the embolization gels. Some more acute, neutrophil-predominant inflammation was also identified in some areas surrounding the gels, and was deemed to be within the expected range around foreign embolization materials. Neovascularization was moderate in both the CH and CH–STS groups, with no significant difference between the two. No intimal hyperplasia was observed. Based on histology, it is not possible to conclude on the extent of gel degradation, but evidence of progressive biodegradation, such as resorptive cell infiltration and tissue growth, was clearly observed (Figure 3.7).

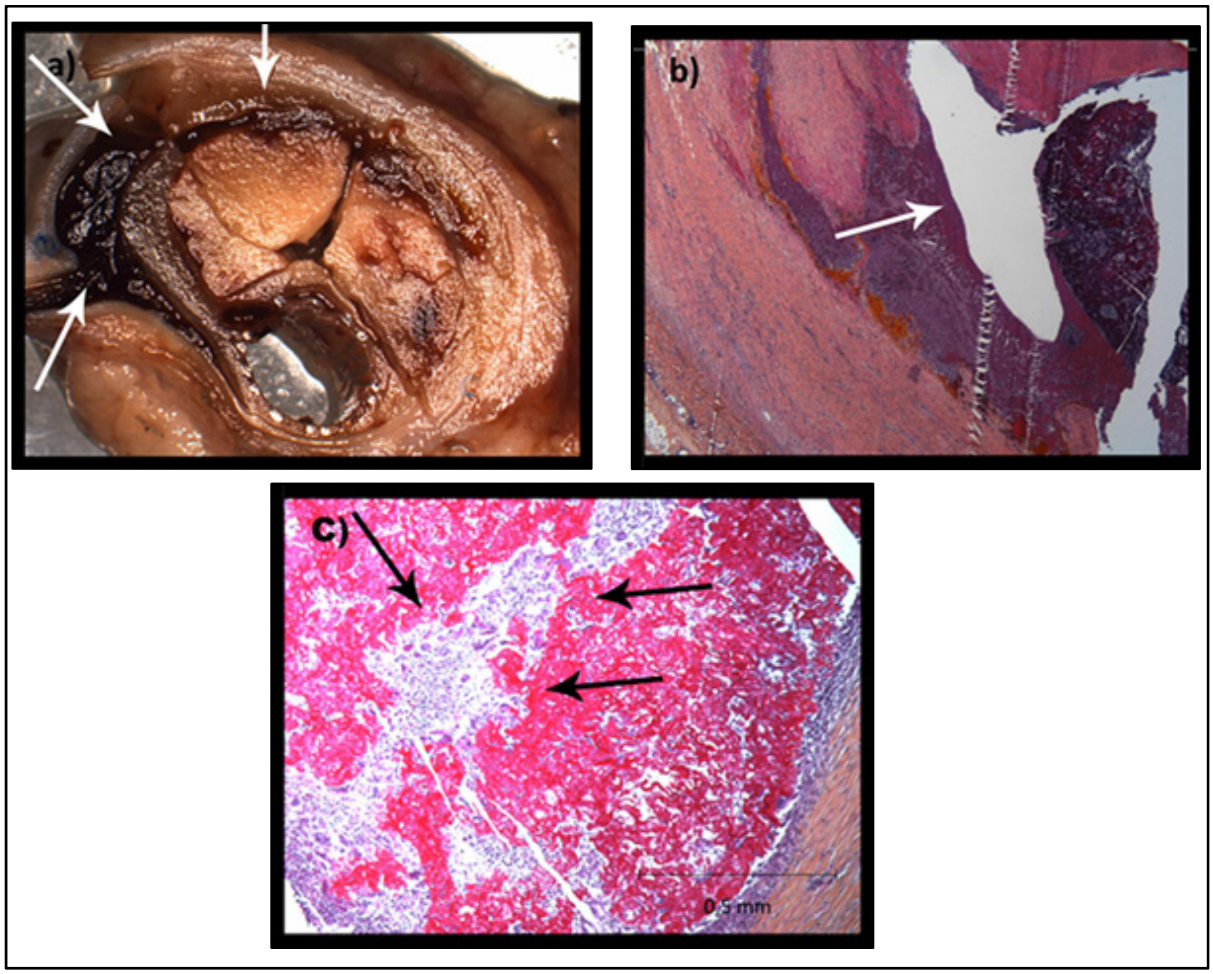


Figure 3.7 A, B Transverse tissue section and histological slide (HPS staining) showing the presence of an endoleak throughout the CH matrix (arrows) (Dog #6); C inflammation and resorption of the embolization agent (arrows) (HPS staining)

### 3.6. Discussion

The hypothesis of this study was that the combination of occlusive properties and sclerotherapy (CH–STS) can provide greater benefits than simple embolization (CH) to permanently occlude aneurysms after EVAR. Although differences observed were not statistically significant given the limited number of animals used, data confirm the potential of CH–STS to decrease the number of residual endoleaks, as compared to an embolic non-sclerosing gel (CH). It was previously demonstrated that CH–STS gels remove the endothelial layer of explanted blood vessels (Fatimi et al., 2012). This may incite a more vigorous thrombotic reaction within the

aneurysm, in addition to preventing thrombus recanalization, as shown in previous studies (Soulez et al., 2008). Interestingly, CH–STS also better casted the aneurysmal sac, as compared to CH, which tends to stick to the SG, but not to the arterial wall. This is important since, according to our hypotheses, and as observed in this animal model, endoleaks generally follow the aneurysm wall (Lerouge et al., 2004; Soulez et al., 2008).

Despite reduced occurrence, two cases of endoleak were observed with CH–STS. These can be explained by the very challenging model used in this study, which is characterized by high flow due to the large misfit created at the proximal neck and the large diameter of the reimplanted collateral artery. This model was chosen since it leads, when untreated, to huge persistent endoleaks (Lerouge et al., 2004). Better results can be expected in a more realistic model of type II endoleaks, where risks of gel migration are lower due to a reversal of blood flow direction.

Recent studies show increasing interest in embolic sclerosing agents for interventional radiology (Dompmartin et al., 2011; Hamada et al., 2002; S. Lerouge et al., 2011; Nakai et al., 2016). While further tests are required to prove its efficacy and safety, CH-STS gel show promising features. In another study, an embolic sclerosing gel made with ethylcellulose and ethanol had been tested in the same animal model (S. Lerouge et al., 2011), but unacceptable rates of gel migration and SG thrombosis were observed, due to the inadequate mechanical properties of the product. In the present case, combining chitosan with BGP leads to thermosensitive hydrogels, whose mechanical properties increase at body temperature (Chenite et al., 2001). Moreover, the addition of STS enables the drastic acceleration of gelation and increase of mechanical properties, while providing the embolization gel with sclerosing properties (Fatimi et al., 2012). No case of SG thrombosis was observed. The injectability through microcatheters was confirmed, even one hour after mixing the two solutions, which means that the risk of catheter occlusion is low. Injection of CH-STS does not require solvent pre-injection. Moreover, Visipaque-containing hydrogels were already shown to present temporary radiopacity (Coutu et al., 2013) which avoids interference with imaging follow-up. Here, the in vivo decrease in gel radiopacity was not studied systematically, but the gel was not visible in the final CT scanner (at 3 months). This may be an advantage

compared to current embolization agents containing tantalum powder (Saeed Kilani et al., 2015). Yet, further studies are needed to confirm that during embolization, radiopacity is enough to ensure good visibility in AAA patients. The biodegradability of chitosan (Ganji et al., 2007) is another potential advantage since the embolization agent could be replaced by fibrous tissue, leading to complete healing (and shrinkage) of the aneurysm after degradation. STS addition is believed to slow down the degradation rate, due to strong interactions between negative STS charges and positively charged chitosan amino groups. This could explain the lower aneurysm shrinkage observed at follow-up in the CH-STS group despite a reduced number of endoleaks. In vivo studies with longer follow-ups will be required to characterize gel biodegradation and aneurysm healing and to verify the absence of endoleak recurrence during the process.

### 3.7. Limitations

The present study is limited by the small number of animals used. A type II model would have been less challenging and probably more appropriate, although embolization agents such as Onyx are also used to treat some type I endoleaks (Chun et al., 2013; Eberhardt et al., 2014). Moreover, embolization was performed here immediately after the creation of the endoleak, while a chronic model would have been more appropriate. Venous patch models lack atherosclerosis and intraluminal thrombus, which are frequently observed in clinical aneurysms, and this may decrease the significance of their endothelial coverage. However, it is well documented that thrombi in clinical aneurysms are permeated by endothelialized channels (Adolph et al., 1997). Finally two cases of tail necrosis were observed, probably due to the migration of one of the embolization compounds. As observed by the operator, migration at injection was more pronounced with CH, probably due to its lower mechanical properties. However, the fact that the two caudal (collateral) arteries were linked to the tail artery makes it impossible to confirm whether CH or CH-STS migration was responsible. Since non-target embolization using a sclerosing agent may cause more tissue necrosis than with a non-sclerosing agent, further safety testing is needed in an aortic aneurysm model reproducing type II endoleaks, with only one embolization agent per animal (Lerouge et al., 2004).

## 3.8. Conclusions

In this challenging type I endoleak model, CH–STS sclerosing gel tends to reduce the occurrence of type I endoleaks compared to a CH non-sclerosing agent. Flow occlusion combined with endothelial denudation appears as a promising new paradigm for the treatment of endoleaks. Further tests in a type II endoleak model and comparisons with commercialized embolization agents such as Onyx are required to better assess the potential of this particular product.

## 3.9. Acknowledgements

This work was supported by the Canadian Institutes of Health Research (PPP-106794) and the Canada Research Chair (S.L). Gilles Soulez is supported by a National Researcher Award from the Fonds de la Recherche en Santé du Quebec. The authors thank Dr. Philippe Roméo for his invaluable help and supervision during the histopathological analysis, Martin Ladouceur for statistical analysis, and Jocelyne Lavoie, Michel Gouin, Elias Assaad, and the animal care staff for their technical help during animal experiments.

## 3.10. Compliance with Ethical Standards

**Conflict of interest** Fatemeh Zehtabi, Vincent Dumont-Mackay, Antony Bertrand-Grenier, and Hélène Héon have no commercial, proprietary, or financial interest in any products or companies described in this article (No potential conflict of interest). Ahmed Fatimi, Gilles Soulez, and Sophie Lerouge are co-inventors on a patent pertaining to chitosan–STS gel and have transferred their rights to their institutions. The technology has been exclusively licensed to Cook Medical. Currently, there is a research contract agreement in place between the academic institutions and Cook Medical to develop the technology.

**Ethical Approval** All surgeries and interventions were performed under general anesthesia according to the guidelines of the Canadian Council on Animal Care, and were approved by the institutional animal committee.

# CHAPTER 4

# NEW ALCOHOL AND ONYX MIXTURE FOR EMBOLIZATION: FEASIBILITY AND PROOF OF CONCEPT IN BOTH *IN VITRO* AND *IN VIVO* MODELS

Mohammad Saeed Kilani[a,b], Fatemeh Zehtabi[c](co-first author), Sophie Lerouge[c], Gilles Soulez[d,e], Jean Michel Bartoli[f], Vincent Vidal[a,g,h], Mohammad F. Badran[i]

[a] Hôpital cardiologique, Centre Hospitalier Universitaire (CHRU) de Lille, Boulevard Jules LECLERQ, 59037 Lille, France
[b] Experimental Interventional Imaging Laboratory, CERIMED, Marseilles, France
[c] Department of Mechanical Engineering, École de technologie supérieure (ETS) & CHUM Research center (CRCHUM), Montreal, Canada
[d] Department of Radiology, Centre Hospitalier de l'Université de Montréal, 1560 Sherbrooke East, H2L 4M1, Montreal, Canada
[e] Department of Radiology, Radio-Oncology and Nuclear Medicine, University of Montreal, Montreal, Canada
[f] Department of Medical Imaging, University Hospital Timone, Marseille, France
[g] Aix-Marseille University, Marseille, France
[h] Interventional Radiology Section, Department of Medical Imaging, University Hospital TIMONE, Marseille, France
[i] Radiology Department, King Faisal Specialist Hospital and Research Center, MBC 28, PO Box 3354, Riyadh 11211, Saudi Arabia

This article has been published in "Cardiovascular Intervent Radiol (2017) 40:735-743"

## 4.1. Context

The purpose of this second article, published in 2017 in the CardioVascular and Interventional Radiology (Volume 40, Issue 5, pp 735–743)(Saeed Kilani et al., 2017), is to respond to the 2nd specific objective of this doctorate: to assess the potential of an embolizing/sclerosing agent developed by addition of a known sclerosing agent (Ethanol) to a present commercialized embolic agent (Onyx) in vitro and in vivo. This project was done equally by two first co-authors F.Zehtabi (design, performance and realization of in vitro experiments, treatment of results, and preparation of figures and manuscript of in vitro part) and MS. Kilani (design, performance and realization of in vivo experiments, treatment of results, and preparation of figures and manuscript of in vivo part).

## 4.2. Abstract

Introduction: Onyx and ethanol are well-known embolic and sclerotic agents that are frequently used in embolization. These agents present advantages and disadvantages regarding visibility, injection control and penetration depth. Mixing both products might yield a new product with different characteristics. The aim of this study is to evaluate the injectability, radiopacity, and mechanical and occlusive properties of different mixtures of Onyx 18 and ethanol in vitro and in vivo (in a swine model).

Materials and Methods: Various Onyx 18 and ethanol formulations were prepared and tested in vitro for their injectability, solidification rate and shrinkage, cohesion and occlusive properties. In vivo tests were performed using 3 swine. Ease of injection, radiopacity, cohesiveness and penetration were analyzed using fluoroscopy and highresolution CT.

Results: All mixtures were easy to inject through a microcatheter with no resistance or blockage in vitro and in vivo. The 50%-ethanol mixture showed delayed copolymerization with fragmentation and proximal occlusion. The 75%-ethanol mixture showed poor radiopacity in vivo and was not tested in vitro. The 25%-ethanol mixture showed good occlusive properties and accepted penetration and radiopacity.

Conclusion: Mixing Onyx and ethanol is feasible. The mixture of 25% of ethanol and 75% of Onyx 18 could be a new sclero-embolic agent. Further research is needed to study the chemical changes of the mixture, to confirm the significance of the added sclerotic effect and to find out the ideal mixture percentages.

**Keywords:** Embolization, Onyx, Ethanol

## 4.3. Introduction and Rationale

The endovascular management of vascular anomalies can be very challenging in current practice. Various techniques have been described in the literature, including embolization, sclerotherapy and combination of both methods. Several materials have been used to achieve vessel occlusion and endothelial disruption (Cho et al., 2006; Do et al., 2007; Do et al., 2005;

Elhammady et al., 2012; Gomes, 1994; Houbballah et al., 2010; Jeong et al., 2006; Jin et al., 2008; Kademani et al., 2004).

Embolization involves vessel occlusion and can be obtained at a proximal level using mechanical agents such as metallic coils and detachable balloons or at a distal level by casting the abnormal vascular network using liquid agents such as cyanoacrylates (N-butyl cyanoacrylates:NBCA) and ethylene-vinyl-alcohol copolymer (Onyx, ev3-Endovascular Inc., Plymouth, MN, USA). A transvenous approach has also been recommended by some authors in some situations (Jackson et al., 1996).

Cyanoacrylates rapidly precipitate upon ionic contact with blood and blood products. These compounds require rapid injection with the consequent risks of reflux, catheter gluing, nontarget embolization and incomplete occlusion as the microcatheter has to be retrieved rapidly (Loh et al., 2010).

Onyx is an alternative liquid embolic agent comprising an ethylene-vinyl-alcohol copolymer (EVOH) dissolved in a solvent (dimethyl sulfoxide, DMSO). This agent is very well visualized under fluoroscopy due to its content of tantalum powder. The solidification process starts when Onyx comes in contact with blood or saline solution. Once injected, DMSO dissipates, and the EVOH then forms a precipitate (Ayad et al., 2006). Due to its high viscosity and non-adhesive cohesive nature, Onyx combines the advantage of a controlled slow injection with a low risk of catheter gluing and systemic migration (Saeed Kilani et al., 2015). However, Onyx is occasionally unable to penetrate sufficiently deeply into very small distal vessels, resulting in unwanted proximal occlusion and reflux with the partial exclusion of the lesion, which may cause its revascularization and regrowth (Ambekar et al., 2016). High clinical and radiological recurrence rates of AVM have been observed after transarterial embolization alone using various embolic materials (Jacobowitz et al., 2001).

Alternatively, sclerotherapy consists of the destruction of the endothelial lining, which results in an inflammatory response; this results in fibroblast proliferation, leading to fibrosis. In addition, the agents used may produce other effects, such as thrombosis and physical obstruction by polymerization. The advantage of sclerotherapy is that it not only results in the

occlusion of vascular structures (similar to embolization) but may also limit recurrence by permanently disrupting the endothelium of the vessels, thus preventing recanalization (Soulez et al., 2008). Sclerotherapy and embolotherapy are considered as a continuum, and some products possess characteristics useful to both, such as cyanoacrylates (Albanese et al., 2010). Absolute ethanol is one of the most effective sclerosing and deeply penetrating agents. It acts by inducing cytotoxic damage through the denaturation of proteins, the hypertonic dehydration of cells, and by coagulation and thrombosis when blood products are present (Ellman et al., 1984; Hyodoh et al., 2005). Together, these factors lead to fibrinoid necrosis (Do et al., 2005). Due to its low viscosity and lack of visibility, the systemic migration of alcohol poses a considerable risk of potentially serious side effects and nontarget embolization. A mortality rate of 0.6% has been reported in AVM treated with ethanol (Yakes et al., 1992). Cases of permanent and transient nerve damage following ethanol injection have also been described (Do et al., 2010). Acute pulmonary hypertension and vasospasm have also been reported during intravascular ethanol use, and skin necrosis and fistulization have also occurred.

An ideal embolic agent would be easily injectable, have good mechanical properties that conform, cast and occlude the target vessels as distally as possible without systemic migration, be radiopaque, cohesive to avoid fragmentation and provide effective permanent and definitive occlusion. Moreover, such an agent should possess both sclerotic and embolic characteristics (Fatimi et al., 2012).

A combination of Onyx with ethanol might be a potential sclero-embolic agent with different characteristics and behavior.

The aim of this study was to evaluate the injectability, radiopacity, and mechanical and occlusive properties of various mixtures of Onyx 18 and ethanol in vitro and in vivo in a swine model.

## 4.4. Materials and Methods

### 4.4.1. Part I: In Vitro Study

Onyx 18 and various formulations of Onyx 18 with absolute ethanol were prepared and tested in vitro for their injectability, solidification rate and shrinkage, cohesion and occlusive properties. Based on radiopacity data obtained in vivo (see below), only the 25%-ethanol mixture (75% Onyx 18, 25% absolute ethanol) and the 50%-ethanol mixture (50% Onyx 18, 50% absolute ethanol) were tested in vitro. All in vitro tests were performed at least in triplicate.

#### Injectability Test

The injectability of the various formulations was evaluated by measuring the force required to inject the solutions through DMSO-compatible catheters (Rebar 18 microcatheters; inner lumen 0.021 inch, EV3-Endovascular Inc., Plymouth, MN, USA) at an injection speed of 0.1 mL/min. This test was performed using a mechanical setup including a Bose® ElectroForce® 3200 Test Instrument equipped with a 225-N load cell, which applied force to a 1-mL syringe (Micro Therapeutics), which was connected to a catheter, which was immersed in a saline bath at 37 °C. Prior to the injection of the tested product, the dead space of the microcatheter was filled with DMSO.

#### Rheometry Test

The rheological properties of Onyx and different mixtures during solidification while in contact with saline solution were studied at 37 °C using rheometry (Physica MCR 301, Anton Paar, Saint-Laurent, Canada) with co-axial cylinder geometry. The evolution of the shear storage modulus, G´ (representing the solid like behavior of the material), and loss modulus G´´ (representing its viscous response) enables to follow the solidification process. The final storage modulus after solidification was also measured to evaluate the elastic properties of the embolizing agent.

**Embolization Test**

To evaluate the occlusive properties of the different mixtures, an in vitro bench test was designed to measure the maximal liquid pressure sustained by the embolic agent before breaking. The system comprised a syringe pump (PHD 2000 Programmable, Harvard Apparatus) pushing a solution of viscosity similar to blood (40% glycerol (v/v) and 60% distilled water (v/v) into silicon tubes of 3.175 mm inner diameter connected to a short tube (3 cm long) filled with the tested mixture. The pressure was measured continuously and was progressively increased up to 220 mmHg, unless migration or breakage of the product occurs.

**Ethanol Release from the Mixture**

To evaluate ethanol release and material shrinkage during polymerization and after injection in water, 1 mL of the tested product was injected into 2 mL of water. After 30 minutes, the volume shrinkage that occurred during precipitation was evaluated by measuring the change in agent volume during solidification.

**4.4.2. Part II: In Vivo Study in a Swine Model**

**Animal Model and Embolization Procedure**

In accordance with the institutional Animal Care and Use Committee, three swine weighing approximately 60 kg each were used. All applicable institutional and/or national guidelines for the care and use of animals were followed. The procedures were performed under general anesthesia. A digital subtraction angiographic Stenoscope system (General Electric Medical System, Minneapolis, USA) was used for radiological procedures. After obtaining femoral arterial access and the superselective catheterization of the target arteries, injections were performed using the same type of microcatheter. Before embolization, the microcatheter was flushed with saline solution prior to filling the dead space of the microcatheter with an adequate volume of DMSO. Onyx was shaken for 20 min using a shaker (Vortex-Genie, Scientific Industries, Bohemia, NY) to homogenize the tantalum powder within the suspension. Before injection, ethanol was added to the desired percentage and mixed in the syringe manually.

Table 4.1 summarizes the mixtures used for the embolization of arterial targets in each swine. Embolization was preceded by a diagnostic angiography series performed using a 6-Fr guiding catheter. Superselective catheterization was performed using the same type of microcatheter. The tip of the microcatheter was positioned immediately proximal to the first bifurcation of each embolized artery. The endpoint of embolization was defined by visualizing the backflow up to the proximal bifurcation. A final angiography run was performed through the guiding catheter to confirm complete occlusion.

Animals were killed at the end of the procedure and underwent high-resolution CT imaging using a thin-slice (0.6 mm) protocol to analyze the penetration depth and the distribution of Onyx through the distal vascularity.

In addition, the first swine was surgically dissected, and the kidneys were explanted and cut into thick slices. Highresolution X-ray and CT scan were performed on the explanted kidneys to analyze the distribution and depth of penetration in each embolized artery.

**Endpoints**

The interventional radiologist who performed all the injections (VV; an interventional radiologist who has more than 10-year experience with the use of liquid embolic agents) evaluated the ease of injection on the following scale: very easy, easy, some resistance and complete blockage. Three observers evaluated (by consensus) the characteristics of tested mixtures in terms of radiopacity and cohesiveness on a four-point scale (excellent, good, fair and poor) and reported their global impression of the product as acceptable or not acceptable (Table 4.2). A consensus score for the evaluation of penetration was designed by adding the distances from the renal cortex and the nearest radio-opaque embolized arterial segment at five points in each embolized territory in swine 1 measured on CT images with MPR reconstructions (Figure 4.1). The nearer the embolic agent was to the cortex (low scores), the higher the penetration. Thus, the largest score corresponded to the least penetration (Table 4.3).

Table 4.1 Various mixtures used for the embolization of target arteries in each swine

| | Target of embolization | Material used |
|---|---|---|
| **Swine 1** | Inferior polar branch of the left renal artery | Onyx 18 |
| | Superior polar branch of the left renal artery | 75%-Ethanol mixture |
| | Superior polar branch of the right renal artery | 50%-Ethanol mixture |
| | Inferior polar branch of the right renal artery | 25%-Ethanol mixture |
| | Left rete mirabilis | 25%-Ethanol mixture |
| **Swine 2** | Right renal artery | Onyx 18 |
| | Left renal artery | 25%-Ethanol mixture |
| | Left rete mirabilis | 25%-Ethanol mixture |
| **Swine 3** | Left rete mirabilis | Onyx 18 |

Table 4.2 Consensus evaluation of the in vivo behavior and characteristics of different mixtures of Onyx and ethanol

| | Radiopacity | Penetration (according to the score shown in Table 3) | Cohesiveness | Acceptable |
|---|---|---|---|---|
| Onyx 18 | Excellent | Good | Excellent | Yes |
| 25%-Ethanol mixture | Excellent | Excellent | Excellent | Yes |
| 50%-Ethanol mixture | Good | Fair | Poor | No |
| 75%-Ethanol mixture | Poor | Excellent | Not analyzable | No |

Table 4.3 Penetration depth score (in mm) for each product tested in swine 1, as measured on CT MPR reconstructions between the renal cortex and the nearest opaque arterial segment at 5 points

| | **P1** | **P2** | **P3** | **P4** | **P5** | **Total** | **Mean** |
|---|---|---|---|---|---|---|---|
| Onyx 18 | 3 | 3.8 | 3.6 | 4.5 | 4 | 18.9 | 3.78 |
| 25%-Ethanol mixture | 3.4 | 3.2 | 3.6 | 2.4 | 3.7 | 16.3 | 3.26 |
| 50%-Ethanol mixture | 4.1 | 4.9 | 7.6 | 7.6 | 6.2 | 30.4 | 6.08 |
| 75%-Ethanol mixture | 3.3 | 3.8 | 2.2 | 2 | 2.3 | 13.6 | 2.72 |


Figure 4.1 Examples of penetration score measurement; coronal oblique CT images of swine 1 with MPR reconstruction. A Right kidney upper pole (50%-ethanol mixture). B Left kidney upper pole (75%-ethanol mixture). C Right kidney lower pole (25%-ethanol mixture). D Left kidney lower pole (Onyx 18). The distances from the renal cortex and the nearest radio-opaque embolized arterial segment at five points in each embolized territory were added to get the score

## 4.5. Results

### 4.5.1. Part I: In Vitro Testing

#### Injectability

All of the tested mixtures were easily injected through the microcatheter and required the application of less force than Onyx 18 (the minimal forces required to inject Onyx, 25%-ethanol and 50%-ethanol mixtures were 3.2 ± 0.5, 1.9 ± 0.1 and 1.3 ± 0.1 N, respectively). Whereas Onyx 18 and the 25%-ethanol mixture formed a cohesive bulky shape in saline solution, the 50%-ethanol mixture failed to form a cohesive and acceptable shape (Figure 4.2).

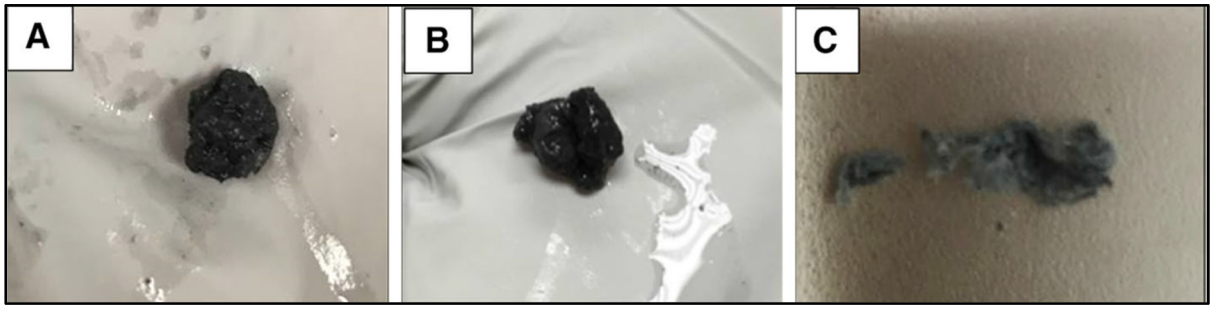


Figure 4.2 Final shape of A Onyx, B 25%-ethanol mixture and C 50%-ethanol mixture after injection in a saline solution bath and polymerization. Note the non-cohesive aspect of 50%-ethanol mixture (C)

#### Rheometry Results

As shown by the evolution of the shear storage modulus (G´) (Figure 4.3A), Onyx rapidly solidified in contact with water. The 25%-ethanol mixture showed quite similar results, but the solidification (copolymerization) rate of the 50%-ethanol mixture was clearly delayed. Increasing ethanol content also drastically decreased the final mechanical properties of the embolizing agent (G´), from 1458 Pa (±244) for Onyx to 617 Pa (±216) for the 25%-ethanol mixture and only 60 Pa (±48) for the 50%-ethanol mixture.

**Occlusive Properties**

Onyx and the 25%-ethanol mixture immediately occluded the tubular structure up to the maximal pressure tested (200 mmHg) (Figure 4.3B); the 50%-ethanol mixture did not occlude and migrated in the tube when the fluid pressure started to increase. Even when increasing the volume of 50%-ethanol mixture to ensure complete initial cast of the tube, poor occlusion and product migration were still observed.

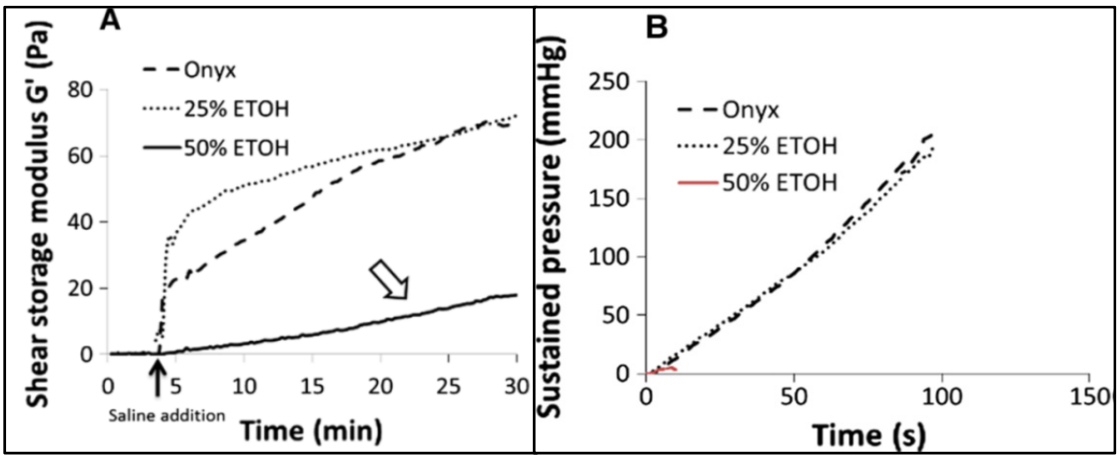


Figure 4.3 A Kinetics of the solidification of the test mixtures in contact with saline as assessed by the evolution of the storage modulus, G0, for Onyx, 25%-ethanol mixture and 50%-ethanol mixture (white arrow) (average curve, n = 3). B In vitro embolization results show good resistance to pressure for Onyx, and 25%-ethanol mixture; 50%-ethanol mixture was resistant only to 10 mmHg

**Ethanol Release**

No significant shrinkage was observed during the solidification of 1 mL Onyx. In contrast, a significant decrease in volume was observed during the solidification of the 25%-ethanol mixture (the final volume was 82% of the initial volume) and 25%-ethanol mixture (60% of the initial volume); most likely, the shrinkage was due mostly to ethanol release (Table 4.4).

### 4.5.2. Part II: *In Vivo* Study

Ethanol and Onyx 18 were easily mixed and were easily injected. No significant resistance was felt compared to Onyx 18. We never experienced catheter blockage. Table 4.2 and Table 4.3 summarize the penetration score data and the consensus evaluation of the mixture characteristics. Using the 75%-ethanol mixture, the visibility under fluoroscopy was rated poor; however, the mixture provided excellent penetration (Table 4.2) and was visible on highresolution X-ray and CT images, reaching distal vessels very close to the renal cortex (Figure 4.4). The cohesiveness of the 75%-ethanol mixture could not be evaluated due to its poor radiopacity.

The 50%-ethanol mixture was not cohesive and fragmented during injection with a significantly lower penetration depth (score = 30.4) than Onyx 18 (score = 18.9). However, the radiopacity remained good (Figure 4.5). With the 25%-ethanol mixture, visibility (radiopacity) was excellent. The mixture was cohesive during injection, and no fragmentation was observed (Figure 4.6). The 25%-ethanol mixture penetrated more deeply (score = 16.3) than Onyx 18 (score = 18.9) in renal arteries (Table 4.3; Figure 4.5, Figure 4.6) and in the rete mirabilis; this resulted in the early migration and embolization of a portion of the contralateral rete mirabilis. In comparison, Onyx 18 resulted in more proximal occlusion and remained localized to the ipsilateral rete mirabilis. By consensus, the 50 and 75%-ethanol mixtures were considered unacceptable for use as embolic agents due to the lack of coherence and radiopacity, respectively.

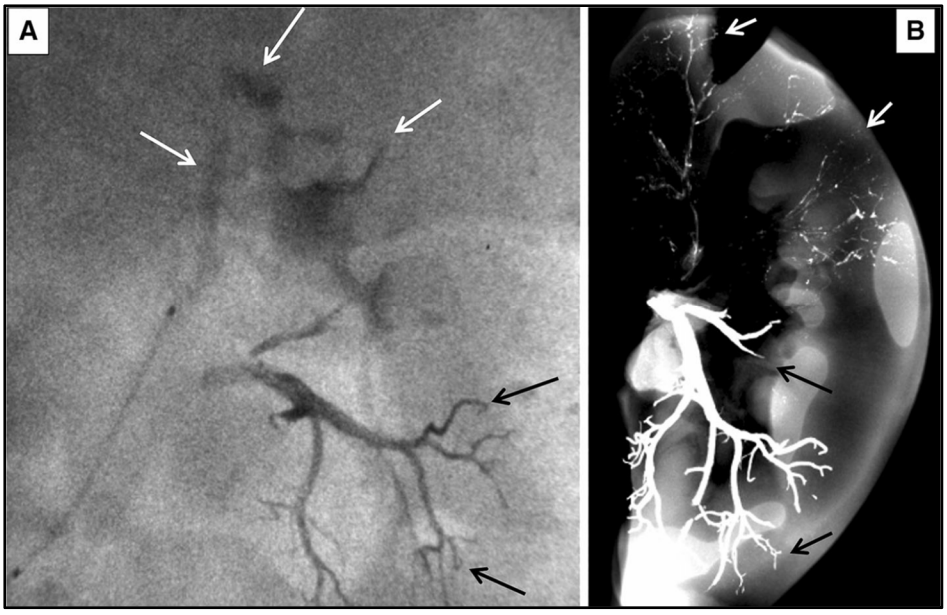


Figure 4.4 Swine 1 left kidney. A Fluoroscopy image of the left kidney of swine 1 showing the poor visualization and faint radiopacity of the 75%-ethanol mixture in the superior polar artery branches (white arrows) compared to Onyx 18 in the inferior polar artery branches (white arrows) compared to Onyx 18 in the inferior polar artery (black arrows). B High-resolution X-ray examination of a thick slice of the explanted left kidney. Compare the deep penetration of the 75%-ethanol mixture, which reached small distal vessels very close to the cortex (white arrows), to the relatively proximal position of the Onyx 18 cast (black arrows)

Table 4.4 Volume decrease during the solidification of different mixtures - most of the decrease is assumed to be due to the release of ethanol

| Formulation (1 mL) | Onyx | 25%ETOH | 50%ETOH |
|---|---|---|---|
| Final volume of the embolizing agent (mL) | 1 | 0.82 | 0.6 |
| Volume shrinkage (mL) | 0 | 0.18 | 0.4 |
| Estimated % initial ethanol volume released | N/A | 72% | 80% |

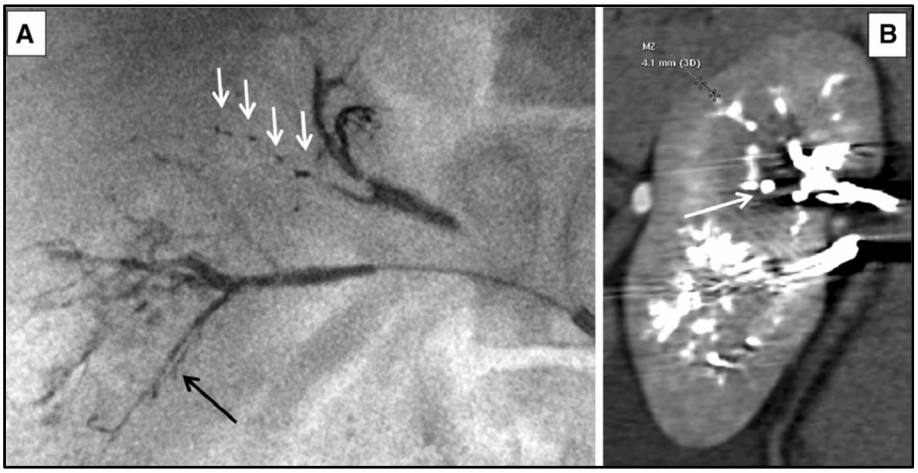


Figure 4.5 Swine 1 right kidney. A Fluoroscopic image of the right kidney of swine 1: Note the fragmentation of 50%-ethanol mixture in the upper pole branches (white arrows) versus the cohesiveness of the 25%-ethanol mixture column in the lower pole branches (black arrow), which appears continuous. B Coronal CT with MPR reconstruction. Note the fragmentation and lack of continuity of 50%-ethanol mixture in the upper pole vessels (white arrow). The distance between the cortex and the nearest embolized artery was 4.1 mm

**4.6. Discussion**

Mixing ethanol and Onyx is technically feasible and provides good visibility under fluoroscopy and preserves the radiopacity and cohesiveness of the 25%-ethanol mixture in both in vivo and in vitro settings. The occlusive properties of the 25%-ethanol mixture were rated as good under high pressure in vitro.

Onyx and the 25%-ethanol mixture immediately occluded the tubular structure up to the maximal pressure tested (200 mmHg) (Figure 4.3B); in contrast, the 50%-ethanol mixture did not occlude the tubular structure and migrated in the tube as the fluid pressure was increased. In vivo, the 50%-ethanol mixture showed a lack of cohesiveness although radiopacity remained acceptable. Fragmentation and proximal occlusion were noted with decreased penetration.

The penetration depth of the 50%-ethanol mixture was higher than that of Onyx alone, probably due to its lower viscosity, as shown by the easier injection through the microcatheter

(less applied force was needed). Mixing 25% absolute ethanol with 75% Onyx seems the most potentially useful dilution among those tested because the other dilutions lacked either cohesiveness (the 50%-ethanol mixture) or radiopacity (the 75%-ethanol mixture). However, a significant amount of ethanol appears to be released from the cast within 30 minutes of precipitation, resulting in cast shrinkage, which may require the volume of the embolizing agent to be increased to maintain cohesiveness. This might be interesting in clinical practice as delivering the released ethanol to the very distal vessels may help to prevent recanalization and therefore further improve the duration and efficacy of the occlusion.

### 4.7. Study Limitations

This preliminary study has many limitations. First, the number of animals tested was very small, and the various dilutions of the mixture were usually tested only once in vivo. No further histological analysis was conducted to confirm the penetration data and the potential sclerotic effect due to the ethanol component in the 25%-ethanol mixture. We believe that this effect would not be very significant considering the short time that elapsed between embolization and animal kill. This study was a preliminary study that was designed only to examine the feasibility and as a proof-of-concept. Only Onyx 18 was tested; other commercially available concentrations (Onyx 34 and 20) were not tested. The target arteries in the study were only normal vessels. However, we think that these data are sufficient to suggest that these different well-known embolic and sclerotic agents can be combined. Further studies are needed to confirm the effect of different mixture dilutions on embolization efficacy and endothelial recanalization. Questions remaining to be addressed involve the chemical changes of the mixtures and its biocompatibility, systemic migration and wash-out of ethanol during injection and after solidification as well as a comparison of the local inflammatory and sclerotic response with those of Onyx.

### 4.8. Potential Clinical Impact

This study represents an initial experience with a new sclero-embolic agent that could be interesting for the endovascular management of various vascular anomalies with the advantages of deep penetration, controlled injection, safe and localized delivery of reduced amount of alcohol to the target and good visibility under fluoroscopy. Further investigation is needed to better understand the chemical changes of the mixture, the behavior of ethanol in the suspension and its effect on tissues compared to Onyx diluted simply with an equivalent amount of DMSO. Studies on other commercially available concentrations of Onyx (Onyx 20 and 34) would certainly be interesting.

### 4.9. Compliance with Ethical Standards

Conflict of interest Gilles Soulez: Dr. Soulez reports grants from Cook Medical, grants from Biotronik Medical, from Siemens Medical, outside the submitted work; in addition, Dr. Soulez has a patent null licensed to Cook Medical.

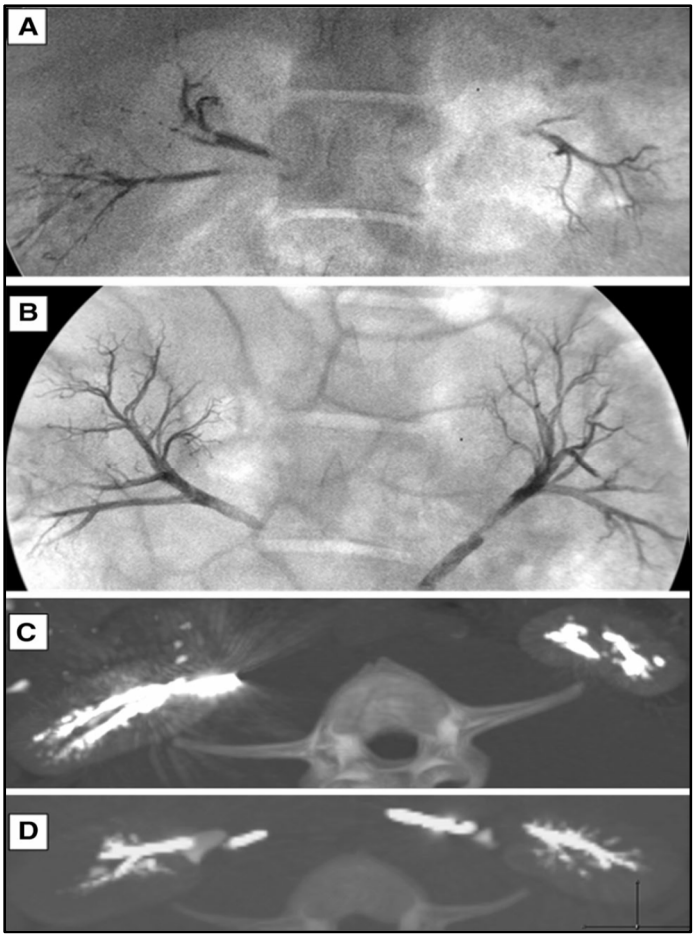


Figure 4.6 Characteristics of the different mixtures compared to those of Onyx 18. A Fluoroscopic image of both kidneys showing Onyx 18 in the left lower pole, 75%-ethanol mixture in the left upper pole, 50%-ethanol mixture in the right upper pole and 25%-ethanol mixture in the right lower pole. B Swine 2: Fluoroscopic image of both kidneys: Onyx 18 in the right renal artery and 25%-ethanol mixture in the left renal artery. The 25%-ethanol mixture also shows good radiopacity and preserved cohesiveness in both swine. C Oblique axial CT image with MIP reconstruction for swine 1 at the lower pole of the kidneys, showing distal penetration of the 25%-ethanol mixture in the right inferior polar branches compared to Onyx 18 on the left side. D Oblique axial CT image with MIP reconstruction for swine 2; this image confirms the better penetration of the 25%-ethanol mixture on the left side than that of Onyx 18 on the right side

# CHAPTER 5

# CHITOSAN-DOXYCYCLINE HYDROGEL: AN MMP INHIBITOR / SCLEROSING EMBOLIZING AGENT AS A NEW APPROACH TO ENDOLEAK PREVENTION AND TREATMENT AFTER ENDOVASCULAR ANEURYSM REPAIR

Fatemeh Zehtabi [a,b], Pompilia Ispas-Szabo [c], Djahida Djerir [c], Lojan Sivakumaran [a,d], Borhane Annabi [c], Gilles Soulez [a,d], Mircea Alexandru Mateescu [c], Sophie Lerouge [a,b,d,*]

[a] CHUM Research Center (CRCHUM), 900 St Denis, Tour Viger, Montréal, QC H2X 0A9, Canada
[b] Department of Mechanical Engineering, École de technologie supérieure, 1100, rue Notre-Dame Ouest, Montreal, QC H3C 1K3, Canada
[c] Department of Chemistry and Pharmaqam Center, Université du Québec à Montréal, C. P. 8888, Branch A, Montreal, QC, Canada
[d] Department of Radiology, Université de Montréal, 2900 Edouard-Montpetit Blvd, Montreal, QC H3T 1J4, Canada
* Corresponding author at: Laboratory of Endovascular Biomaterials, CHUM research center, 900 St Denis, Tour Viger, Montreal, QC H2X 0A9, Canada.

This article has been published in "Acta Biomaterialia 64 (2017) 94-105"

## 5.1. Context

The aim of this third article, published in 2017 in the Acta Biomaterialia journal (Volume 64, Pages 94-105)(Zehtabi, Ispas-Szabo, et al., 2017), is to respond to the 3rd specific objective of this doctorate: to develop an injectable radiopaque MMP inhibitor/sclerosing embolizing agent by integration of doxycycline (DOX), a well-known sclerosing and MMP inhibitor agent, into a chitosan-based matrix for the treatment of AAAs. The majority of this work has been done by F. Zehtabi (design, performance and realization of experiments, treatment of results, preparation of figures and manuscript). Work on this article was presented at Journée académique du département radiologie (2016 & 2017) and 10th world biomaterials congress (WBC2016).

## 5.2. Abstract

The success of endovascular repair of AAAs remains limited due to the development of endoleaks. Sac embolization has been proposed to manage endoleaks, but current embolizing materials are associated with frequent recurrence. An injectable agent that combines vascular

occlusion and sclerosing properties has demonstrated promise for the treatment of endoleaks. Moreover, the inhibition of aneurysmal wall degradation via matrix metalloproteinases (MMPs) may further prevent aneurysm progression. Thus, an embolization agent that promotes occlusion, MMP inhibition and endothelial ablation was hypothesized to provide a multi-faceted approach for endoleak treatment.

In this study, an injectable, occlusive chitosan (CH) hydrogel containing doxycycline (DOX)—a sclerosant and MMP inhibitor—was developed. Several CH-DOX hydrogel formulations were characterized for their mechanical and sclerosing properties, injectability, DOX release rate, and MMP inhibition. An optimized formulation was assessed for its short-term ability to occlude blood vessels *in vivo*.

All formulations were injectable and gelled rapidly at body temperature. Only hydrogels prepared with 0.075 M sodium bicarbonate and 0.08 M phosphate buffer as the gelling agent presented sufficient mechanical properties to immediately impede physiological flow. DOX release from this gel was in a two-stage pattern: a burst release followed by a slow continuous release. Released DOX was bioactive and able to inhibit MMP-2 activity in human glioblastoma cells. Preliminary *in vivo* testing in pig renal arteries showed immediate and delayed embolization success of 96% and 86%, respectively. Altogether, CH-DOX hydrogels appear to be promising new multifunctional embolic agents for the treatment of endoleaks.

### 5.3. Statement of Significance

An injectable embolizing chitosan hydrogel releasing doxycycline (DOX) was developed as the first multifaceted approach for the occlusion of blood vessels. It combines occlusive properties with DOX sclerosing and MMP inhibition properties, respectively known to prevent recanalization process and to counteract the underlying pathophysiology of vessel wall degradation and aneurysm progression. After drug release, the biocompatible scaffold can be invaded by cells and slowly degrade.

Local DOX delivery requires lower drug amount and decreases risks of side effects compared to systemic administration.

This new gel could be used for the prevention or treatment of endoleaks after endovascular aneurysm repair, but also for the embolization of other blood vessels such as venous or vascular malformations.

## 5.4.Introduction

Abdominal aortic aneurysms (AAAs) are abnormal dilatations of the abdominal aorta that may result in fatal rupture. They are one of the most significant causes of morbidity and mortality in the elderly (Ahmed et al., 2016). Current recommendations suggest that patients with AAAs greater than ≥5.5 cm undergo treatment via open surgery or its minimally invasive alternative, endovascular aneurysm repair (EVAR). In EVAR, a stent-graft is deployed into the aorta transarterially to exclude blood flow from the aneurysmal sac (Fatimi et al., 2012). While associated with an increase in initial survival (Siracuse et al., 2016b), the long-term success of EVAR remains limited in part due to the development of endoleaks. Endoleaks are characterized by the persistent perfusion of the aneurysm sac outside of the stent-graft. They may attain pressures comparable to those found in the systemic circulation and are associated with adverse outcomes (Fatimi et al., 2012).

Transarterial or translumbar needle embolization is recommended for the treatment of expanding endoleaks, especially type II endoleaks (Stavropoulos et al., 2009). However, current embolic agents are associated with high rates of recurrence (Martin et al., 2001; Stavropoulos, Kim, et al., 2005). Recent studies have suggested that the endothelial layer plays a major role in the development and persistence of endoleaks; in animal models, aneurysms that were mechanically denuded of their endothelium showed a decrease in the persistence of endoleaks (Soulez et al., 2008). Furthermore, the underlying pathophysiology of aneurysm progression—which has been linked to persistent, localized inflammation associated with excessive activity of matrix metalloproteinases (MMPs) resulting in the progressive vessel wall destruction (Baxter et al., 2016)—has yet to be addressed. Therefore, we hypothesized that an embolization agent that occludes the endoleak, inhibits MMP and promotes endothelial sclerosis would provide a multi-faceted approach for endoleak prevention and treatment.

The aim of the present study was to develop an injectable and radiopaque chitosan-based embolization agent containing doxycycline (DOX) as an adjunct to EVAR for the treatment of AAAs. DOX is one of the most investigated medications in the management of AAAs. When injected locally, DOX causes irreversible endothelial injury promoting thrombosis and occlusion (Albanese et al., 2010). It is also an MMP inhibitor that limits AAA growth by inhibiting extracellular matrix (ECM) remodelling and localized inflammation (Kroon et al., 2015). In patients with AAAs, systemic administration of DOX has been shown to decrease MMP activity at the site of the aneurysm, resulting in decreased AAA progression (R. W. Thompson et al., 1999). In a preclinical model, this effect was achieved with just local administration of DOX, which theoretically would mitigate concerns of systemic toxicity (Bartoli et al., 2006). We hypothesized that the administration of DOX in an occlusive embolic matrix would maximize localized DOX exposure and could act as an adjunct to EVAR to prevent aortic expansion and to prevent or treat endoleaks.

Chitosan-based hydrogels were selected as the embolic matrix since they are desirable for their biocompatibility, biodegradability, injectability at room temperature and adhesion properties (Kim et al., 2008; Wu et al., 2005). Also they and can rapidly undergoing sol-gel transition at body temperature (Ahmadi et al., 2015). They have been studied extensively for intravascular embolization (Fatimi et al., 2016; Wang et al., 2011). Furthermore, these gels can be prepared with commercial contrast agents to help monitor injection and migration under fluoroscopy (given that chitosan and doxycycline are not radiopaque) (Coutu et al., 2013).

We hypothesized that DOX could be integrated into chitosan hydrogels while maintaining injectability and favourable mechanical properties. We expected a two-stage release of DOX from the hydrogel, including an initial burst release—to promote sclerosis and initiate MMP inhibition—and a continuous release thereafter to sustain MMP inhibition.

## 5.5.Materials and methods

### 5.5.1. Preparation of hydrogels

*In situ* gelling hydrogels were prepared by mixing two solutions. Shrimp shell chitosan (CH) (Marinard Biotech, MW 250 kDa, DDA 94%) was first purified as previously published (Assaad et al., 2015). Solution A was prepared by dissolving the CH powder at 3.33% (w/v) in HCl (0.1M) solution with or without Visipaque 320® (VIS) contrast agent (GE Healthcare, Rahway, USA) at room temperature under constant magnetic stirring. It was sterilized by autoclave (AMSCO® Evolution® Steam Sterilizer, Oh, USA) at 121°C for 20 min and stored at 4°C until further use. Solution B contained the gelling agent with or without DOX sterilized by 0.2 µm filtration.

Several gelling agents were investigated to obtain a final gel with a rapid gelation rate and optimal mechanical properties, based on previous work (Assaad et al., 2015). Specifically, the initial G´ needed to be higher than 800 Pa upon injection to resist flow up to 200 mm Hg (Fatimi et al., 2016). Sodium bicarbonate $NaHCO_3$ (SHC) (MP Biomedicals, Solon, OH, USA) was mixed with phosphate buffer (PB) at pH 8, which was prepared by dissolving sodium phosphate monobasic (SPM) and sodium phosphate dibasic (SPD) salts in Milli-Q water at w/w ratio of 0.06. β-Glycerophosphate disodium salt pentahydrate (BGP) (Sigma Aldrich, Oakville, ON, Canada) was chosen as a control due to its favourable gelation kinetics. BGP solutions were prepared by dissolving the salt in Milli-Q water (Assaad et al., 2015). DOX was dissolved at different concentrations in the gelling agent solutions. To increase DOX stability, sodium thiosulfate as an antioxidant (1% w/v) and creatine as a stabilizer (1% w/v) were also added (Gilbard et al., 2012).

To form CH-DOX and CH hydrogels, solution A and B were loaded in separate syringes joined by a Luer lock connector and then mixed just prior to their use. The abbreviations, initial and final concentration of each compound in the gels are summarized in Table 5.1. In the first part of the manuscript, the names of the hydrogels indicate their final composition. For example, CH/SHC0.075PB0.08/VIS50/DOX0.1 represents a hydrogel containing 2% w/v CH, SHC0.075PB0.08M as gelling agent, 50% v/v radiopaque agent (VIS) and 0.1 w/v % DOX.

All hydrogels were prepared to reach a final concentration of 2% w/v CH. Starting from section 5.5.3, once the final gelling agent was selected, the name of gel was simplified to indicate only DOX concentration in the gel (CH-DOX0.1 for DOX 0.1%w/v).

### 5.5.2. Characterization of hydrogels as an embolic agent

The kinetics of gelation, occlusive properties and injectability of gels were evaluated. First, gelation kinetics and occlusive properties were used to select an optimal gelling agent based on previous work (Fatimi et al., 2016). Subsequently, the impact of adding VIS50% and different concentrations of DOX on these parameters was reassessed to ensure favourable mechanical properties.

#### *5.5.2.1.* Rheology

Rheological properties were studied using the Physica MCR 301 rheometer (Anton Paar; Saint-Laurent, QC, Canada) with co-axial cylinder geometry. Time sweep experiment was performed in the linear viscoelastic region (frequency (1 Hz), strain (1%)). The evolution of the storage (G´) and loss (G´´) moduli as a function of time at body temperature (37 °C) was determined.

#### *5.5.2.2.* Occlusive properties

The effectiveness of the gels in occluding blood flow after different gelation times (2 and 7 min) was tested using an *in vitro* bench test previously developed (Fatimi et al., 2016). In brief, a glycerol (40%v/v) and water (60%v/v) solution of viscosity similar to blood (5 cps) was pushed by a syringe pump towards a tube filled with the gel with increasing pressure (up to 200 mmHg) while possible leakage was monitored. Only gels that were able to immediately resist pressured flow were assessed in subsequent experiments.

#### *5.5.2.3.* Gel injectability

Gel injectability by microcatheter (FasT-325, Boston Scientific; internal diameter of 0.61 mm (0.024 inch); length of 140 cm) (Coutu et al., 2013) was verified by measuring the maximal

force needed to eject CH gels after different gelation times (t = 0 and 5 min) at 37°C. The force was measured using an ElectroForce® 3200 Test Instrument (TA Instrument; 225 N load cell).

Table 5.1 Initial and final concentrations (in the syringe and in the gel respectively) of each component and pH of the various hydrogels tested.

| Gel name | Chitosan (%w/v) | | VIS (% v/v) | | DOX (% w/v) | | Gelling agent Concentration (M) | Hydro gel pH |
|---|---|---|---|---|---|---|---|---|
| | *Initial* | *Final* | *Initial* | *Final* | *Initial* | *Final* | *Final* | *Final* |
| CH/BGP0.4 | 3.33 | 2 | 0 | 0 | 0 | 0 | BGP : 0.4<br>SHC:0.075 | 7.2 |
| CH/SHC0.075PB0.04 | 3.33 | 2 | 0 | 0 | 0 | 0 | PB: 0.04<br>SHC:0.075 | 7.2 |
| CH/SHC0.075PB0.08 | 3.33 | 2 | 0 | 0 | 0 | 0 | PB: 0.08<br>SHC:0.075 | 7.2 |
| CH/SHC0.075PB0.08/VIS50 | 3.33 | 2 | 83.3 | 50 | 0 | 0 | PB: 0.08<br>SHC:0.075 | 7.2 |
| CH/SHC0.075PB0.08/VIS50/DOX0.1 | 3.33 | 2 | 83.3 | 50 | 0.25 | 0.1 | PB: 0.08<br>SHC:0.075 | 7.1 |
| CH/SHC0.075PB0.08/VIS50/DOX0.3 | 3.33 | 2 | 83.3 | 50 | 0.75 | 0.3 | PB: 0.08<br>SHC:0.075 | 7.0 |
| CH/SHC0.075PB0.08/VIS50/DOX1 | 3.33 | 2 | 83.3 | 50 | 2.5 | 1 | PB: 0.08 | 7.0 |

### 5.5.3. DOX cytotoxic dose-response on endothelial cells

DOX cytotoxic dose-response was studied on human umbilical vascular endothelial cells (HUVECs) (Lonza, CC-2519, ON, Canada). HUVECs were cultivated in flasks coated with 1% gelatin in EGM-2 bullet kit (Lonza, CC-3156, ON, Canada) and used between passages 3 and 5. The HUVECs (9000 cells/well) were then seeded in 96-well plates and cultured until 80% confluence in culture medium containing 1% penicillin and streptomycin (Wisent, 450-204-EL, QC, Canada). The cells were then exposed to different concentrations of DOX from 0 to 0.75% (w/v) for 24 h. Fresh culture medium was used as a negative control while culture medium supplemented with 10% (v/v) dimethyl sulfoxide solution (DMSO) was used as

positive control. Cell viability was evaluated via cell metabolic activity assayed using 10% AlamarBlue (Cedarlane Corp., Burlington, ON, Canada) with fluorescence measurements (Ex 560 nm/Em 590 nm).

### 5.5.4. *Ex vivo* de-endothelialization

The ability of prepared hydrogels containing different DOX concentrations to remove endothelial lining was evaluated *ex vivo* using the aortas of dogs sacrificed in the framework of other experiments. Aortic segments were harvested, rinsed and sutured at one end and then were embolized by gel containing 0, 0.1, 0.3 or 1% w/v DOX; one aorta was kept as control. Embolized tissues and the control were incubated at 37 °C with 5% $CO_2$ for 3 h in RPMI 1640 (25.03 mM Hepes and 2.05 mM L-glutamine) supplemented with 20% FBS, 100 U $mL^{-1}$ penicillin, 100 $mgmL^{-1}$ streptavidin, and 2.5 $mgmL^{-1}$ gentamicin. Arteries were fixed in buffered formalin and embedded with paraffin. Histological analysis was performed to detect vessel wall damage; factor VIII staining was used to detect the presence of endothelial cells.

### 5.5.5. Indirect cytotoxicity tests

Indirect cytotoxicity tests were performed on gel extracts obtained after incubation of the gel in culture media at different timepoints (1, 2, 3 and 7 days) following ISO 10993-5:2001 standards. They aimed to confirm the desirable toxicity of extracts due to large DOX release within the first 24 h (sclerosing effect), but also the absence of gel toxicity once DOX and radiopaque agent are mostly released (next extracts). To prepare hydrogel extracts, samples (1 mL each, n = 3) were left to gel in a 12-well plate for 3 h at 37 °C in an incubator, and then 3 mL of culture medium were added on the top of each hydrogel. At days 1, 2, 3 and 6 the medium was recovered and replaced by a fresh medium. Extracts were frozen at -20°C until the assay. L929 fibroblast cells (ATCC, Manassas, VA, USA) were seeded in 96-well plates (10000 cells/well) and cultured until 90% confluence in Dulbecco's Modified Eagle's Medium (Gibco BRL, Invitrogen, Grand Island, NY, USA) supplemented with 10% fetal bovin serum (FBS; Medicor, Montreal, QC, Canada). The culture medium was then removed and replaced with medium containing the extract. After 24 h, the viability of the cells was estimated by

measuring their metabolic activity using AlamarBlue compared to that of negative and positive controls (media without extract and media with 10% DMSO, respectively).

### 5.5.6. In vitro drug release and swelling studies

Drug release rate was studied using an USP Dissolution Apparatus I (Distek 3200). CH-DOX 0.1 gels (3 mL) were prepared (Section 5.5.1), allowed to gel for 5 min and then placed in the basket of the apparatus and submerged in PBS at 37 °C. DOX liberation was monitored over 1 week with constant stirring at 30 rpm. Aliquots of sample were withdrawn at different time intervals and analyzed by spectrophotometry at 390 nm. The amount of released DOX at each time point was determined by using a calibration curve obtained in the range of 0–50 µg/mL.

The drug release kinetics was quantified using Korsemeyer-Peppas formula:

$$M_t/M_\infty = kt^n$$

where $Mt/M_\infty$ is the amount of drug released at t time, k is a constant including structural and geometrical characteristic of the dosage form, and n is the diffusion exponent indicative of the release mechanism (Peppas, Huang, et al., 2000).

Swelling behaviour of the hydrogels was also investigated, by following the weight of samples immersed in PBS at 37 °C over 7 days (Peppas, Huang, et al., 2000). Samples (2 mL) were first left to gel in a cylindrical holder for 24 h. Then the slabs were placed in similar conditions as those used for drug release tests (baskets of USP apparatus I, in PBS medium at 37 °C and 30 rpm). Samples were removed at predetermined time points, weighted after removal of the superficial liquid and reported as a function of the initial mass:

$$Q = (W_0 - W_t) / W_t \times 100$$

Where $W_0$ and $W_t$ are the sample weights at time 0 and time t, respectively.

### 5.5.7. MMP inhibition

The bioactivity of DOX released from the CH-DOX hydrogels was assessed in terms of its ability to inhibit MMP-2 secreted from human U-87 glioblastoma cells (U-87MG). MMP-2 inhibition was assessed at different time points and compared to the bioactivity of DOX solutions with known concentrations. U-87MG cells (ATCC, Manassas, VA) were cultivated ($2.5 \times 10^5$ cells/well) in 6-well plates in Eagle's minimum essential Medium containing 10% (v/v) calf serum (HyClone Laboratories, Logan, UT), 1 mM sodium pyruvate, 2 mM glutamine, 100 units/mL penicillin and 100 mg/mL streptomycin. After two days incubation at 37 °C with 5% $CO_2$, tissue culture plate inserts (VWR®, Radnor, PA) were used to submerge the hydrogel in the media without directly contacting cells. To determine whether DOX remained bioactive for several days in the gel, these hydrogels were placed in the wells either immediately after gelation or after pre-incubation in culture media for one or three days. The cells were then incubated for 24 h in the presence of the hydrogel, before performing viability and gelatin zymography tests. In parallel, the concentration of DOX released in the media at each time point was estimated based on DOX release in PBS in similar conditions, as measured by spectrometry.

Gelatin zymography was used to assess the extent of MMP-2 gelatinolytic activity and activation status as previously described (Sina et al., 2010). Briefly, an aliquot (20 µL) of the culture medium was subjected to SDS-PAGE in a gel containing 0.1 mg/mL gelatin, a substrate that is efficiently hydrolyzed by proMMP-2 and MMP-2. The gels were then incubated in 2.5% Triton X-100 and rinsed in nanopure distilled $H_2O$. Gels were further incubated at 37 °C for 20 h in 20 mM NaCl, 5 mM CaCl2, 0.02% Brij-35, 50 mM Tris-HCl buffer, pH 7.6, then stained with 0.1% Coomassie Brilliant blue R-250 and destained in 10% acetic acid, 30% methanol in $H_2O$. Gelatinolytic activity was detected as unstained bands on a blue background.

### 5.5.8. Structural and morphological analyses

SEM and FTIR were performed on the final CH-DOX solution.

#### 5.5.8.1. Scanning electron microscope (SEM)

Samples were left for 24 h of gelation at 37 °C then vacuum freeze dried. Slices of each sample were cut using a surgical blade and sputter-coated with a thin gold layer. The morphology of the samples was examined using a Hitachi 3.0 kV scanning electron microscope (S-4300SE/N) under vacuum (Hitachi High Technologies America, Pleasanton, CA, USA).

#### 5.5.8.2. Fourier transform infrared spectroscopy (FTIR)

Potential interactions between CH gels and DOX were evaluated by comparing the FTIR spectra of CH, DOX and a mixture of CH and DOX (all as dry powders) with spectra obtained from lyophilized CH and CH-DOX gels (left to gel for 48 h). The FTIR spectra of all samples were recorded (32 scans at a resolution of 4 $cm^{-1}$) using a Thermo-Nicolet 6700 (Madison, WI, USA) FTIR spectrometer equipped with a deuterated triglycine sulfate-KBr (DTGS-KBr) detector and a diamond smart attenuated total reflection platform. Data were analyzed with Omnic software.

### 5.5.9. *In vivo* assays

The feasibility of using CH/SHC0.075PB0.08/VIS50/DOX0.1 gel selected as an embolic agent was assessed during a short-term preliminary *in vivo* study on six pigs planned for sacrifice in the framework of another experimental protocol. The animals did not undergo aneurysm surgery or EVAR. Bilateral embolization of the caudal branch of the renal artery was performed to determine whether the agent could promote an embolization of a complete arterial territory including the parent artery and its branch divisions. The renal physiology and cardiovascular anatomy of pigs are quite similar to human physiology. We chose this acute model of renal artery embolization in a cohort of pigs already enrolled for a terminal experimentation to minimize the number of animals involved and associated costs. The procedures were approved by the CHUM institutional animal care committee (CIPA).

The animals were placed under general anesthesia and intubated for the duration of the procedure. Following a femoral artery access, either the right or left renal artery was selectively catheterized with a 5 French cobra catheter (Terumo, Tolyo, Japan) and a hyperselective

catheterization of the caudal segmental artery was performed with a co-axial microcatheter (FasT-325, Boston Scientific). Contrast material was injected and digital subtraction angiograms (DSAs) were taken. Subsequently, approximately 5 mL of gel was injected under fluoroscopic guidance until satisfactory occlusion up to the tip of the microcatheter. Immediate and delayed successes were evaluated by DSAs taken immediately and 10–20 min post-embolization respectively, to detect possible rapid reopening of the occluded arterial territory. The procedure was repeated for the contralateral caudal renal artery.

A semi-quantitative method was employed to assess the occlusion of distal branches (modified from (Maeda et al., 2013). In this method, the downstream divisions of the caudal branch were classified from D1-D3 (Figure 5.1), where D1 referred to the immediate and largest branches of the caudal artery, following subsequent branches from this artery were labelled D2, and further branches were labelled as D3. After D3, the resolution of the arteries was too variable to be assessed systematically, thus this was the most distal division assessed. It should be noted that the diameter of the branches and their presumed location in 3-D space were also taken into consideration to determine whether a branch was D1, D2 or D3; thus, a major branch (e.g. D2) could give off multiple D3 branches before finally bifurcating into terminal D3 branches. All pre-embolization angiograms were coded for the number of divisions presents (Figure 5.1); subsequently, the immediate and delayed post-embolization angiograms were coded similarly for visible branches. Embolization success was calculated as:

$$\text{Percentage occlusion} = 100\% \times (!!!\ \text{INVALID CITATION}\ !!!)$$

Percentage occlusion was calculated for each division level as well as globally.
A few hours after in vivo embolization, animals were euthanized. Histological analysis of embolized kidneys was performed. Factor VIII staining was used to detect possible damage to endothelium.

### 5.5.10. Statistical analysis

Results are presented as the mean ± standard deviation (SD) except where otherwise indicated. One-way or two-way ANOVA with Tukey's multiple comparison tests were performed as

appropriate. Statistical significance was defined as $p < 0.05$. Statistical analysis was performed using GraphPad Prism 7.0.

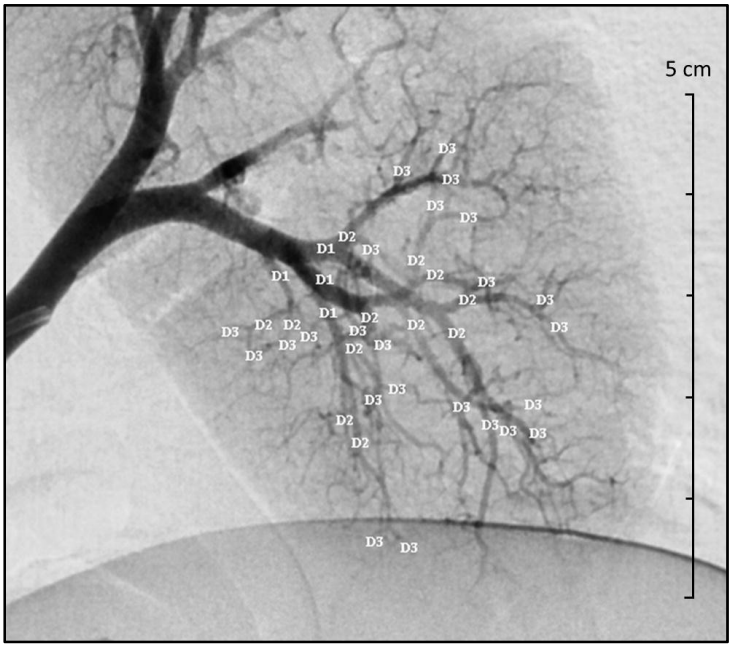


Figure 5.1 Division system method: D1 referred to the immediate and largest branches of the caudal artery; subsequent branches from this artery were labelled D2, and further branches were labelled as D3

## 5.6. Results

### 5.6.1. Hydrogel rheological and in vitro occlusive properties

A single gelling agent formulation was selected based on rheology and *in vitro* embolization results in order to create a hydrogel which gels rapidly and is occlusive. Figure 5.2 presents the evolution of the storage modulus G´ (indicative of elastic properties) with time of CH hydrogels mixed with the three different gelling agents at 37 °C. While all gels reached G´ values higher than 2000 Pa after 1 h, gels with SHC0.075PB0.08M had the highest initial mechanical properties ($G'_0$= 2233 ± 202) at 37 °C. This was also the only formulation to be able to immediately resist flow against the mixture of glycerol and water during in vitro embolization tests (Figure 5.3). Gels prepared with BGP0.4M and SHC0.075PB0.04M were able to withstand the pressurized flow, but only after 7 min of gelation.

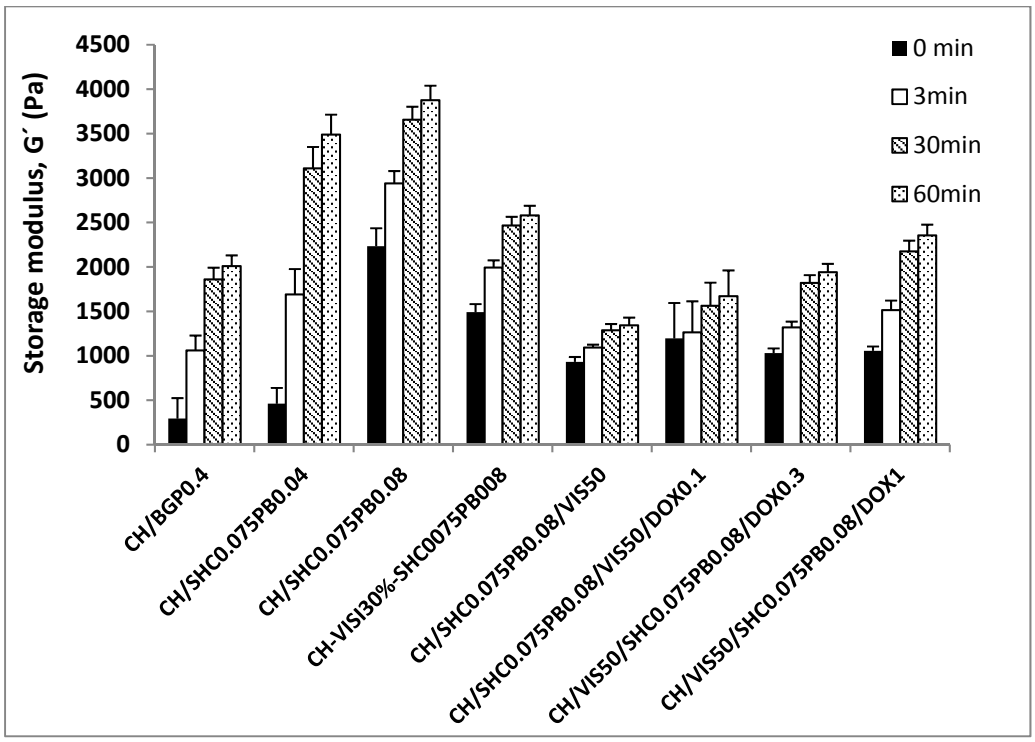


Figure 5.2 Evolution of the storage modulus (G´) at 37 °C as a function of time for chitosan hydrogels prepared with different gelling agents (BGP04M, SHC0.075PB0.04M and SHC0.075PB0.08M), as well as SHC0.075PB0.08M chitosan gels containing VIS (50% v/v) and DOX (0.1%, 0.3% and 1% w/v)

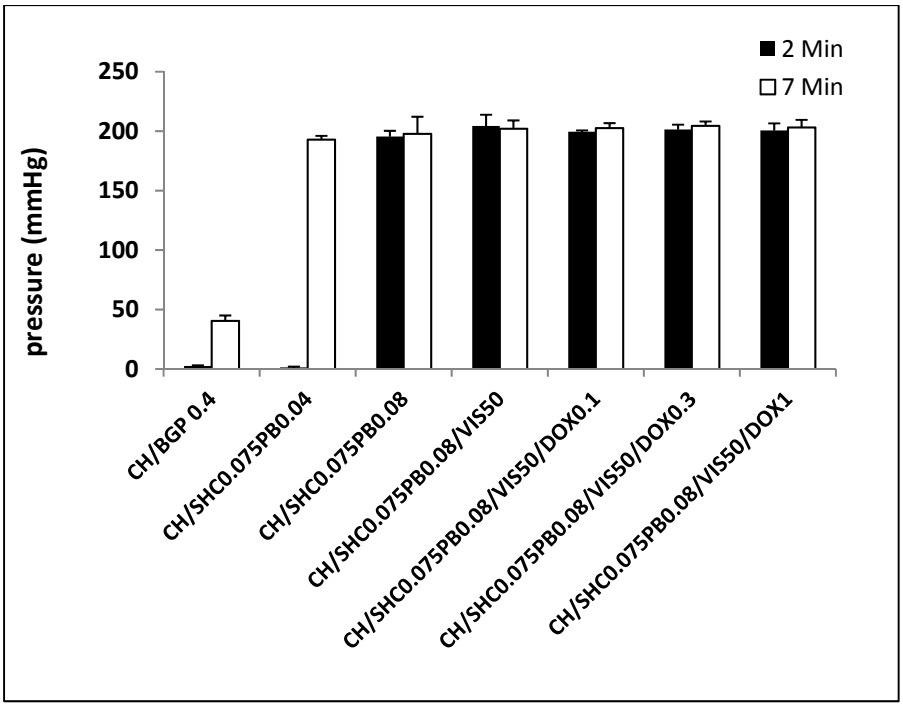


Figure 5.3 Maximum liquid pressure sustained by chitosan hydrogels prepared with different gelling agents (BGP04M, SHC0.075PB0.04M and SHC0.075PB0.08 M), as well as SHC0.075PB0.08 chitosan gels with VIS (50% v/v) and DOX (0.1%, 0.3% and 1% w/v). The maximum pressure reached by the bench test was 200 mmHg.

Therefore, only gels made with SHC0.075PB0.08M as gelling agent were kept for further tests.

The addition of VIS (50% v/v) and DOX delayed the kinetics of gelation, but the initial G' values remained above the 800 Pa threshold previously identified (Fatimi et al., 2016) (Figure 5.2). The gels were also immediately able to resist flow up to 200 mmHg in the *in vitro* embolization test (Figure 5.3). While the rheological properties of the gel rapidly increased at body temperature, they remained low and stable at room temperature (22 °C) (data not shown).

The hydrogel was injectable through a 0.61 mm diameter catheter. The force required to inject the gel immediately after mixing the components (23.4 ± 0.5N) was also only slightly increased (27.1 ± 2.2N) when waiting for up to 5 min before injection. These values were still largely

below the maximal force that could be applied by hand by clinicians on a 1 mL syringe, as tested by an experienced interventional radiologist.

### 5.6.2. DOX effect on endothelial cell viability

HUVECs were incubated with varied concentrations of DOX solution for 24 h. Cells showed a substantial decrease in viability when exposed to DOX concentrations above 0.5 mg/mL ($LD_{50\%} \approx 0.8$ mg/mL) (Figure 5.4a). Factor VIII staining on *ex vivo* embolized arteries demonstrated the removal of the endothelial layer by DOX (Figure 5.4b). While injection of CH gel only slightly affected the endothelial cells layer (Figure 5.4b (II)), all tested CH-DOX gels effectively removed the endothelial layer (Figure 5.4b (III-V)).

### 5.6.3. Indirect cytotoxicity of CH hydrogels

The incubation of L929 fibroblast cells with the hydrogel extracts showed significant cytotoxic effect of the first extract (retrieved after the first 24 h incubation) for all the hydrogels containing DOX.

However, extracts from the subsequent incubations (48 h, 72 h and 1 week) showed more than 85% of viability except CH-DOX0.3, which resulted in 75% of viability at 48 h (Figure 5.5).

### 5.6.4. DOX in vitro release rate and hydrogels swelling

DOX release from CH-DOX 0.1 and CH-DOX 1 gels exhibited a two-stage profile, with a rapid burst release observed within the first 24 h, followed by slow and continuous release for up for the next 168 h (Figure 5.8a). The kinetic parameters calculated from Eq. (1) were n = 0.89 (k = 4.5) for CH-DOX 1 and n = 0.96 (k = 1.81) for CH-DOX0.1 indicating a controlled drug release close to zero order. Swelling studies (Figure 5.8b) showed that weight decrease once the gel was immersed in PBS, with the decrease being slower for CH-DOX compared to CH gel.

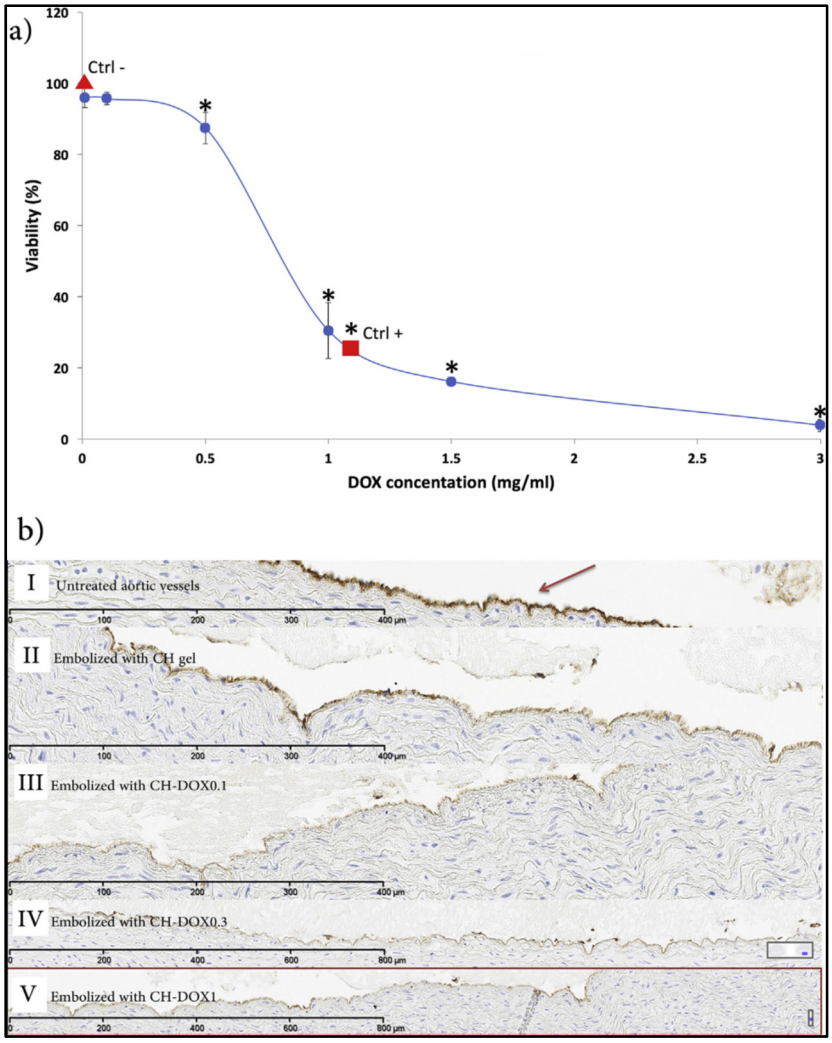


Figure 5.4 a) Dose response of DOX on HUVECs showing LD50% around 0.8 mg/mL in media solution. Data were normalized according to the AlamarBlue fluorescence signal of the negative control. Four samples were tested for each condition and the experiment was done in triplicate. Data are shown as mean ± SD. * $p < 0.05$ compared to negative control. b) Factor VIII immunostaining of aortic vessels: (I) untreated or embolized ex vivo with (II) CH gel; (III) CH-DOX0.1 gel; (IV) CH-DOX0.3 gel; (V) CH-DOX1 gel. Endothelial cells (Arrow, brown staining) are present at the lumen of untreated artery and still partially present after embolization by CH gel, but absent after embolization with DOX-containing CH gels. Embolization with each formulation was performed in triplicate

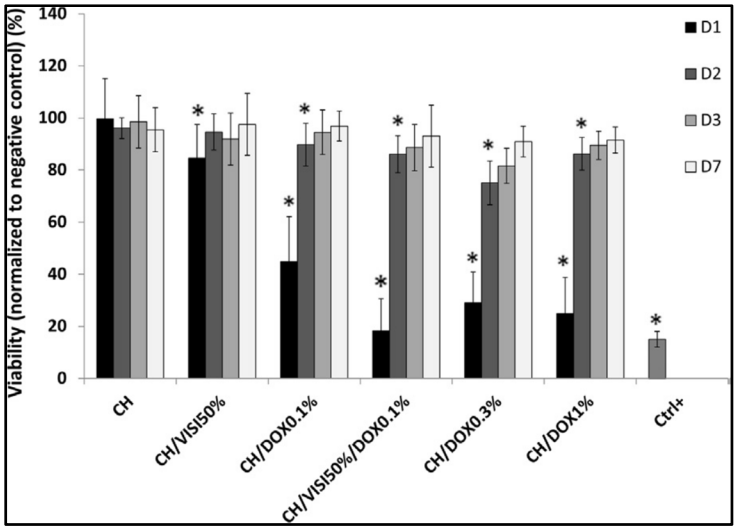


Figure 5.5 Viability of L929 fibroblasts exposed to extracts recovered at days 1, 2, 3 and 7 during incubation with various CH hydrogels (n = 18, mean ± SD). (Ctrl- = cells in medium culture, Ctrl+ = cells exposed to 10% DMSO). Data are shown as mean ± SD. * $p < 0.05$ compared to control

### 5.6.5. MMP inhibition

Figure 5.9a shows the reduction of MMP-2 gelatinolytic activity of U-87 cells after 24 h of contact with DOX—either when directly added into solution (triangles, dotted line) or when released from the CH-DOX gels (squares, continuous line)—as a function of DOX concentration. In both cases, there was a concentration dependent inhibition of MMP. The half maximal inhibitory concentrations (IC50) were estimated to be 0.01 mg/mL and 0.03 mg/mL for the DOX solutions and the DOX extracts of the gels, respectively. The MMP inhibition by gels containing different concentrations of DOX—that were pre-incubated for 1 or 3 days—is displayed in Figure 5.9b. Gelatin zymography images are added to the Supplementary Results section (Figure 5.6). All concentrations of DOX significantly reduced MMP activity compared to control ($p < 0.05$). These results confirmed that encapsulation of DOX within a CH gel does not alter its bioactivity and that DOX remains bioactive in the gel for at least 4 days.

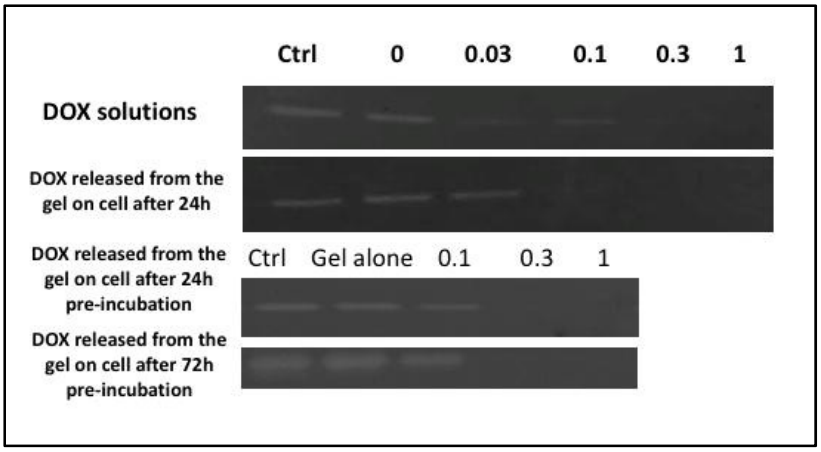


Figure 5.6 Gelatin zymogram showing the MMP inhibition by gels containing different concentrations of DOX—that were in solutions, released from the gel for 24h and pre-incubated for 1 or 3 days respectively

### 5.6.6. FTIR and SEM

Chitosan powder had a characteristic band at 1150 $cm^{-1}$ for C-N stretching of the amine group. DOX powder had a peak at 1661 $cm^{-1}$ characteristic of a C=O amide and at 1604 $cm^{-1}$ characteristic of a ketone C@O stretch. DOX also had two peaks at 1574 $cm^{-1}$ and 1556 $cm^{-1}$ (Tamimi et al., 2008) characteristic of NAH bending of the amide groups; these were well distinguished in the spectrum of the powder mixture. The FTIR spectrum of the lyophilized CH-DOX gel was different to that of the physical mixture of their powders. The band shifted from 1661 $cm^{-1}$ to 1691 $cm^{-1}$ and the bands at 1556 $cm^{-1}$ and 1574 $cm^{-1}$ were no longer observed (Figure 5.7).

SEM of freeze-dried hydrogels confirmed the presence of a homogeneous porous three-dimensional structure. As shown in Figure 5.10 (a & b) the pore size was smaller for gel containing VIS and DOX compared to CH gels.

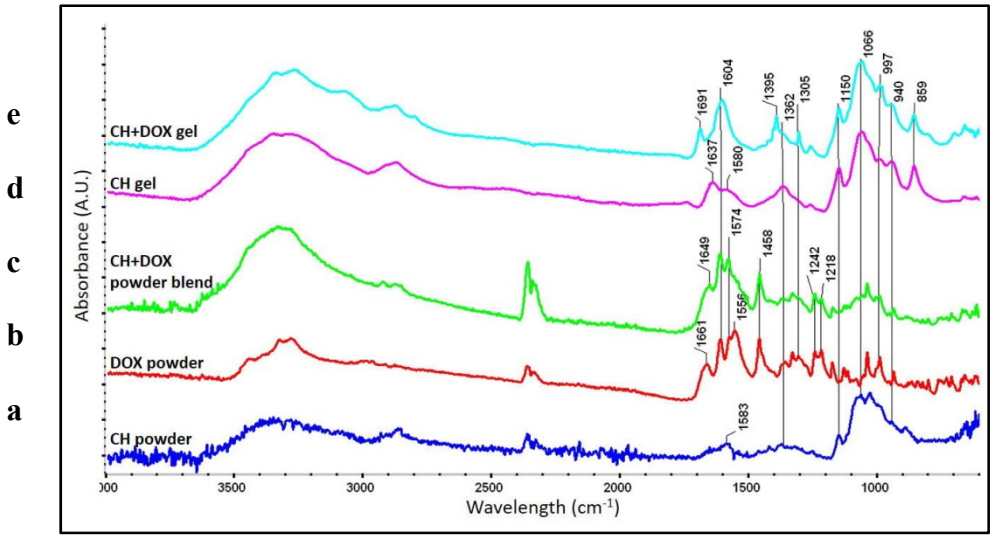


Figure 5.7 FT-IR spectra taken a) chitosan powder b) DOX powder c) physical mixture of CH and DOX d) lyophilized CH gels without DOX e) lyophilized CH-DOX gels

### 5.6.7. *In vivo* testing

Short term *in vivo* embolization of the renal porcine caudal polar artery with CH-DOX0.1 gels was successfully performed through the 0.61 mm internal diameter micro-catheter (Table 5.2). Figure 5.11a and b show digital subtraction angiography (DSA) images before and after complete embolization of the artery, respectively. This gel formulation (containing 50%v/v VIS) had good visibility during injection under fluoroscopy, as confirmed by a 25-year experienced interventional radiologist (Figure 5.11c). We did not observe any evidence of proximal or distal gel migration nor catheter gluing during and after embolization. The efficacy of embolization is summarized in Table 5.2 where the percentage of occluded vessels immediately and after a delay is indicated. Immediate success was excellent (96%), but it was reduced to 86% after 20 min. Histology of the embolized kidney confirmed that the gel was able to induce endothelial ablation (Figure 5.12b).

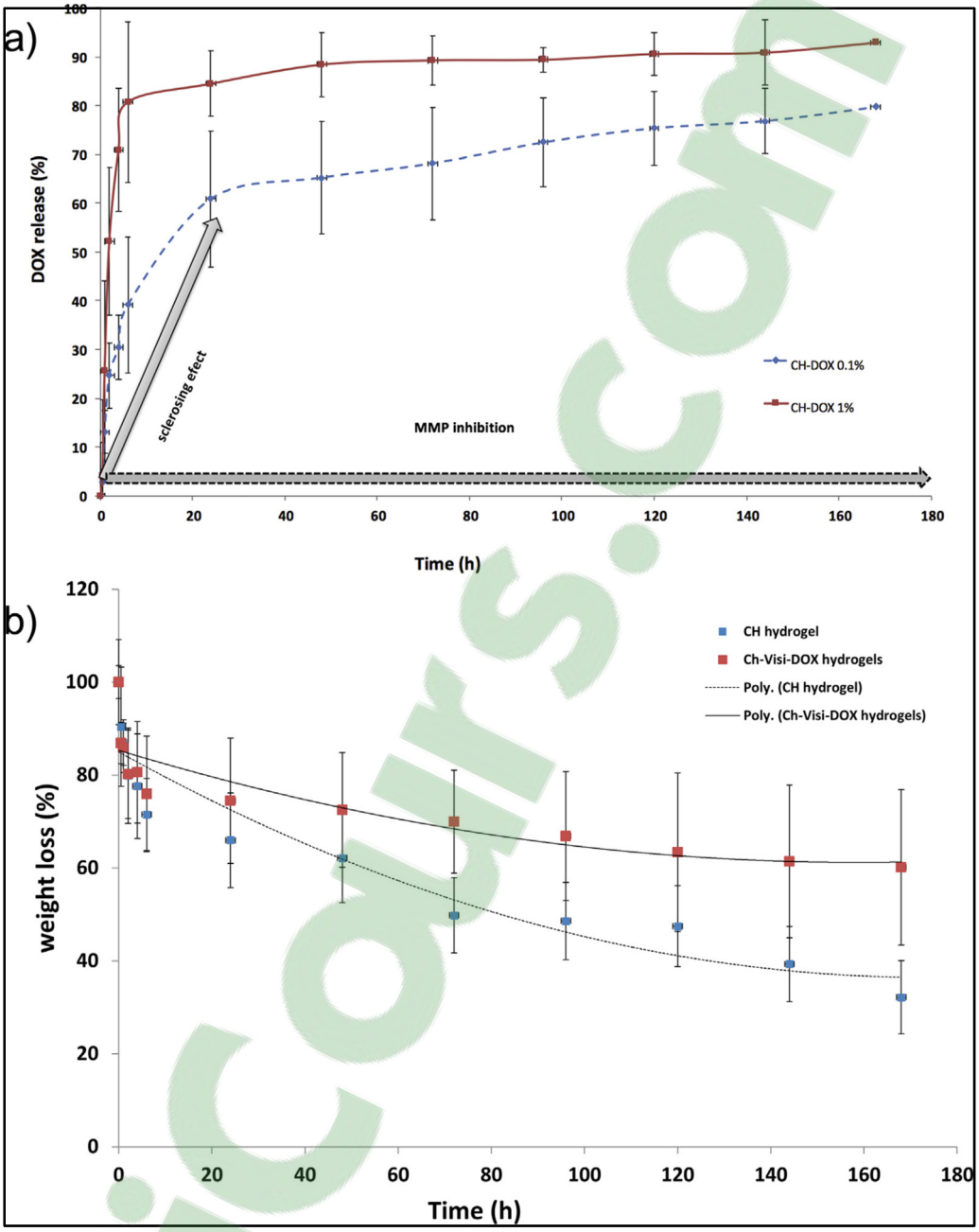


Figure 5.8 a) DOX release rate from CH-DOX0.1 and CH-DOX1 gels done by release test. Aliquots of sample were withdrawn at different time intervals (0.5,1,2,4,6,24,48,72,96,120,144, 168 h). b) Evaluation of swelling behaviour of the hydrogels in PBS at 37 ºC using weight loss measurements at equal time intervals to the release test. Poly (polynomial trendline) is a curved line that is used when data fluctuates

## 5.7. Discussion

In this study we developed an injectable, radiopaque CH hydrogel for DOX delivery. We hypothesized that the combination of the occlusive properties of CH hydrogels with the sclerosing and MMP inhibiting properties of DOX would create an embolic agent particularly well suited to manage endoleaks. To achieve this, we first optimized the mechanical properties of the CH hydrogel by mixing CH with different gelling agents (Assaad et al., 2015). We found that only gels prepared with SHC0.075PB0.08M offered sufficient initial mechanical properties suitable for embolization (Fatimi et al., 2016); thus, further experimentation was performed with this gelling agent only. Next, VIS was added to the hydrogel to confer radiopacity; the gel's mechanical properties remained adequate. Finally, DOX was added to the hydrogel to confer sclerosing and MMP-inhibiting properties.

DOX is a promising agent to prevent aneurysm progression and rupture. The pathophysiology of aneurysm progression is related to the degradation of the vascular wall by MMPs present within the inflammatory microenvironment (Annabi et al., 2002). Recent studies employing DOX have shown aneurysm suppression in experimental animal models and short term clinical trials (Hackmann et al.; Kroon et al., 2015; Prall et al., 2002; R. W. Thompson et al., 1999). The mechanism of DOX-mediated MMP inhibition is ascribed to its ability to competitively bind with zinc, which is a co-factor required for MMP function (Shanmuganathan et al., 2008). However, DOX may also prevent the progression of AAAs through other mechanisms. Indeed, AAAs could be considered an autoimmune condition given that AAA tissue shows clonal expansion of T cells (Lu et al., 2014). It has been proposed that DOX, which can inhibit mitochondrial protein synthesis and arrest cell proliferation, also may prevent the local clonal expansion of T cells and the progression of disease (Lindeman et al., 2009).

While DOX therapy is promising, certain studies have concluded that oral DOX treatment is not effective for long-term or for the treatment of small AAA (Meijer et al., 2013). However, this may have been due to insufficient dosing; as high, long-term, systemic dosing may have been avoided due to the risk of negative side-effects. Local DOX delivery is an alternative to solve these issues. Local delivery was shown to provide effective short term treatment in experimental models of AAAs in rat (Sho et al., 2004), requiring lower drugs amount and

theoretically avoiding dose-related side effects upon systemic administration (Bartoli et al., 2006; Sho et al., 2004). Such side effects include pulmonary fibrosis, hair loss and pigmentation (Albanese et al., 2010; Patricia E. Burrows et al., 2004).

In addition to MMP inhibition, DOX also offers sclerosing properties. The ability of DOX (10 mg/mL in serum) to act as a sclerosing agent has been widely reported in lymphatic malformations (Cahill et al., 2011; Caouette-Laberge). The vascular endothelial layer is known to play an important role in the recanalization process and in the persistence of endoleaks (Soulez et al., 2008). Indeed, previous preclinical work has shown that an embolizing agent combining occlusive and sclerosing properties tends to reduce endoleak persistence compared to an agent with simple occlusive properties (Fatimi et al., 2012). However, this agent was limited by suboptimal mechanical properties, which were improved upon in this study with a superior gelling agent. Furthermore, neither this gel nor commercial embolic agents have not sought to address the underlying pathophysiology of aneurysm progression associated with excessive activity of MMPs and resulted in the progressive vessel wall destruction.

Again, the *in situ* DOX delivery within a hydrogel could help reduce the dosage of DOX required to induce endothelial sclerosis by increasing local drug retention. This is advantageous as it avoids exposure to large quantities of sclerosants.

DOX was released from the hydrogel in a two-stage pattern. There was an initial fast-burst release of DOX that followed first order kinetics within the first 24 h, continued by a slow, sustained release of DOX over the following week. We believe that immediate exposure of the vascular endothelium to high concentrations of DOX would elicit a sclerosing effect-as per the *ex vivo* studies and *in vivo* histology-and initiate MMP inhibition. The following sustained release, conversely, would sustain MMP inhibition, as per the MMP inhibition zymography, while avoiding prolonged inflammatory reaction of the surrounding tissue, as evidenced by the lack of cytotoxicity after one day.

The fast burst release of DOX is likely explained by both rapid water loss and rapid diffusion of the drug from the gel surface; the continuous release can be explained by the slow diffusion of DOX from the gel core. The swelling tests showed substantial mass loss (35%) of the

hydrogel during the first 24h, which likely corresponded to both water loss and the release of VIS. The rapid release of VIS has previously been studied and occurs within hours of exposure to fluid (Coutu et al., 2013). The slow release of DOX in the second phase could be due to either its low solubility or to hydrogel-drug interactions. The similarity of the DOX release profile and swelling analysis support the role of the hydrogel in controlling the release of the agent.

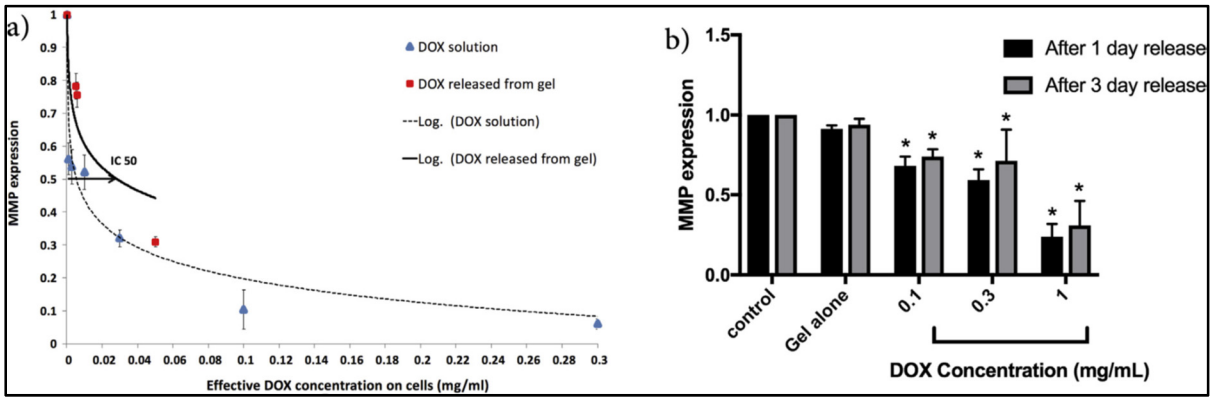


Figure 5.9 a) Effect of DOX on MMP-2 gelatinolytic activity after 24 h contact with cells, when directly added in solution (blue triangles (dotted line)) or when released from the CH-DOX gels (Red squares; continuous line).The similar trend confirms that DOX remains bioactive within the gel. b) MMP inhibition from gels with different concentrations of DOX that have been pre-incubated for 1 and 3 days. Data are shown as mean ± SD. * $p < 0.05$ compared to control

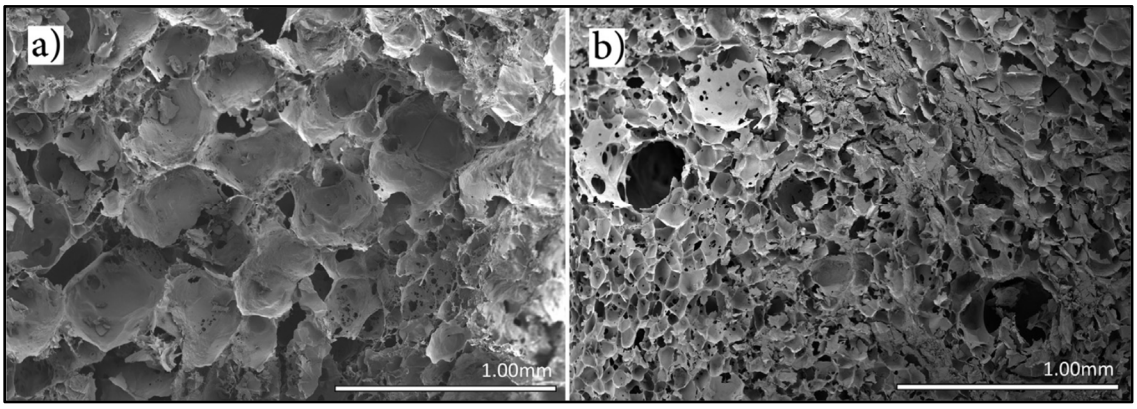


Figure 5.10 SEM images of freeze dried a) CH hydrogel b) CH -DOX hydrogel

Table 5.2 Percentage of immediate and delayed (after 17 min ± 5 min) successful occlusion of porcine renal caudal artery branches at various division levels and overall after embolization with CH/SHC0.075PB0.08/VIS50/DOX0.1, as measured by digital subtraction angiography

| Division | Immediate occlusion (%) Mean ± SD (n=11) | Delayed occlusion (%) Mean ± SD (n=8) |
|---|---|---|
| D1 | 87.5 ± 7.2 | 66.5 ± 12.6 |
| D2 | 96.6 ±2.3 | 83 ± 5.6 |
| D3 | 97.3 ± 1.8 | 90.4 ± 4.1 |
| **Total:** | **96.4 ±2.4** | **85.8 ±4.8** |

Addition of DOX and VIS did not prevent gelation and led to gels with sufficient mechanical properties to impede blood circulation. Injectability of the gel through a microcatheter without risk of catheter blockage was confirmed both *in vitro* and *in vivo*. The visibility of CH-DOX on fluoroscopy was sufficient for accurate targeting and monitoring of migration. These properties demonstrated feasibility for blood vessel embolization. Furthermore, one of the appealing features of the hydrogel is that its injection does not require the use of toxic solvents, which is a requirement of some current embolic agents (Saeed Kilani et al., 2015). As previously mentioned, indirect cytotoxicity testing suggested that after the initial DOX burst release, CH-DOX 0.1 should have no toxic effect. The gel should also become a biocompatible and biodegradable scaffold that can be invaded by cells , as previously shown with a quite similar chitosan gel (Zehtabi, Dumont-Mackay, et al., 2017).

The main challenge of this project was to determine the optimal DOX concentration to include in the final gel. In agreement with previous studies (Shanmuganathan et al., 2008), free DOX was shown to promote a concentration-dependent decrease in cell viability, with about 50% survival after 24h exposure to 0.8 mg/mL. Translation of *in vitro* data to *in vivo* situations remains difficult, however. E*x vivo* embolization was also performed and de-endothelialization was demonstrated at all DOX concentrations tested (0.1 to 1%w/v). MMP tests also

demonstrated that 1) DOX contained in hydrogels was still bioactive after 4 days and 2) the gel containing 0.1% DOX was able to suppress MMP-2 activity by 70% after 24 h.

SEM showed no evidence of DOX crystallization on the surface of the gel, indicating the homogeneous dispersion. The smaller pore size of the CH-DOX hydrogel compared to CH alone may have been due to the presence of both VIS, which confers higher viscosity to the gel, and/or DOX, whose low solubility slows down matrix formation. These interactions may have resulted in the tighter network structure, which we suspect would be able to better control drug release.

The FTIR data (i.e. the shifting of the 1661 $cm^{-1}$ band and disappearance of the 1556 $cm^{-1}$ and 1574 $cm^{-1}$ bands of DOX) indicates that there are weak interactions between the amide groups of DOX and hydroxyl groups of CH, which limits vibrational motion (Tamimi et al., 2008). DOX may be entrapped in the CH hydrogel network and lose molecular freedom.

Based on these data, we selected to use 0.1% (w/v) DOX as the concentration tested during *in vivo* assays. This low concentration was selected to reduce risks of adverse side effect such as possible chronic inflammation (due to DOX sclerosing properties) and delayed healing (Albanese et al., 2010). Furthermore, CH-DOX with 0.1% had a lower risk of DOX oxidation which we felt would facilitate more scalable production in the future.
However, the *in vivo* data suggest that a higher DOX concentration may have been more appropriate. While CH-DOX 0.1 initially led to occlusion of 96% of target arteries, post-embolization recanalization was noted, particularly of the proximal branches (Figure 5.11).

This finding could be explained by inadequate thrombus formation or insufficient mechanical properties. While *ex vivo* results demonstrated that de-endothelialization occurred when the vascular lumen was exposed to DOX at 0.1% after 3h, the *in vivo* tests showed that this concentration may not have been sufficient to promote an immediate and robust thrombotic reaction secondary to vascular sclerosis (Kumar et al., 2010). Furthermore, hydrogels containing 0.3% DOX demonstrated slightly better mechanical properties. Therefore, although this hydrogel appears promising for the treatment of aneurysms and endoleaks, further

optimization of the concentration of DOX will be pursued to promote optimal de-endothelialization, leading to a faster and more robust thrombotic reaction.

Further tests will also be required to better assess the risks of off-target embolization, which is a concern for all liquid-based embolic agents. Yet, CH-DOX has several features that mitigate this risk. Its viscosity which makes it less likely to migrate in conditions of high flow and its rate of injection can be slow down to prevent distal migration, since there is no risk of catheter gluing as observed with cyanoacrylates. Embolization can also be performed through a balloon catheter to prevent not only off target embolization but reflux as well.

The present study is limited by the small number of animals and unavailability of appropriate animal models. The short-term preliminary animal study was useful as proof of concept of occlusive properties in the macro and microvasculature. However, more comprehensive animal studies in an experimental aneurysm model are needed to evaluate long term occlusion, gel degradation and severity of inflammation in the future. Such a model should mimic aneurysmal pathology (including atherosclerotic disease) in order to assess the efficacy of the product not only as an embolizing agent but also as a MMP inhibition strategy. Unfortunately, no such models currently exist.

CH-DOX hydrogels also has the potential to use for the embolization of intracranial aneurysms and embolization of AVMs which are associated with increased MMP-2 and MM-9 expression respectively. CH-DOX could either replace or act as an adjunct with current embolic agents (especially since we believe that it can withstand systemic pressures based on our *in vitro* results and that it can reliably inhibit MMP expression) (Health Quality, 2006; Wei et al., 2016).

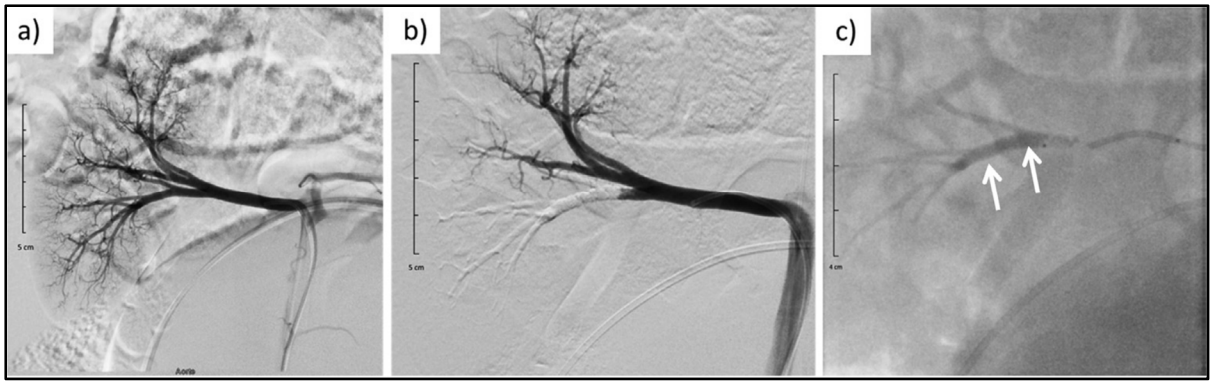


Figure 5.11 DSA before a) and after b) complete embolization of the right lower polar artery of kidney by CH-DOX0.1 gels c) radiopaque embolizing gel visible without substraction (arrows)

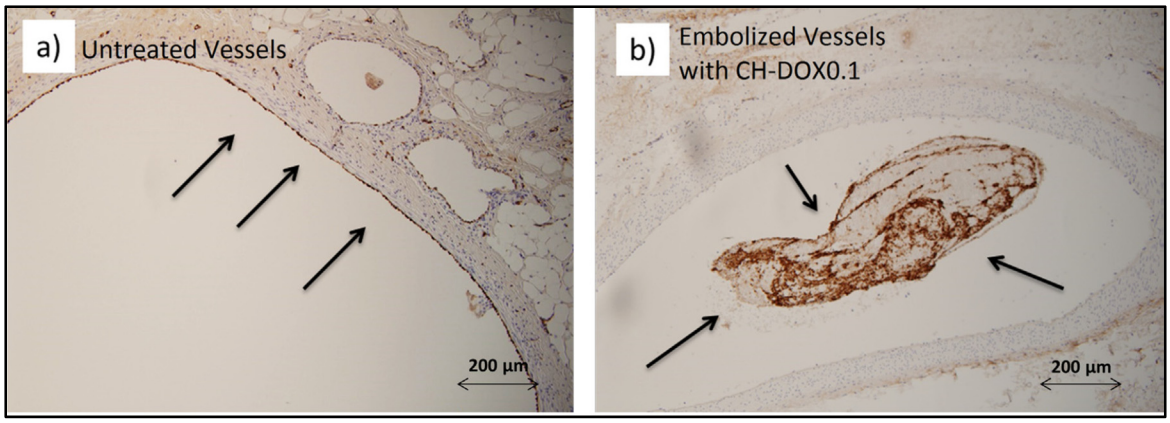


Figure 5.12 Factor VIII immunostaining of *in vivo* embolized vessels: (a) untreated; (b) embolized with CH-DOX0.1. The figure shows that the endothelial lining is removed *in vivo* after embolization with CH-DOX0.1 gels, while it is clearly visible on untreated arteries (brown stain, arrows)

## 5.8.Conclusion

An injectable radiopaque chitosan-based physical hydrogel was developed as carrier system for local controlled drug (DOX) delivery and evaluated for its potential as injectable embolizing agent for blood vessel and endoleaks. The gel is injectable through a microcatheter and has sufficiently rapid gelation and mechanical properties to block tubular structures subjected to physiological pressure. The two inter-related stage DOX delivery enables the release of a large amount of drug to remove the endothelium and induce vessel thrombosis

(sclerosing properties) and initiate MMPs inhibition, while the prolonged slow release stage that follows is favorable to continue MMP inhibition. This could therefore counteract ECM degradation and aneurysm progression. While preliminary short-term *in vivo* testing with DOX 0.1% concentration confirmed feasibility for blood vessel embolization and showed promising data, it also suggested that higher DOX concentration might be required to avoid recanalization of vessels after embolization. Altogether, these injectable radiopaque chitosan-based hydrogels therefore present very interesting features for blood vessel and aneurysm embolization.

## 5.9.Funding

This work was supported by NSERC (RGPIN-2015-05169) and by the Canada Research Chair in Endovascular Implants and Biomaterials (950-229036).

## 5.10. Acknowledgments

The authors thank Dr. Louis Gaboury (UdeM) for help and supervision during the histological analysis, Marion Maire and Eve Hui (CRCHUM) for assistance during cell and tissue culture, Marc-André Labelle for help during FTIR analysis and Michel Gouin, Helene Heon and the CRCHUM animal care staff for technical help during animal tests.

## 5.11. Appendix A. Supplementary data

Supplementary data associated with this article can be found, in the online version, at http://dx.doi.org/10.1016/j.actbio.2017.09.021

# CHAPTER 6

# DISCUSSION

While sac embolization has potential to treat or prevent endoleaks after EVAR, the presently commercialized embolizing materials have several drawbacks and lead to frequent recurrence, as described in chapter 1. For instance, Onyx, which is one of the most well-known embolic agents in the market, leads to high rate of recurrence of endoleaks and reintervention is needed in 44% (Khaja et al., 2014).

This lack of effectiveness can be explained by their mechanism of action, which is only based on occlusive properties originated from their mechanical properties. They don't prevent the recanalization process which can reopen blood clots thanks to the endothelial cell lining (Soulez et al., 2008), and do not counteract mechanisms involved in AAA formation and progression, which is at least partly due to excessive activity of matrix metalloproteinase (MMPs) (Annabi et al., 2002).

To address these gaps, during this PhD project, we proposed to evaluate and optimize sclerosing embolizing agents, with the goal of creating an ideal multi-faceted embolic agent for the prevention and treatment of endoleak and other vascular diseases. Different engineering tools were developed to assess embolizing agents in vitro, in complement to preliminary in vivo testing in animal models. The objectives are achieved in three complementary projects. In this section, we discuss the results and present some new results that did not fit in the 3 articles but help to compare the three formulations developed during this PhD in terms of mechanical properties, injectability, biocompatibility and their potential as embolic agent based on design criteria.

## CH-STS hydrogels as sclerosing embolizing agent

Our team previously developed a sclerosing embolizing agent based on chitosan combined with STS as sclerosing agent (Fatimi et al., 2012). The first objective of this PhD was therefore to demonstrate in a canine model of endovascular aneurysm repair the superiority of such embolizing sclerosing agent (CH-STS hydrogels), compared with an embolizing but non

sclerosing agent (CH hydrogels) to treat endoleak. The underlying hypothesis is that combining embolization and endothelial ablation using an embolic agent with sclerosing properties could be a promising strategy to prevent endoleak persistence and/or recurrence after EVAR.

The results can be summarized as follows; although CH and CH-STS gelled rapidly ($G_{Initial} \geq$ 800 Pa), adding more STS results in higher gelation rate and higher initial storage moduli. Indeed, both gels present rapid gelation and occlude blood flow up to physiological pressure *in vitro*. In *in vivo* experiments, the occurrence of endoleaks type I seems to be less in CH-STS sclerosing gel compared to a CH non-sclerosing agent (2/9 versus 6/9, $p = 0.069$) however, no significant difference between groups were observed, possibly due to the small number of animals. This is the main limitation of this part of the project. We initially determined, based on power analysis, that 9 animals would be sufficient to observe difference between the CH and CH-STS. However, based on the previous results we assumed that there would be only 1 or less endoleak in the Ch-STS group. We didn't expect that two aneurysms treated with CH-STS would be left only very partially embolized (Zehtabi, Dumont-Mackay, et al., 2017).

As secondary endpoints, it was observed that CH-STS led to better initial nidus embolization, which can be explained by its mechanical properties and by its higher thrombogenicity effect (Zehtabi, Dumont-Mackay, et al., 2017). Moreover, it tends to stick to the vessel wall, which is a good feature to prevent recanalization process.

**Recommendation and perspectives on CH-STS gels:**

In the scope of modification of CH-STS degradability and biocompatibility, some of the important points have not been studied which could be interesting for the future researches. In particular, the STS release rate from the hydrogel should be investigated and, if possible, expedite. In vitro cytotoxicity of CH-STS extract suggest that STS release is long (see later, Figure 6.5). Moreover some STS may remain in the gel structure with time, through ionic interactions. Modifying the STS release or changing hydrogel composition by reducing STS or replacing STS might help to have higher degradation rate and improved biocompatibility of the hydrogel. However, it is not a simple solution since decreasing STS concentration is known to lead to a decrease of mechanical properties (Fatimi et al., 2012).

Also, due to our limited number of animal model and failure to obtain acceptable statistical results, further animal tests and comparisons between CH and CH-STS to reach significant statistical results would be recommended. For this project we chose the type I endoleak model to ensure very challenging endoleaks and better reproducibility than we would have had with a type II endoleak model. Not only results could be extended to type II but we would expect better results with type II model since they present reverse flow and less embolizing agent migration due to the backflow of collateral vessels. To prove our claim, we need to have better assessment of the potential of this product by running animal tests with type II endoleak model and comparing the results with commercialized embolizing agents such as Onyx.

According to these results, the combination of chemical endothelial ablation and flow blockage seems to be promising for endoleaks treatment. Given that the Chitosan-STS gel may not easily be transferred to the clinics, we evaluated both *in vitro* and *in vivo*, the potential of an embolizing sclerosing agent prepared by adding a sclerosing agent (Ethanol) to a currently commercialized embolic agent (Onyx).

**Onyx- Ethanol mixture as a sclerosing embolizing agent**

The purpose of the second project was to investigate the potential of an embolizing sclerosing agent prepared by adding a sclerosing agent (Ethanol) to a currently commercialized embolic agent (Onyx). Based on our previous work on CH-STS, we hypothesized that by combining Onyx with ethanol, which is a well-known sclerotic agent, the efficacy of the embolizing agent will be improved. However, by mixing the two products, various characteristics might be seen in a new product regarding visibility, injection control and penetration depth. Therefore, the first step consisted in studying these properties as a function of ethanol concentration (at 25, 50 and 75% v/v) both *in vitro* and *in vivo* in various porcine arteries, a simple and much less costly animal model, compared to the canine aneurysm model.

In brief, the 25%-ethanol 75% Onyx mixture showed the best properties, with good injectability, good occlusive properties *in vitro*, good radiopacity and deeper penetration than Onyx. Lower concentration of Onyx and higher concentrations of ethanol lead to lower

viscosity and deeper penetration of the mixture into small vessels before the completion of the polymerization process which is desirable in some of AVM model treatment.

While these are promising results, these are only very preliminary and several steps are required to further assess the potential of this product for AAA in endoleak model and in other animal models for other applications such as cerebral AVM or cerebral aneurysms.

While both embolizing agents (CH-STS and Onyx-EtOH) present interesting features, they did not fill one of the gaps identified in the literature review, namely, the prevention of the aneurysm progressive enlargement. This led us to the third part of this PhD.

**CH-DOX hydrogels as an MMP inhibitor/sclerosing embolizing agent**

The third aim of this thesis was to address the gaps present in the current embolic agents, by developing an embolizing agent able to stop recanalization and aneurysm progression at the same time. We hypothesized that decreasing MMP excessive activity in the aneurysmal wall could help to prevent aneurysm progression. We therefore developed an injectable and radiopaque chitosan-based embolization agent containing doxycycline (DOX) as an MMP inhibitor/sclerosing embolizing agent for the treatment of AAAs.

Results showed that a CH-DOX hydrogel formulation could be found which is injectable through a microcatheter and has sufficient rapid gelation and mechanical properties to block tubular structures subjected to physiological pressure. As expected, DOX release from CH hydrogels followed the two inter-related stage (release of a large amount of drug to remove the endothelium and initiate MMPs inhibition, while the prolonged slow release stage that follows is favorable to continue MMP inhibition). CH-DOX gels led to ablation of endothelial layer of embolized arteries in an *ex vivo* model within 3h. Released DOX was still bioactive and able to reduce MMP expression in human glioblastoma cells. Preliminary short-term *in vivo* testing of DOX 0.1% concentration in pig renal arteries confirmed its injectability, good radiopacity and good initial embolization of small blood vessels (with diameter from 2.19± 0.7mm (Fabian Alejandro et al., 2017)). However one of the limitations outlined in the project is some

reopening of blood flow within a few minutes post embolization. This could be due to inadequate thrombus formation or insufficient mechanical properties.

Recommendation: we suggest increasing DOX concentration in the gel to 3 mg/mL or 5 mg/mL). We hypothesize that such gel would be better for long term embolization. Indeed, as will be seen later, increasing drug level was shown to increase the gel final mechanical properties (Figure 6.1) Moreover, it should increase endothelial ablation, therefore thrombogenicity, and thus better prevent the reopening process.

**Comparison of the three embolizing agents**

Some further tests have been performed to compare the three formulations and evaluate their ability to fulfill the design criteria of an ideal embolizing agent. They are presented and discussed in the following paragraphs.

Table 6.1, at the end of this section, summarizes the strength and weaknesses of each embolizing agent in regards to the design criteria, in comparison to commercialized Onyx, according to the results gathered in this PhD and in previous literature data. The values of each feature of products are shown with a number of + signs and its exact meaning is explained in each specific section.

Gel mechanical properties : To compare the final mechanical properties of the gels, Rheolution test were performed for all the formulations by ElastoSensTMBio (Ceccaldi et al., 2017). To perform this test, 2 mL of each formulation solution was added to a specific detachable sample holder and then 2mL of PBS were added on the samples and incubation at 37 °C was continued until 24h. Subsequently supernatants were removed and sample holders were firmly attached to the instrument before measuring storage moduli (G'). Obtained results showed that CH and CH-STS gels with radiopaque agent present relatively poor mechanical properties. This is in contradiction with rheometry results where CH-STS presented high G' values, probably due to some precipitation.

Addition of DOX increased the mechanical properties, especially at concentration equal or above 0.3%. These tests were however performed only once and should be repeated (Figure 6.1).

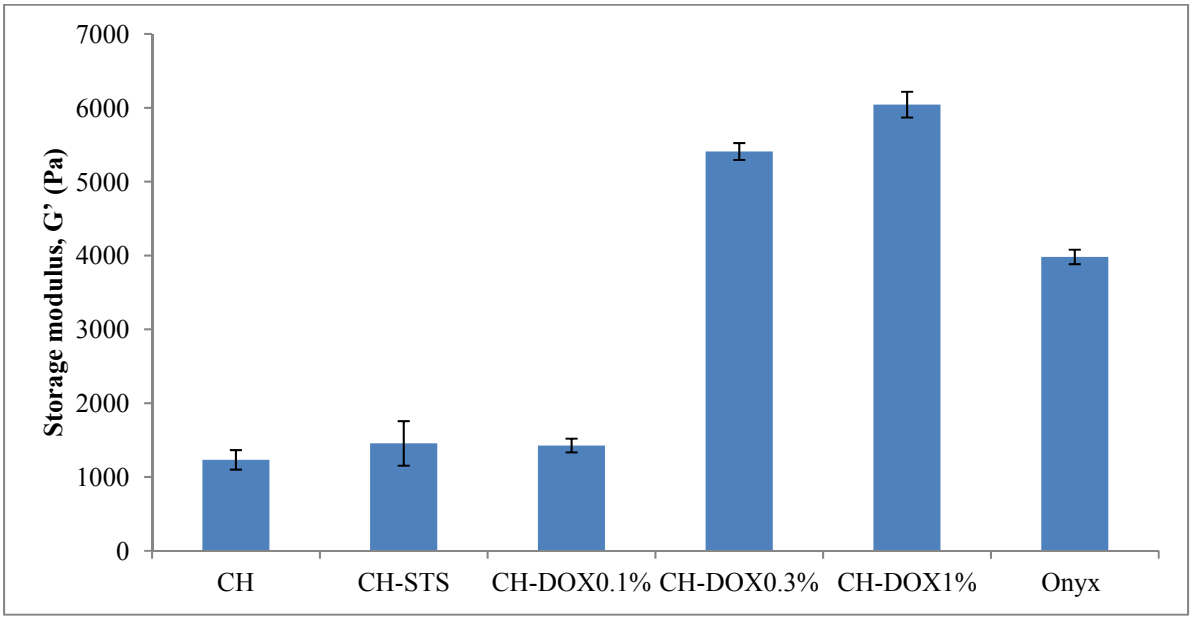


Figure 6.1 Final Storage modulus, G' (Pa) after 24 h of gelation at 37ºC for different chitosan hydrogels formulations (Visi 50%, GA: SHC 0.075 PB0.08) (n=3)

Control & deliverability is one of the most significant designs of criteria of embolic agents which are affected by two factors: Injectability and polymerization time and initial mechanical properties. Injection of both CH-STS or CH-DOX does not require any special pre-treatment prior to gel injection, in contrast to Onyx which requires the injection of DMSO, a very toxic product, through the catheter before Onyx injection (Chaloupka et al., 1999). Embolization by Onyx is time consuming because it must be injected slowly (Ideal: 0.16ml / min; Max: 0.3ml / min, risk of angionecrosis if faster, Min: 0.05ml / min: risk of catheter occlusion and rupture if slower) and requires changing the catheter for each feeder embolization. In contrast CH-DOX (as well as CH-STS) enables successive injections without changing the catheter (Saeed Kilani et al., 2015).

To compare the injection force and the cohesion of each product after passage through the catheter, injectability test were performed for CH-STS, CH-DOX, Onyx and Onyx-25%ET

using a microcatheter (FasT-325, Boston Scientific; internal diameter of 0.61 mm (0.024 inch); length of 140 cm) (Fatimi et al., 2016). Even though all formulations were injectable, they have different process of solidification, which impact on the force required for injection (Figure 6.2). The solidification process of Onyx is a copolymerization or precipitation type which starts once Onyx encounters blood or saline solution (Ayad et al., 2006). Therefore, it is liquid at the time of the injection and can easily be injected. While the solidification of CH-STS and CH-DOX is a gelification process which starts immediately after mixing gelling agent and CH solution before injection. So, at the time of injection, we have a hydrogel that gets tighter and harder with time. Indeed, as seen in the Figure 6.2, CH-STS required the highest force for injection due to the high rate of gelation, which is partially associated with precipitation, while CH-DOX, which gels less rapidly, required lower force. In contrast, Onyx and Onyx-25%Et which remain liquid as long as not in contact with water, could be injected with about 10 times less forces. These difference in terms of solidification process also impact on the shapes of the product after coming out of catheter (Figure 6.3). Onyx-25%ET has a bulky shape while CH-DOX and CH-STS have a filament shape.

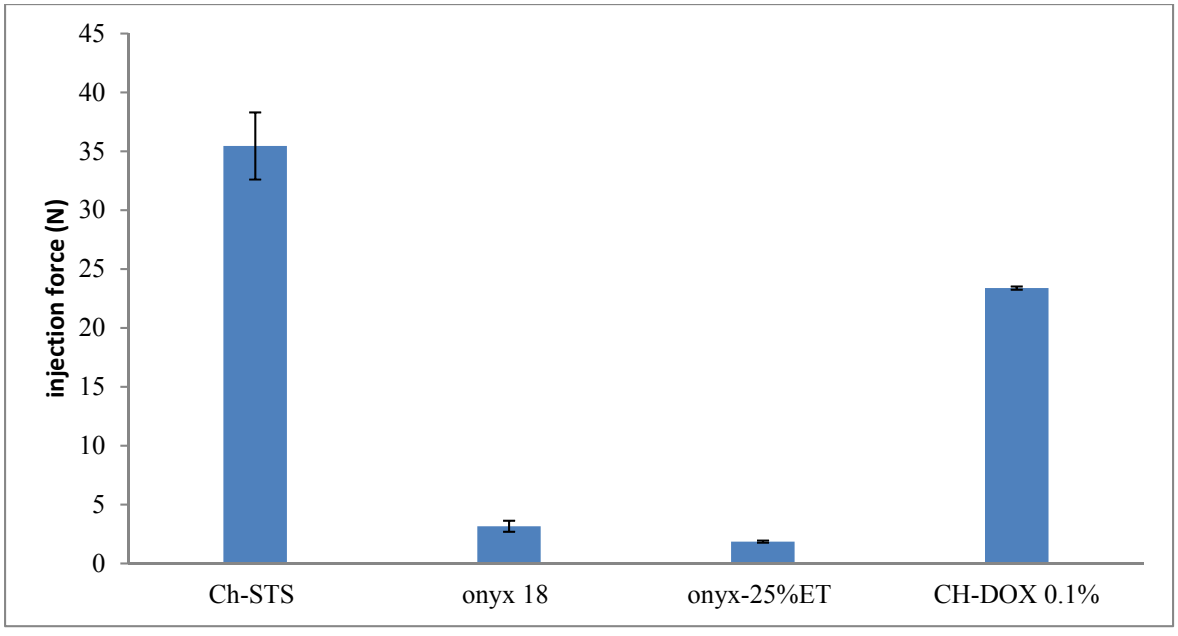


Figure 6.2 Maximum force required to inject the gel through the catheter (Øint = 0,61mm) after different times of gelation (mean ±SD; n=3)

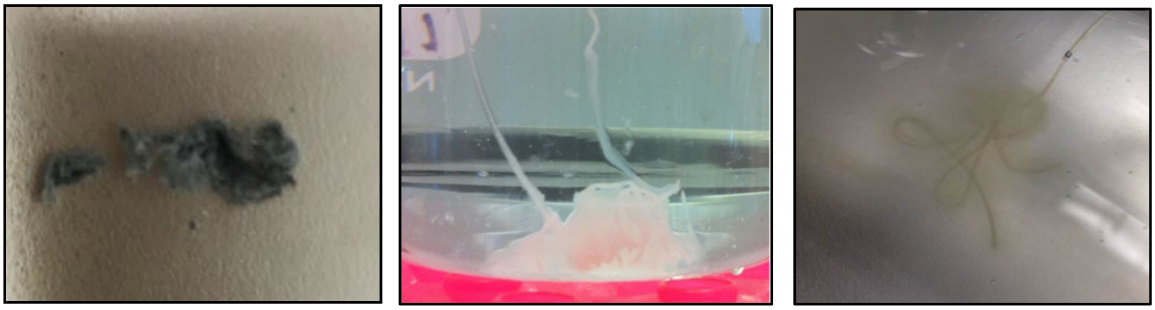

a) Onyx-25%ET b) CH-STS 3% c) CH-DOX 0.1%

Figure 6.3 the shape of Onyx 18, CH-STS3% and CH-DOX 0.1% after coming out of 0.21" catheter

Control & deliverability as a function of injectability (from easy (+++) to hard (+)) and initial mechanical properties (from low (+) to high (+++) are shown in

Table 6.1. As shown in the Figure 6.4, although the initial mechanical property of Onyx seems to be low due to its fluidity, from embolization results (Saeed Kilani et al., 2017) it was shown that initial mechanical properties of Onyx is high enough to resist to the flow up to the 220 mmHg (+++). CH-STS (+++) shows higher initial mechanical properties than CH-DOX (++) due to its faster gelation rate. For instance, CH-STS shows high initial mechanical properties (+++) and high injection force (+++). Although there are some difficulties with control during injection because of the great required injection force, CH-STS is able to fill the cavity properly due to high initial mechanical properties.

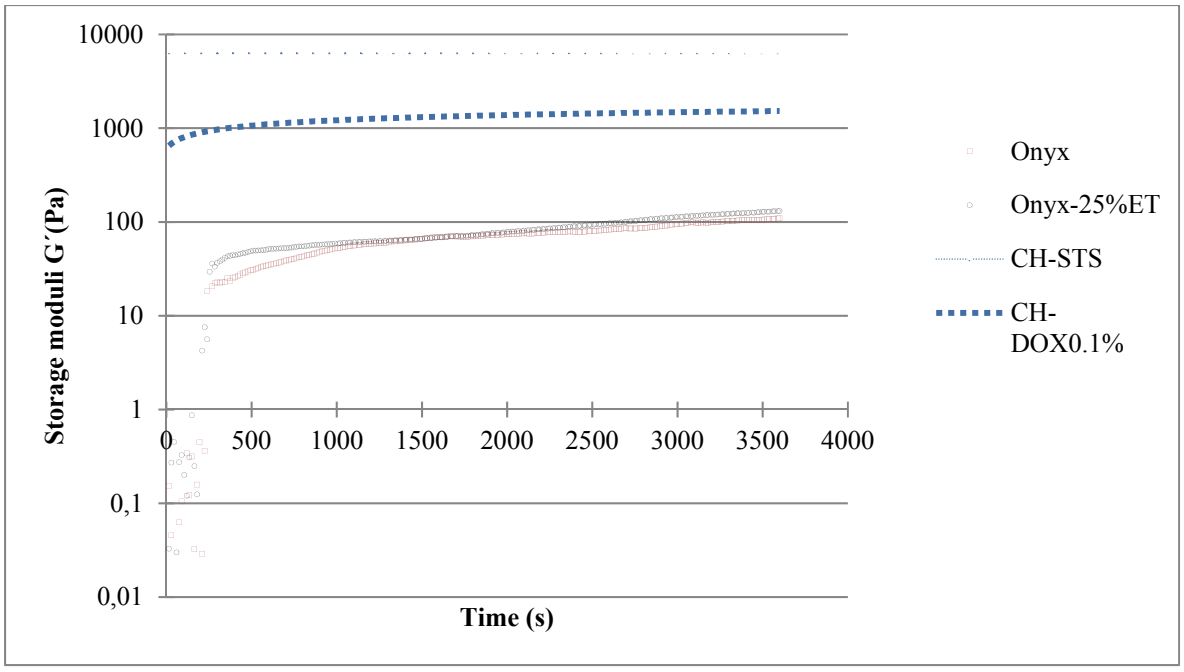


Figure 6.4 Evolution of the storage modulus (G') with time for different formulations at 37°C (n=3)

Biocompatibility: To evaluate possible toxicity of CH-STS, CH-DOX and Onyx *in vitro* indirect cytotoxicity tests were performed on gel extracts which were obtained after incubation of the gel in culture media at different timepoints (1, 2, 3 and 7 days). DMSO10% was used as a positive control since it is known to induce cell death following ISO 10993-5:2001 standards. Results are presented in Figure 6.5 and expressed in percentage of viable cells compared to negative control (cells in media without extracts). They showed that even after 7 days, the CH-STS still releases toxic products (it shows by "0" in the table which means product is toxic), most probably STS (Figure 6.5) which means that STS release is not complete during this time. While STS release and toxic effect is beneficial in short term (to induce endothelial ablation), it is important to verify whether the amount and release kinetics is appropriate and drug will be completely released. Indeed the slow release of STS might lead to long-term toxicity of the hydrogel and impair tissue healing. Furthermore, in contrast to CH-STS where STS is believed to remain in the gel in long term due to ionic interactions, once burst release of DOX is achieved, CH-DOX gel does not release toxic products and therefore form a biocompatible scaffold (+++). Indeed, as already showed by our team, the gelling agent and radiopaque agent

are also rapidly released (Coutu et al., 2013), leading to simple CH physical hydrogels which biocompatibility was already confirmed by others teams. The short and long-term biocompatibility of the CH-DOX remains however to be confirmed by further *in vitro* and *in vivo* tests.

Biodegradation: The release rate of the STS from chitosan hydrogels also might effect on the rate of hydrogel degradation, the slow release of the STS could be a reason that hydrogels are visible even six months after implantation (Zehtabi, Dumont-Mackay, et al., 2017).

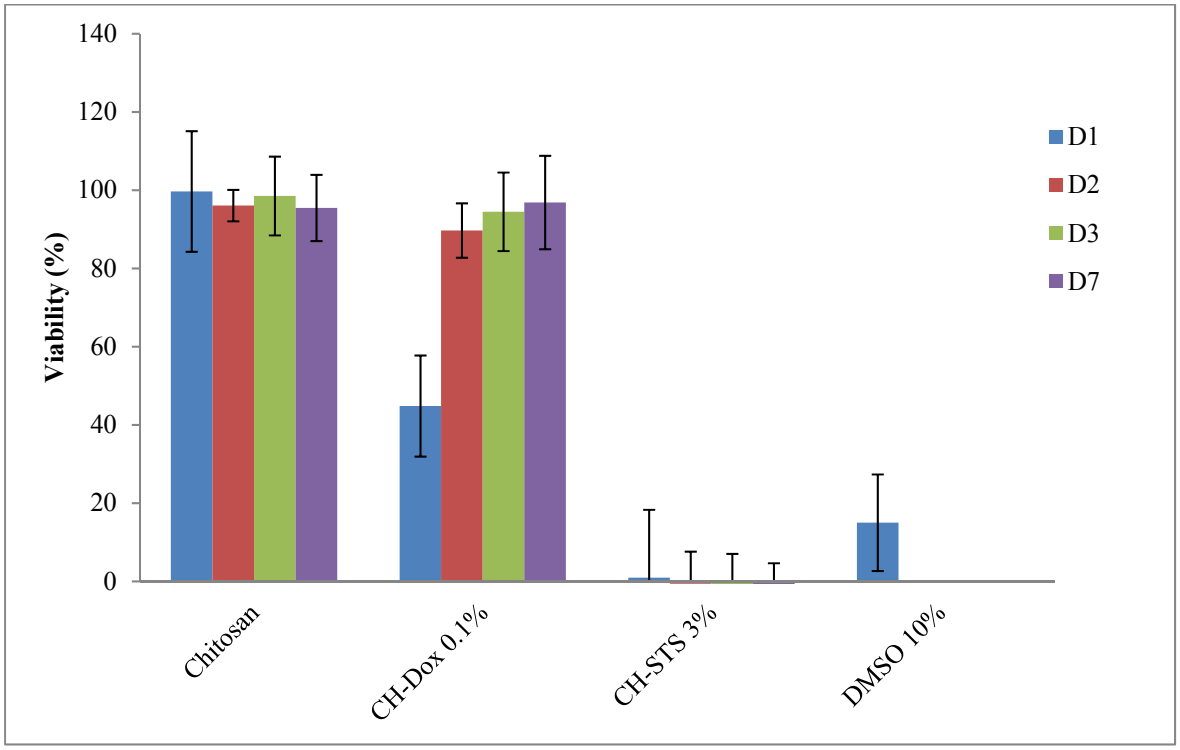


Figure 6.5 Viability of L929 fibroblasts exposed to extracts recovered at days 1, 2, 3 and 7 during incubation with various CH hydrogels (n = 18, mean ± SD). (Ctrl- = cells in medium culture, Ctrl+ = cells exposed to 10% DMSO).

CH and STS could form a chitosan-anionic surfactant complex in the solution by binding of STS molecules to chitosan chains (Figure 6.6). Presence of STS in the gel as anionic surfactant may also explain the slower degradation rate of CH-STS, compared to CH hydrogels, which in term could explain why the rate of reduction in aneurysm size was found to be lower during

our animal study. Aneurysm size is a practical way to follow endoleak treatment since aneurysm growth is considered as a failure and increased risk of aneurysm rupture (White et al., 2009). However following embolization with permanent agent, sac shrinkage is rarely observed and physician are looking more at sac expansion combined with residual endoleaks . Therefore, we do not believe that aneurysm shrinkage should be considered as a key result here to evaluate the success of endoleak treatment. The reduced aneurysm shrinkage is mostly due to the fact that CH-STS is only very slowly degradable.

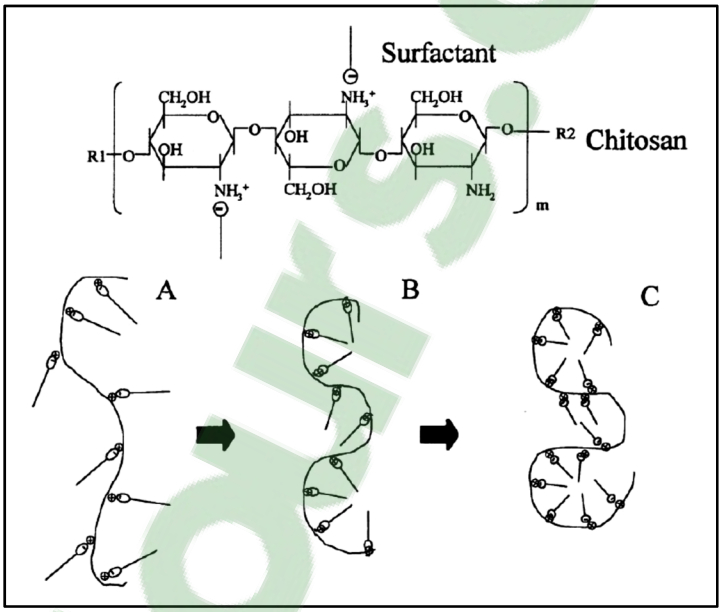


Figure 6.6 Tentative model of the Chitosan-STS (anionic surfactant) complex formation in the solution (Huang et al., 2001)

Whether this is an advantage or limitation is still unclear. The biodegradability and porous structure of the embolizing agent is very important to favor replacement by fibrous tissue, result in the aneurysm shrinking and healing completely after degradation. We did not study the biodegradation rate of CH-DOX and CH-STS since the degradation rates of chitosan hydrogels have already been extensively studied. The degradation rate of CH gels depends on the degree of deacetylation (DDA) of chitosan (Thein-Han et al., 2007). In the present works

we used chitosan with a DDA of 95%, which means that chitosan gels will slowly degrade over several weeks. But this could be accelerated by using chitosan with lower DDA.

Biodegradation of CH-STS is slower than CH hydrogels according to the limited aneurysm shrinkage and to the fact that most of the aneurysmal sac is still filled with the gel after 3 or 6 months after embolization (Zehtabi, Dumont-Mackay, et al., 2017). While it was impossible to quantify the gel degradation percentage in this study, histology showed qualitative evidence of progressive biodegradation, including resorptive cell infiltration and development of tissue. For the same reason, CH-DOX (+++) degradation rate may be accelerated compared to CH-STS gel (+) because we also expect an almost complete release of contrast agent and gelation agent within the first 24h (Coutu et al., 2013); furthermore, after 1 week, we demonstrated that 80% of the DOX was released from CH-DOX thus, we are confident that rapidly only chitosan hydrogel will remain *in situ*, and will demonstrate similar degradation with CH-DOX. However, according to previous researches, Onyx is not a biodegradable embolic agent and it remains in the body after the implantation (Ayad et al., 2006).

Radiopacity: Although all the developed formulations are radiopaque, the radiopacity of CH-DOX (+++) due to higher concentration of radiopaque agent is better than that of CH-STS (++). CH-STS and CH- DOX, unlike Onyx, are temporary radiopaque and they are created to rapidly release the contrast agent, to not interfere with imaging follow-up (Coutu et al., 2013). *In vitro* studies showed rapid (despite incomplete) decrease of radiopacity after only 24h rinsing (Coutu et al., 2013).

Occlusion properties: To investigate the occlusive properties of each formulation, *in vitro* embolization test by a bench test were performed (Fatimi et al., 2016). *In vitro* embolization results showed that all the formulations have resistance to a simulated blood stream up to a pressure of 220 mmHg. Also *in vivo* results confirmed good occlusive properties for CH-STS (+++) and Onyx (+++), while CH-DOX (++) showed some reopening after 20 min.

Sclerosing effect or inducing endothelial ablation is another design of criteria which can prevent recanalization processes and stop endoleak formation and persistence. Due to chemical nature of STS and its high concentrations in the CH-STS, this hydrogel has a strong

sclerotherapy effect (+++). Although we have not done a specific test to compare the sclerotherapy strength of different products, with regard to the cytotoxicity test results, it can be concluded that CH-DOX is a weaker sclerosing agent (++) than CH-STS due to its lower drug concentration and faster release of DOX. Onyx is not a sclerosing agent, but Onyx-25%Et has its own sclerosing properties due to the addition of ethanol, which is a strong sclerosing agent. However, due to the rapid release of ethanol, we anticipate lower sclerosing properties of Onyx-25%Et compare to CH-STS, but further investigation is needed to prove our claim (++).

MMP inhibition: AAA formation and development which is characterized by progressive destruction of extracellular matrix components of the artery is believed to be associated with the excessive activity of MMP-2 and MMP-9. Among the three developed products, only CH-DOX due to the presence of DOX, a known MMP inhibitor, in the hydrogel structure can effectively reduce the excessive activity of MMPs (+++).

Table 6.1 Summary of the strength and weaknesses of each embolizing agent according to the results gathered in this PhD and in previous literature data and design criteria

| **Agent** | | **CH-STS** | **Onyx100%** | **Onyx-25%ET** | **CH-DOX** |
|---|---|---|---|---|---|
| Control & deliverability | Injectability | + | +++ | +++ | + |
| | Initial mechanical properties | +++ | +++ | +++ | ++ |
| Occlusion | | +++ | +++ | +++ | ++ |
| Sclerosing effect | | +++ | 0 | ++ | ++ |
| biocompatibility | | 0 | 0 | 0 | +++ |
| Biodegradability | | ++ | 0 | 0 | +++ |
| Radiopacity | | ++ | +++ | +++ | +++ |
| MMP inhibition | | 0 | 0 | 0 | ++ |

**Potential of developed agents for other applications**

All the developed formulations in this PhD are sclerosant/embolization agents. Therefore, in addition to endoleak treatment and prevention after EVAR, they could be used to treat other vascular diseases such as arteriovenous malformations (AVM) and lymphatic malformations (Jayaraman et al., 2008).

An AVM (arteriovenous malformation) is a congenital disorder of blood vessels occurring mostly in the brain, brainstem, or spinal cord that is characterized by a complex, tangled web of abnormal arteries and veins connected by one or more fistulas (abnormal communications) (Cho et al., 2006). The cause of AVMs is not clear. Most people are born with them, but they can occasionally form later in life. They are rarely passed down among families genetically. An AVM puts extreme pressure on the walls of the affected arteries and veins, causing them to become thin or weak. This may result in the AVM rupturing and bleeding into the brain (a hemorrhage). One of the options for AVM treatment and prevention of haemorrhage is Embolization, also known as Embolotherapy or Endovascular therapy, which has been used to treat AVM since the early 1980's. This procedure involves the injection of an embolic agent material into the AVM in order to block it off. One of the most known agents for treating AVM is ethanol, but it leads to some complications such as pulmonary hypertension, hemoglobinuria, skin necrosis, nerve injury and muscular fibrosis(Prasetyono et al., 2010).

Combining vascular occlusion and sclerosis could have a more effective potential for treatment of AVMs. Onyx-25%ET and CH-STS and CH-DOX could be potential candidates in a territory at risk for ethanol such as nerve territory, orbiteal area, pancreas, small, large bowel and pelvis (bladder, rectum)(S. Lerouge et al., 2011). In addition to being able to remove endothelial lining like ethanol, they have other advantages over ethanol such as cohesiveness, radiopacity, and better control during delivery. In addition to all the aforementioned advantages of three formulations, CH-DOX can help to better treatment of AVM by preventing excessive activity of MMP-9 which is associated with AVMs (Chen et al., 2006). However, using these formulations may also be associated with some complications such as having difficulty in access to the Nidus, which can be solved by plug and push method.

A lymphatic malformation is a mass in the head or neck that results from a localized abnormality of lymphatic vessels. There are several treatment options depending on the problems due to the lymphatic malformation, the location in the body, the degree of tissue involvement and the size of the lymphatic malformation such as surgery and/or injection sclerotherapy. The treatment consists of a percutaneous (through skin) injection of a substance into the abnormal veins of the venous malformation. Substances used in sclerotherapy include Doxycline, OK-432, Bleomycin and a number of other sclerosing agents. These agents cause an irritation of the wall lining the lymph cyst (sclerosing effect) which then becomes inflamed and shuts down (Bloom et al., 2004).

As it was previously shown, lymphatic malformations are also associated with excessive activity of MMPs. Therefore, Combination of vascular occlusion, sclerosis and MMP inhibition could be multifaceted approach for lymphatic malformation treatment (Patricia E Burrows et al., 2008). CH-DOX seems to have a good potential to be used for injection sclerotherapy for lymphatic malformation. This product can also reduce the number of injection with the help of drug release strategy and so increase the safety of the treatment.

# CONCLUSION

The superiority of CH-STS (an embolizing/sclerosing agent) compared to CH hydrogels (an embolizing but non sclerosing agent) to treat endoleak in a canine model of endovascular aneurysm repair, showed that combination of sclerosing effect and occlusive properties could increase the efficacy of the embolization treatment.

To transfer this approach to the clinics, an embolizing sclerosing agent prepared by adding a sclerosing agent (Ethanol) to a currently commercialized embolic agent (Onyx) were developed and in vitro and in vivo properties were evaluated. Obtained results showed that this new sclero-embolic agent could be interesting for the endovascular management of various vascular anomalies with the advantages of deep penetration, controlled injection, safe and localized delivery of reduced amount of alcohol to the target and good visibility under fluoroscopy. Further investigation is required to check the ability of this product to prevent endoleak.

Finally the obtained results showed that CH-DOX as an MMP inhibitor/sclerosing embolizing agent is able to occlude the blood flow, remove the endothelial lining and inhibit MMPs. This shows that embolizing agent which are able to target the mechanism leading to AAA/endoleak formation, such as endothelial ablation or MMP inhibition, in addition to its occlusive properties, might have a better potential for AAA/endoleak treatment.

For future investigations, it would be interesting to increase the DOX concentration to improve efficacy of the embolization by increasing the thrombogenicity effect. Also in vivo tests to compare different formulations in an endoleak model are recommended in order to evaluate the features of each material for this application.

The originality of this PhD is the design and characterization of new radiopaque injectable sclerosing embolizing agents, in particular the first radiopaque injectable matrix with sclerosing and MMP inhibition properties. Combining these properties is believed to improve the efficacy of sac embolization after EVAR. Moreover, these materials should be able to compete with the current embolic agents in terms of its efficiency and price. CH-STS hydrogels

have been patented and licensed by Cook Medical Company. Based on the considered composition for our hydrogels we expect to have an injectable radiopaque hydrogel with the minimum toxicity, enough mechanical properties to occlude blood flowing and stop the mechanism of recanalization and aneurysm progression.

## Appendix 1 – Description of in vitro tests

Some of the main in vitro techniques developed or used to assess the potential of embolizing agents are described below, since they are only shortly described in each article.

**Embolization test**

Embolization is a method to occlude the aneurysm sac or collateral artery feeding the aneurysm sac. The occlusive properties of embolic agents (their ability to resist against blood pressure) could be determined *in vivo* or *in vitro*. *In vivo* embolization tests are limited by costs, time and ethical issues. Therefore, an in vitro bench test was designed in Lerouge's laboratory (LBEV) for the first assessment of occlusive properties.

**Principle:** Components used to design an in vitro bench test mimic the body conditions, such as blood pressure and temperature, however cannot imitate perfectly.

The bench test was designed to apply increasing pressure to the embolic agent filling a tube mimicking a blood vessel, while the pressure is measured accurately and continuously, in order to detect possible leakage through the gel. The applied pressure must be as large as 200 mmHg since mean blood systolic pressure is 95-140 mmHg but can reach up to 200 mmHg at least.

**Experimental section**

The solution used in this test has a viscosity similar to blood (dynamic viscosity of 5 cps). This is obtained with a mixture of 40% glycerol (v / v) and 60% distilled water (v / v). Silicon is chosen for the tubes, in order to achieve mechanical properties close to those of arteries (Young's modulus of 1.50 MPa) [Raz, 2007 #182]. The silicon tubes of 3.175 mm inside diameter and 1.6 mm thickness (VWR) are used to mimic the arteries. The tubes are immersed in a water bath at 37ºC to simulate body temperature. The applied pressure is increased continuously and can be recorded to obtain reproducible curves.

A syringe pump (PHD 2000 Programmable, Harvard Apparatus) could push the liquid (40% glycerol (v / v) and 60% distilled water (v / v)) in the tubes increasing the pressure until a minimum pressure of 220 mm Hg.

First a tubular segment filled with embolic product is left to gel in an incubator during various periods. Then the filled tube is placed in the embedded position and the applied pressure is increased until all of the fluid elapsed or until the embolizing fluid passes. The pressure gauge (DPM4, Fluke Biomedical) allows measuring the pressure continuously. It is also possible to connect to a computer to record the data obtained. On the other hand, it only measures the pressure of the gases. This requires an expansion chamber to allow the liquid to enter and increase the pressure without coming into direct contact with the pressure gauge. The final design of the test bench is shown in (Fig.E1).

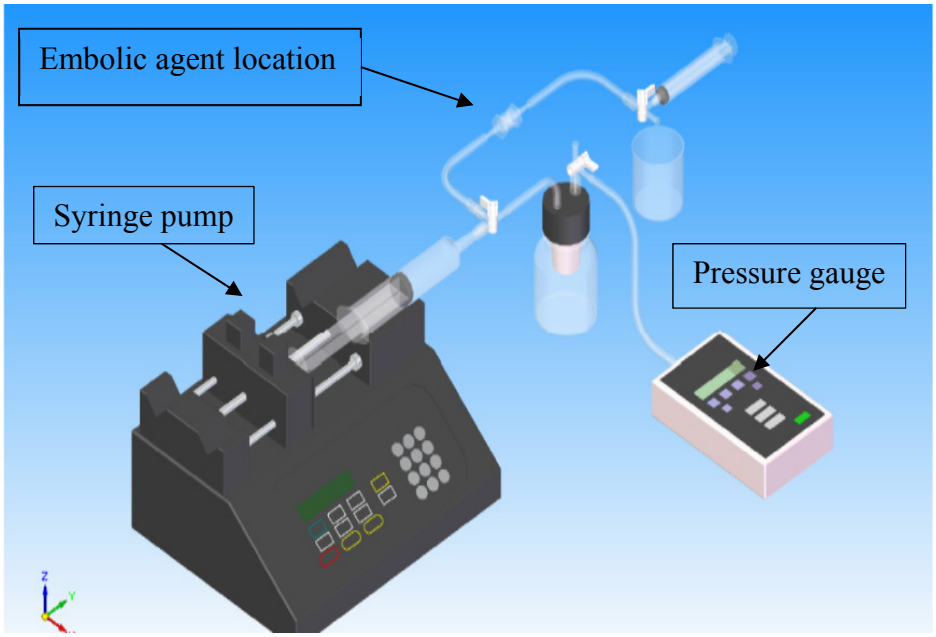


Figure E1 Schematic representation of the in vitro embolization bench test

## Injectability test

**Principle**: To verify injectability of the gel and evaluate the maximal force needed for injection as a function of time, the injectability test was developed. The embolizing agent must be able to flow through the microcatheter when applying a reasonable force at controlled displacement rate of the injection syringe.

**Experimental procedure**

The test was designed on a BOSE system ElectroForce® 3220 Series II test instrument with standard 0.5 inch (12.5 mm) displacement transducer and 50 lb (225 N) force transducer (Load cell 1) applying on the 1 ml syringe (Micro Therapeutics) connected to an infusion catheter (137 cm length and 0.61 mm internal diameter, FasT-325, Boston scientific, cork, Ireland) (see Fig. E3). The displacement rate is 0.8 mm/s to inject the gel, on a distance of 12mm. The required force to flow the gel outside the catheter after different times of gelation (0, 20, 60 min) was evaluated and recorded.

The curves (force N versus time) allow finding the maximum force value. Figure E2 presents the schematic representation of the injectability test.

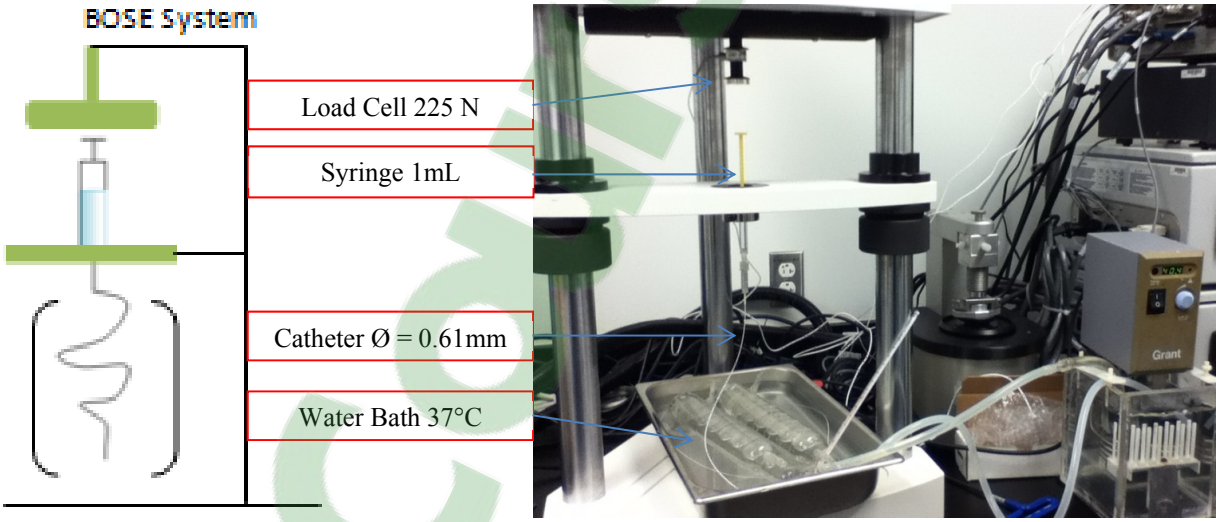


Figure E2 Injectability test set up using the Electroforce 3200 (Bose)

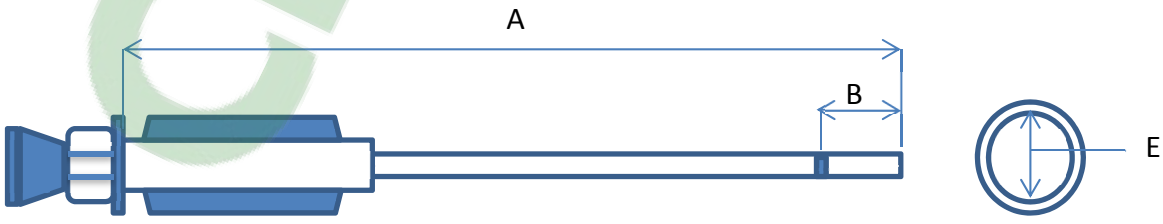

| A | B | E |
|---|---|---|
| 140 cm | 8 cm | 0.61mm |

Figure E3 Schematic representation of the catheter (FasT-325, Boston scientific, cork, Ireland

**Rheological properties**

**Principle**: Rheological properties are measured by deformation of sample under the influence of imposed stress. Strain sweep and frequency sweep were first performed to determine the linear viscoelastic region (LVE) and then rheological properties were evaluated in this region.

Shear modulus (G*) is composed of the storage modulus (G') and the loss modulus (G"). In fact, for solid materials, we can neglect the viscous module, as it is very small compared to the elastic module. So the shear module is approximately equal to the elastic modulus for solids. Conversely, for liquids shear modulus is approximately equal to the viscous modulus.

For gels, which are a form of material between the solid phase and the liquid phase, both the elastic modulus and the viscous modulus must be taken into account to evaluate the shear modulus.

The rheological properties of the embolic agents will be determined and compared. In this test, viscoelastic and gelation properties (gelation time and gelation rate) of the hydrogel solution as a function of time and temperature is determined immediately after mixing the two solutions of hydrogels or Onyx-Et mixture, using a rheometer (Physica MCR301 (Anton Paar) with coaxial cylinder geometry (CC10/T200) (Fig.E4).

An embolic agent requires a rapid solidification and for hydrogels enhanced viscoelastic properties after gelation. So the storage (G') and loss (G'') moduli versus time is evaluated as a function of gel composition, temperature etc.

**Gelation time:** the time interval between the addition of the "catalyst" into a liquid adhesive system and the formation of a gel.

According to the theory of Winter [Winter, 1986 #180], as shown in the Fig.E5, the crossover point of G' and G" correspond to the gelation time.

Figure E4 Rheometer (Physica MCR301 (Anton Paar)

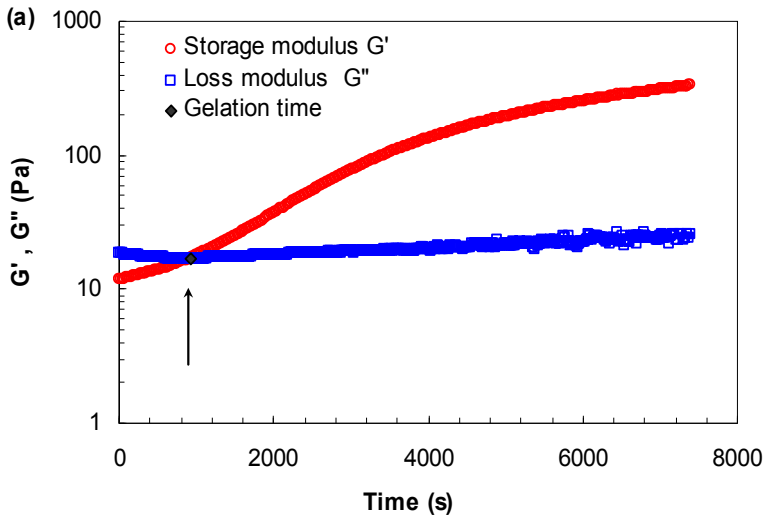


Figure E5 Storage (G') and loss (G'') moduli versus time for a radiopaque chitosan hydrogel (2% w/v CH, 12% w/v b-GP, 20% v/v IOP). Measurement was performed at a fixed temperature (37℃), frequency (1 Hz), strain (1%)

Fig E5 shows a typical curve for solutions containing 0% STS. Initially, G' is lower than G'', but it continually increases with time, while the loss modulus reaches a pseudo-plateau.

The quicker increase in G' compared with G'' with time leads to a crossover point which shows the gelation time.

**Rheolution test**

**Principle**: VeTBiM is a novel measurements technique of viscoelastic properties of the hydrogels after complete gelation as a function of time or temperature in real time, without contact, and nondestructively. It has been implemented in the analytical instrument ElastoSens™Bio (Rheolution, Montreal, Canada) which specifically measures the storage (G´) and loss (G") moduli of the complex linear shear modulus of gels. By this method, materials may be mechanically tested in three configurations using the dynamic displacement response of a material to a low amplitude vibration.

**Experimental procedure**: This non-destructive and contactless method was previously described in details and validated [Ceccaldi, 2016 #312]. Briefly, 2 mL of each formulation solution was added to a specific detachable sample holder containing an elastic membrane at its bottom and then 2mL of PBS were added on top of the samples and incubation at 37 °C was continued until 24h. Subsequently supernatants were removed and sample holders were firmly attached to the instrument before measuring storage moduli (G'). Free resonances of the samples in the LVE were detected between 20 and 200 Hz. In this technique, a laser is applied to measure the displacement of the material during the vibration and then this data is converted to storage (G′) and loss (G″) moduli by a theoretical model that takes into account the volume of the sample, the properties of the sample holder membrane and the excitation signal.

# LIST OF BIBLIOGRAPHICAL REFERENCES


Abularrage, C. J., Patel, V. I., Conrad, M. F., Schneider, E. B., Cambria, R. P., & Kwolek, C. J. (2012). Improved results using Onyx glue for the treatment of persistent type 2 endoleak after endovascular aneurysm repair. *Journal of vascular surgery, 56*(3), 630-636.

Adolph, R., Vorp, D. A., Steed, D. L., Webster, M. W., Kameneva, M. V., & Watkins, S. C. (1997). Cellular content and permeability of intraluminal thrombus in abdominal aortic aneurysm. *Journal of vascular surgery, 25*(5), 916-926.

Ahmadi, Oveisi, Z., Samani, S. M., & Amoozgar, Z. (2015). Chitosan based hydrogels: characteristics and pharmaceutical applications. *Research in Pharmaceutical Sciences, 10*(1), 1-16.

Ahmadi, R., & de Bruijn, J. D. (2008). Biocompatibility and gelation of chitosan–glycerol phosphate hydrogels. *Journal of Biomedical Materials Research Part A, 86*(3), 824-832.

Ahmed, R., Ghoorah, K., & Kunadian, V. (2016). Abdominal Aortic Aneurysms and Risk Factors for Adverse Events. *Cardiology in Review, 24*(2), 88-93.

Ailawadi, G., Eliason, J. L., & Upchurch, G. R., Jr. (2003). Current concepts in the pathogenesis of abdominal aortic aneurysm. *Journal of vascular surgery, 38*(3), 584-588.

Albanese, G., & Kondo, K. L. (2010). Pharmacology of Sclerotherapy. *Seminars in Interventional Radiology, 27*(4), 391-399.

Ambekar, S., Gaynor, B. G., Peterson, E. C., & Elhammady, M. S. (2016). Long-term angiographic results of endovascularly "cured" intracranial dural arteriovenous fistulas. *Journal of Neurosurgery, 124*(4), 1123-1127.

Annabi, B., Shédid, D., Ghosn, P., Kenigsberg, R. L., Desrosiers, R. R., Bojanowski, M. W., Béliveau, R. (2002). Differential regulation of matrix metalloproteinase activities in abdominal aortic aneurysms. *Journal of vascular surgery, 35*(3), 539-546.

Assaad, E., Maire, M., & Lerouge, S. (2015). Injectable thermosensitive chitosan hydrogels with controlled gelation kinetics and enhanced mechanical resistance. *Carbohydrate Polymers, 130*, 87-96.

Ayad, M., Eskioglu, E., & Mericle, R. A. (2006). Onyx: a unique neuroembolic agent. *Expert Review of Medical Devices, 3*(6), 705-715.

Barnett, B. P., & Gailloud, P. (2011). Assessment of EmboGel—A Selectively Dissolvable Radiopaque Hydrogel for Embolic Applications. *Journal of vascular and interventional radiology, 22*(2), 203-211.

Barnett, B. P., Hughes, A. H., Lin, S., Arepally, A., & Gailloud, P. H. (2009). In Vitro Assessment of EmboGel and UltraGel Radiopaque Hydrogels for the Endovascular Treatment of Aneurysms. *Journal of vascular and interventional radiology, 20*(4), 507-512.

Bartoli, M. A., Parodi, F. E., Chu, J., Pagano, M. B., Mao, D., Baxter, B. T., Thompson, R. W. (2006). Localized administration of doxycycline suppresses aortic dilatation in an

experimental mouse model of abdominal aortic aneurysm. *Annals of vascular surgery, 20*(2), 228-236.

Bastos, R. M., Razuk Filho, A., Blasbalg, R., Caffaro, R. A., Karakhanian, W. K., & Rocha, A. J. (2011). A multidetector tomography protocol for follow-up of endovascular aortic aneurysm repair. *Clinics, 66*, 2025-2029.

Baxter, B. T., Matsumura, J., Curci, J., McBride, R., Blackwelder, W. C., Liu, X., Terrin, M. L. (2016). Non-invasive Treatment of Abdominal Aortic Aneurysm Clinical Trial (N-TA3CT): Design of a Phase IIb, placebo-controlled, double-blind, randomized clinical trial of doxycycline for the reduction of growth of small abdominal aortic aneurysm. *Contemporary clinical trials, 48*, 91-98.

Berger, J., Reist, M., Mayer, J., Felt, O., & Gurny, R. (2004). Structure and interactions in chitosan hydrogels formed by complexation or aggregation for biomedical applications. *European Journal of Pharmaceutics and Biopharmaceutics, 57*(1), 35-52.

Bernkop-Schnürch, A., Humenberger, C., & Valenta, C. (1998). Basic studies on bioadhesive delivery systems for peptide and protein drugs. *International journal of pharmaceutics, 165*(2), 217-225.

Bloom, D. C., Perkins, J. A., & Manning, S. C. (2004). Management of lymphatic malformations. *Current Opinion in Otolaryngology & Head and Neck Surgery, 12*(6), 500-504.

Bonvini, R., Alerci, M., Antonucci, F., Tutta, P., Wyttenbach, R., Bogen, M., Gallino, A. (2003). Preoperative Embolization of Collateral Side Branches: A Valid Means to Reduce Type II Endoleaks After Endovascular AAA Repair. *Journal of Endovascular Therapy, 10*(2), 227-232.

Bosman, W. M. P. F., Vlot, J., van der Steenhoven, T. J., van den Berg, O., Hamming, J. F., de Vries, A. C., Jacobs, M. J. (2010). Aortic Customize: An In Vivo Feasibility Study of a Percutaneous Technique for the Repair of Aortic Aneurysms Using Injectable Elastomer. *European journal of vascular and endovascular surgery, 40*(1), 65-70.

Brewster, D. C., Jones, J. E., Chung, T. K., Lamuraglia, G. M., Kwolek, C. J., Watkins, M. T., Cambria, R. P. (2006). Long-term outcomes after endovascular abdominal aortic aneurysm repair: the first decade. *Annals of surgery, 244*(3), 426-438.

Burrows, P. E., & Mason, K. P. (2004). Percutaneous Treatment of Low Flow Vascular Malformations. *Journal of vascular and interventional radiology, 15*(5), 431-445.

Burrows, P. E., Mitri, R. K., Alomari, A., Padua, H. M., Lord, D. J., Sylvia, M. B., Mulliken, J. B. (2008). Percutaneous sclerotherapy of lymphatic malformations with doxycycline. *Lymphatic research and biology, 6*(3-4), 209-216.

Cabrera, J., Cabrera, J., Jr., Garcia-Olmedo, M. A., & Redondo, P. (2003). Treatment of venous malformations with sclerosant in microfoam form. *Archives of dermatology, 139*(11), 1409-1416.

Cahill, A. M., Nijs, E., Ballah, D., Rabinowitz, D., Thompson, L., Rintoul, N., Low, D. (2011). Percutaneous sclerotherapy in neonatal and infant head and neck lymphatic malformations: a single center experience. *Journal of pediatric surgery, 46*(11), 2083-2095.

Cao, P., De Rango, P., Verzini, F., & Parlani, G. (2010). Endoleak after endovascular aortic repair: classification, diagnosis and management following endovascular thoracic and abdominal aortic repair. *Journal of Cardiovascular Surgery, 51*(1), 53.

Caouette-Laberge, L. Emmanuel A. Ameh Louise Caouette-Laberge Jean-Martin Laberge.

Carter, A. J., Aggarwal, M., Kopia, G. A., Tio, F., Tsao, P. S., Kolata, R., Falotico, R. (2004). Long-term effects of polymer-based, slow-release, sirolimus-eluting stents in a porcine coronary model. *Cardiovascular Research, 63*(4), 617-624.

Ceccaldi, C., Assaad, E., Hui, E., Buccionyte, M., Adoungotchodo, A., & Lerouge, S. (2017). Optimization of Injectable Thermosensitive Scaffolds with Enhanced Mechanical Properties for Cell Therapy. *Macromolecular Bioscience*. 17(6), 1600435.

Ceccaldi, C., Strandman, S., Hui, E., Montagnon, E., Schmitt, C., Hadj Henni, A., Lerouge, S., (2017). Validation and application of a nondestructive and contactless method for rheological evaluation of biomaterials. *Journal of Biomedical Materials Research Part B: Applied Biomaterials,105(8), 2565-257.*

Chaloupka, J. C., Huddle, D. C., Alderman, J., Fink, S., Hammond, R., & Vinters, H. V. (1999). A Reexamination of the Angiotoxicity of Superselective Injection of DMSO in the Swine Rete Embolization Model. *American Journal of Neuroradiology, 20*(3), 401-410.

Chaudry, G., Burrows, P. E., Padua, H. M., Dillon, B. J., Fishman, S. J., & Alomari, A. I. (2011). Sclerotherapy of abdominal lymphatic malformations with doxycycline. *Journal Of Vascular And Interventional Radiology, 22*(10), 1431-1435.

Chen, Y., Fan, Y., Poon, K., Achrol, A. S., Lawton, M. T., Zhu, Y., Barbaro, N. M. (2006). MMP-9 expression is associated with leukocytic but not endothelial markers in brain arteriovenous malformations. *Frontiers in bioscience: a journal and virtual library, 11*, 3121-3128.

Chenite, A., Buschmann, M., Wang, D., Chaput, C., & Kandani, N. (2001). Rheological characterisation of thermogelling chitosan/glycerol-phosphate solutions. *Carbohydrate Polymers, 46*(1), 39-47.

Cho, S. K., Do, Y. S., Shin, S. W., Kim, D.-I., Kim, Y. W., Park, K. B., Choo, I.-W. (2006). Arteriovenous malformations of the body and extremities: analysis of therapeutic outcomes and approaches according to a modified angiographic classification. *Journal of Endovascular Therapy, 13*(4), 527-538.

Choke, E., Cockerill, G., Wilson, W. R., Sayed, S., Dawson, J., Loftus, I., & Thompson, M. M. (2005). A review of biological factors implicated in abdominal aortic aneurysm rupture. *European Journal of Vascular and Endovascular Surgery, 30*(3), 227-244.

Chu, J. F. (2006). *Patent Identifier No. US2008005043 6A1*, Methods and compounds for obliteration of vessels: Google Patents.

Chun, J. Y., & Morgan, R. (2013). Transcatheter embolisation of type 1 endoleaks after endovascular aortic aneurysm repair with Onyx: when no other treatment option is feasible. *European journal of vascular and endovascular surgery, 45*(2), 141-144.

Chung, R., & Morgan, R. A. (2015). Type 2 Endoleaks Post-EVAR: Current Evidence for Rupture Risk, Intervention and Outcomes of Treatment. *CardioVascular and Interventional Radiology, 38*(3), 507-522.

Coutu, J. M., Fatimi, A., Berrahmoune, S., Soulez, G., & Lerouge, S. (2013). A new radiopaque embolizing agent for the treatment of endoleaks after endovascular repair: influence of

contrast agent on chitosan thermogel properties. *Journal of Biomedical Materials Research Part B: Applied Biomaterials, 101*(1), 153-161.

Creech, O., Jr. (1966). Endo-aneurysmorrhaphy and treatment of aortic aneurysm. *Annals of Surgery, 164*(6), 935-946.

Crotty, K. L., Orihuela, E., & Warren, M. M. (1993). Recent Advances in the Diagnosis and Treatment of Renal Arteriovenous Malformations and Fistulas. *The Journal of Urology, 150*(5, Part 1), 1355-1359.

Do, Y. S., Park, K.-B., & Cho, S. K. (2007). How do we treat arteriovenous malformations (tips and tricks)? *Techniques in vascular and interventional radiology, 10*(4), 291-298.

Do, Y. S., Park, K. B., Park, H. S., Cho, S. K., Shin, S. W., Moon, J. W., Lee, S. H. (2010). Extremity arteriovenous malformations involving the bone: therapeutic outcomes of ethanol embolotherapy. *Journal of vascular and interventional radiology, 21*(6), 807-816.

Do, Y. S., Yakes, W. F., Shin, S. W., Lee, B.-B., Kim, D.-I., Liu, W. C., Choo, I.-W. (2005). Ethanol embolization of arteriovenous malformations: interim results. *Radiology, 235*(2), 674-682.

Dompmartin, A., Blaizot, X., Theron, J., Hammer, F., Chene, Y., Labbe, D., Boon, L. M. (2011). Radio-opaque ethylcellulose-ethanol is a safe and efficient sclerosing agent for venous malformations. *European Radiology, 21*(12), 2647-2656.

Dondelinger, R. F., & Adler, O. B. (1990). *Interventional radiology*: New York : Georg Thieme.

Dubois, J., Soulez, G., Oliva, V. L., Berthiaume, M. J., Lapierre, C., & Therasse, E. (2001). Soft-tissue venous malformations in adult patients: imaging and therapeutic issues. *Radiographics, 21*(6), 1519-1531.

Durdu, S., Deniz, G. C., Balci, D., Zaim, C., Dogan, A., Can, A., Akar, A. R. (2012). Apoptotic vascular smooth muscle cell depletion via BCL2 family of proteins in human ascending aortic aneurysm and dissection. *Cardiovascular therapeutics, 30*(6), 308-316.

Eberhardt, K. M., Sadeghi-Azandaryani, M., Worlicek, S., Koeppel, T., Reiser, M. F., & Treitl, M. (2014). Treatment of type I endoleaks using transcatheter embolization with onyx. *Journal of Endovascular Therapy, 21*(1), 162-171.

Elhammady, M. S., Peterson, E. C., Johnson, J. N., & Aziz-Sultan, M. A. (2012). Preoperative onyx embolization of vascular head and neck tumors by direct puncture. *World neurosurgery, 77*(5), 725-730.

Ellman, B. A., Parkhill, B. J., Marcus, P. B., Curry, T. S., & Peters, P. C. (1984). Renal Ablation with Absolute Ethanol: Mechanism of Action. *Investigative radiology, 19*(5), 416-423.

Fabian Alejandro, G., Luis Ernesto, B., & Hernando Yesid, E. (2017). Morphological Characterization of the Renal Arteries in the Pig. Comparative Analysis with the Human. *International Journal of Morphology, 35*(1).

Fang, J.-Y., Chen, J.-P., Leu, Y.-L., & Hu, J.-W. (2008). Temperature-sensitive hydrogels composed of chitosan and hyaluronic acid as injectable carriers for drug delivery. *European Journal of Pharmaceutics and Biopharmaceutics, 68*(3), 626-636.

Fatimi, A., Chabrot, P., Berrahmoune, S., Coutu, J. M., Soulez, G., & Lerouge, S. (2012). A new injectable radiopaque chitosan-based sclerosing embolizing hydrogel for endovascular therapies. *Acta Biomaterialia, 8*(7), 2712-2721.

Fatimi, A., Zehtabi, F., & Lerouge, S. (2016). Optimization and characterization of injectable chitosan-iodixanol-based hydrogels for the embolization of blood vessels. *Journal of biomedical materials research. Part B, Applied biomaterials, 104*(8), 1551-1562.

Fievez, M. (1989). Aneurysms and Arterial Dissections. In J.-P. Camilleri, C. L. Berry, J.-N. Fiessinger, & J. Bariéty (Eds.), *Diseases of the Arterial Wall* (pp. 533-545). London: Springer London.

Franklin, I. J., Harley, S. L., Greenhalgh, R. M., & Powell, J. T. (1999). Uptake of tetracycline by aortic aneurysm wall and its effect on inflammation and proteolysis. *British Journal of Surgery, 86*(6), 771-775.

Gandhi, R., & Bryce, Y. (2016). Management of Type II Endoleaks: Available Options for Treating the Most Common Type of Endoleak After EVAR. *Endovascular Today, 15*(4).

Ganji, F., Abdekhodaie, M. J., & Ramazani S.A., A. (2007). Gelation time and degradation rate of chitosan-based injectable hydrogel. *Journal of Sol-Gel Science and Technology, 42*(1), 47-53.

Geisbusch, P., Katzen, B. T., Tsoukas, A. I., Arango, D., Pena, C. S., & Benenati, J. F. (2011). Endovascular repair of infrarenal aortic aneurysms in octogenarians and nonagenarians. *Journal of Vascular Surgery, 54*(6), 1605-1613.

George, M., & Abraham, T. E. (2006). Polyionic hydrocolloids for the intestinal delivery of protein drugs: Alginate and chitosan — a review. *Journal of Controlled Release, 114*(1), 1-14.

Ghouri, M., & Krajcer, Z. (2010). Endoluminal abdominal aortic aneurysm repair: the latest advances in prevention of distal endograft migration and type 1 endoleak. *Texas Heart Institute Journal, 37*(1), 19.

Gibas, I., & Janik, H. (2010). Review: synthetic polymer hydrogels for biomedical applications. *Chemistry & Chemical Technology*, 4(4), 297-304

Gilbard, J. P., Gilbard, E., Fieldson, G., & Huson, R. B. (2012). *Patent Identifier No. US20120190653A1*, Therapeutic eye drop comprising doxycycline and a stabilizer: Google Patents.

Golzarian, J., Dussaussois, L., Ait Said, K., Abada, H. T., Dereume, J. P., & Struyven, J. (2002). Embolization of large aneurysms with long wire coils. *Cardiovascular and Interventional Radiology, 25*(1), 26-29.

Golzarian, J., Maes, E. B., & Sun, S. (2005). Endoleak: treatment options. *Techniques in vascular and interventional radiology, 8*(1), 41-49.

Golzarian, J., Struyven, J., Abada, H. T., Wery, D., Dussaussois, L., Madani, A., Dereume, J. P. (1997). Endovascular aortic stent-grafts: transcatheter embolization of persistent perigraft leaks. *Radiology, 202*(3), 731-734.

Gomes, A. S. (1994). Embolization therapy of congenital arteriovenous malformations: use of alternate approaches. *Radiology, 190*(1), 191-198.

Grzela, T., Bikowska, B., & Litwiniuk, M. (2011). Matrix metalloproteinases in aortic aneurysm-executors or executioners? *Etiology, Pathogenesis and Pathophysiology of Aortic Aneurysms and Aneurysm Rupture*: InTech.

Guidebook, M. (2012). *Medifocus Guidebook On: Abdominal Aortic Aneurysm*: CreateSpace Independent Publishing Platform.

Gulrez, S. K. H., & Al-Assaf, S. (2011). *Hydrogels: Methods of Preparation, Characterisation and Applications*.

Hackmann, A. E., Rubin, B. G., Sanchez, L. A., Geraghty, P. A., Thompson, R. W., & Curci, J. A. A randomized, placebo-controlled trial of doxycycline after endoluminal aneurysm repair. *Journal of vascular surgery, 48*(3), 519-526.

Hamada, J., Kai, Y., Morioka, M., Kazekawa, K., Ishimaru, Y., Iwata, H., & Ushio, Y. (2002). A mixture of ethylene vinyl alcohol copolymer and ethanol yielding a nonadhesive liquid embolic agent to treat cerebral arteriovenous malformations: initial clinical experience. *Journal of Neurosurgery, 97*(4), 881-888.

Hashimoto, T., Wen, G., Lawton, M. T., Boudreau, N. J., Bollen, A. W., Yang, G.-Y., Halbach, V. V. (2003). Abnormal expression of matrix metalloproteinases and tissue inhibitors of metalloproteinases in brain arteriovenous malformations. *Stroke, 34*(4), 925-931.

Health Quality, O. (2006). Coil Embolization for Intracranial Aneurysms: An Evidence-Based Analysis. *Ontario Health Technology Assessment Series, 6*(1), 1-114.

Heinemann, C., Heinemann, S., Bernhardt, A., Lode, A., Worch, H., & Hanke, T. (2010). In vitro osteoclastogenesis on textile chitosan scaffold. *European cells & materials, 19*, 96-106.

Henderson, E. L., Geng, Y.-J., Sukhova, G. K., Whittemore, A. D., Knox, J., & Libby, P. (1999). Death of smooth muscle cells and expression of mediators of apoptosis by T lymphocytes in human abdominal aortic aneurysms. *Circulation, 99*(1), 96-104.

Hennink, W. E., & van Nostrum, C. F. (2002). Novel crosslinking methods to design hydrogels. *Advanced Drug Delivery Reviews, 54*(1), 13-36.

Henrikson, O., Roos, H., & Falkenberg, M. (2011). Ethylene vinyl alcohol copolymer (Onyx) to seal type 1 endoleak. A new technique. *Vascular, 19*(2), 77-81.

Hinterseher, I., Gäbel, G., Corvinus, F., Lück, C., Saeger, H., Bergert, H., Kuivaniemi, H. (2012). Presence of Borrelia burgdorferi sensu lato antibodies in the serum of patients with abdominal aortic aneurysms. *European journal of clinical microbiology & infectious diseases, 31*(5), 781-789.

Hiramoto, J. S., Reilly, L. M., Schneider, D. B., Sivamurthy, N., Rapp, J. H., & Chuter, T. A. M. (2007). Long-term outcome and reintervention after endovascular abdominal aortic aneurysm repair using the Zenith stent graft. *Journal of vascular surgery, 45*(3), 461-466.

Hobo, R., & Buth, J. (2006). Secondary interventions following endovascular abdominal aortic aneurysm repair using current endografts. A EUROSTAR report. *Journal of Vascular Surgery, 43*(5), 896-902.

Houbballah, R., Mallios, A., Poussier, B., Soury, P., Fukui, S., Gigou, F., & Laurian, C. (2010). A new therapeutic approach to congenital pelvic arteriovenous malformations. *Annals of vascular surgery, 24*(8), 1102-1109.

Huang, R. Y. M., Moon, G. Y., & Pal, R. (2001). Chitosan/anionic surfactant complex membranes for the pervaporation separation of methanol/MTBE and characterization of the polymer/surfactant system. *Journal of Membrane Science, 184*(1), 1-15.

Joseph D., (1976), *Hydrogels for Medical and Related Applications*. Utah:American chemical society.

Hyodoh, H., Hori, M., Akiba, H., Tamakawa, M., Hyodoh, K., & Hareyama, M. (2005). Peripheral vascular malformations: imaging, treatment approaches, and therapeutic issues. *Radiographics, 25*(suppl_1), S159-S171.

Jackson, J. E., Mansfield, A. O., & Allison, D. J. (1996). Treatment of high-flow vascular malformations by venous embolization aided by flow occlusion techniques. *CardioVascular and Interventional Radiology, 19*(5), 323-328.

Jacobowitz, G. R., Rosen, R. J., Rockman, C. B., Nalbandian, M., Hofstee, D. J., Fioole, B., . . . Riles, T. S. (2001). Transcatheter embolization of complex pelvic vascular malformations: results and long-term follow-up. *Journal of vascular surgery, 33*(1), 51-55.

Jayaraman, M. V., Marcellus, M. L., Hamilton, S., Do, H. M., Campbell, D., Chang, S. D., Marks, M. P. (2008). Neurologic Complications of Arteriovenous Malformation Embolization Using Liquid Embolic Agents. *American Journal of Neuroradiology, 29*(2), 242-246.

Jeong, H.-S., Baek, C.-H., Son, Y.-I., Wook Kim, T., Bung Lee, B., & Sik Byun, H. (2006). Treatment for extracranial arteriovenous malformations of the head and neck. *Acta oto-laryngologica, 126*(3), 295-300.

Jin, Y., Lin, X., Li, W., Hu, X., Ma, G., & Wang, W. (2008). Sclerotherapy after embolization of draining vein: a safe treatment method for venous malformations. *Journal of vascular surgery, 47*(6), 1292-1299.

Kademani, D., Costello, B. J., Ditty, D., & Quinn, P. (2004). An alternative approach to maxillofacial arteriovenous malformations with transosseous direct puncture embolization. *Oral Surgery, Oral Medicine, Oral Pathology, Oral Radiology, and Endodontology, 97*(6), 701-706.

Kaito, K., Urayama, H., & Watanabe, G. (2003). Doxycycline treatment in a model of early abdominal aortic aneurysm. *Surgery today, 33*(6), 426-433.

Khaja, M. S., Park, A. W., Swee, W., Evans, A. J., Fritz Angle, J., Turba, U. C., Matsumoto, A. H. (2014). Treatment of type II endoleak using Onyx with long-term imaging follow-up. *CardioVascular and Interventional Radiology, 37*(3), 613-622.

Kim, I.-Y., Seo, S.-J., Moon, H.-S., Yoo, M.-K., Park, I.-Y., Kim, B.-C., & Cho, C.-S. (2008). Chitosan and its derivatives for tissue engineering applications. *Biotechnology Advances, 26*(1), 1-21.

Kroon, A. M., & Taanman, J.-W. (2015). Clonal Expansion of T Cells in Abdominal Aortic Aneurysm: A Role for Doxycycline as Drug of Choice? *International journal of molecular sciences, 16*(5), 11178-11195.

Kuivaniemi, H., Ryer, E., Richard Yoon, H., Elmore, J., & Tromp, G. (2013). *Genetic risk factors for abdominal aortic aneurysms (AAA)*, 1-30.

Kuivaniemi, H., Ryer, E. J., Elmore, J. R., & Tromp, G. (2015). Understanding the pathogenesis of abdominal aortic aneurysms. *Expert review of cardiovascular therapy, 13*(9), 975-987.

Kumar, D. R., Hanlin, E., Glurich, I., Mazza, J. J., & Yale, S. H. (2010). Virchow's Contribution to the Understanding of Thrombosis and Cellular Biology. *Clinical Medicine & Research, 8*(3-4), 168-172.

Lerouge, S., Bonneviot, M. C., Salazkin, I., Raymond, J., & Soulez, G. (2011). Endothelial denudation combined with embolization in the prevention of endoleaks after

endovascular aneurysm repair: an animal study. *Journal of Endovascular Therapy, 18*(5), 686-696.

Lerouge, S., Raymond, J., Salazkin, I., Qin, Z., Gaboury, L., Cloutier, G., Soulez, G. (2004). Endovascular aortic aneurysm repair with stent-grafts: experimental models can reproduce endoleaks. *Journal of vascular and interventional radiology*
*15*(9), 971-979.

Lerouge, S., Soulez, G., Fatimi, A., Coutu, J., & Raymond, J. (2011). *Patent Identifier No. US8840867B2,* Embolizing Sclerosing Hydrogel: Google Patents.

Lindeman, J. H., Abdul-Hussien, H., van Bockel, J. H., Wolterbeek, R., & Kleemann, R. (2009). Clinical trial of doxycycline for matrix metalloproteinase-9 inhibition in patients with an abdominal aneurysm doxycycline selectively depletes aortic wall neutrophils and cytotoxic t cells. *Circulation, 119*(16), 2209-2216.

Liu, J., Xiong, W., Baca-Regen, L., Nagase, H., & Baxter, B. T. (2003). Mechanism of inhibition of matrix metalloproteinase-2 expression by doxycycline in human aortic smooth muscle cells. *Journal of vascular surgery, 38*(6), 1376-1383.

Loh, Y., & Duckwiler, G. R. (2010). A prospective, multicenter, randomized trial of the Onyx liquid embolic system and N-butyl cyanoacrylate embolization of cerebral arteriovenous malformations. *Journal of Neurosurgery, 113*(4), 733-741.

Lu, S., White, J. V., Lin, W. L., Zhang, X., Solomides, C., Evans, K., Monos, D. S. (2014). Aneurysmal lesions of patients with abdominal aortic aneurysm contain clonally expanded T cells. *The Journal of Immunology*, 1301009.

Madan, M., Bajaj, A., Lewis, S., Udupa, N., & Baig, J. A. (2009). In Situ Forming Polymeric Drug Delivery Systems. *Indian Journal of Pharmaceutical Sciences, 71*(3), 242-251.

Maeda, N., Verret, V., Moine, L., Bedouet, L., Louguet, S., Servais, E., Laurent, A. (2013). Targeting and recanalization after embolization with calibrated resorbable microspheres versus hand-cut gelatin sponge particles in a porcine kidney model. *Journal Of Vascular And Interventional Radiology, 24*(9), 1391-1398.

Martin, M. L., Dolmatch, B. L., Fry, P. D., & Machan, L. S. (2001). Treatment of Type II Endoleaks with Onyx. *Journal of vascular and interventional radiology, 12*(5), 629-632.

Meijer, C. A., Stijnen, T., Wasser, M. N., Hamming, J. F., van Bockel, J. H., & Lindeman, J. H. (2013). Doxycycline for stabilization of abdominal aortic aneurysms: a randomized trial. *Annals of internal medicine, 159*(12), 815-823.

Moulakakis, K. G., Dalainas, I., Mylonas, S., Giannakopoulos, T. G., Avgerinos, E. D., & Liapis, C. D. (2010). Conversion to open repair after endografting for abdominal aortic aneurysm: a review of causes, incidence, results, and surgical techniques of reconstruction. *Journal of Endovascular Therapy, 17*(6), 694-702.

Moxon, J. V., Parr, A., Emeto, T. I., Walker, P., Norman, P. E., & Golledge, J. (2010). Diagnosis and monitoring of abdominal aortic aneurysm: current status and future prospects. *Current problems in cardiology, 35*(10), 512-548.

Mujumdar, S. K., & Minnesota, U. o. (2008). *Stimuli Sensitive Hydrogels for Controlled Drug Delivery and Sensing Applications*: University of Minnesota.

Muller-Wille, R., Wohlgemuth, W. A., Heiss, P., Wiggermann, P., Guntner, O., Schreyer, A. G., Zorger, N. (2013). Transarterial embolization of type II endoleaks after EVAR: the

role of ethylene vinyl alcohol copolymer (Onyx). *CardioVascular and Interventional Radiology, 36*(5), 1288-1295.

Nakai, M., Ikoma, A., Sato, M., Sato, H., Nishimura, Y., & Okamura, Y. (2016). Prophylactic Intraoperative Embolization of Abdominal Aortic Aneurysm Sacs Using N-Butyl Cyanoacrylate/Lipiodol/Ethanol Mixture with Proximal Neck Aortic Balloon Occlusion during Endovascular Abdominal Aortic Repair. *Journal of vascular and interventional radiology, 27*(7), 954-960.

Nevala, T., Biancari, F., Manninen, H., Aho, P.-S., Matsi, P., Mäkinen, K., Perälä, J. (2010). Type II Endoleak After Endovascular Repair of Abdominal Aortic Aneurysm: Effectiveness of Embolization. *CardioVascular and Interventional Radiology, 33*(2), 278-284.

Nguyen, M. K., & Lee, D. S. (2010). Injectable Biodegradable Hydrogels. *Macromolecular Bioscience, 10*(6), 563-579.

Nicpon-Marieb, E., & Martin, T. (1998). *Human anatomy & physiology*: Benjamin Cummings.

Nordon, I. M., Karthikesalingam, A., Hinchliffe, R. J., Holt, P. J., Loftus, I. M., & Thompson, M. M. (2010). Secondary Interventions Following Endovascular Aneurysm Repair (EVAR) and the Enduring Value of Graft Surveillance. *European journal of vascular and endovascular surgery, 39*(5), 547-554.

Park, K., Ottenbrite, R. M., & Okano, T. (2010). *Biomedical Applications of Hydrogels Handbook*: Springer New York.

Parodi, J. C., Palmaz, J. C., & Barone, H. D. (1991). Transfemoral intraluminal graft implantation for abdominal aortic aneurysms. *Ann Vasc Surg, 5*(6), 491-499.

Peppas, N. A., Bures, P., Leobandung, W., & Ichikawa, H. (2000). Hydrogels in pharmaceutical formulations. *European Journal of Pharmaceutics and Biopharmaceutics, 50*, 27-46.

Peppas, N. A., Huang, Y., Torres-Lugo, M., Ward, J. H., & Zhang, J. (2000). Physicochemical foundations and structural design of hydrogels in medicine and biology. *Annual Review of Biomedical Engineering, 2*, 9-29.

Petrinec, D., Liao, S., Holmes, D. R., Reilly, J. M., Parks, W. C., & Thompson, R. W. (1996). Doxycycline inhibition of aneurysmal degeneration in an elastase-induced rat model of abdominal aortic aneurysm: preservation of aortic elastin associated with suppressed production of 92 kD gelatinase. *Journal of vascular surgery, 23*(2), 336-346.

Piai, J. F., Rubira, A. F., & Muniz, E. C. (2009). Self-assembly of a swollen chitosan/chondroitin sulfate hydrogel by outward diffusion of the chondroitin sulfate chains. *Acta Biomaterialia, 5*(7), 2601-2609.

Pollack, A. A., & Wood, E. H. (1949). Venous pressure in the saphenous vein at the ankle in man during exercise and changes in posture. *Journal of Applied Physiology, 1*(9), 649-662.

Prall, A. K., Longo, G. M., Mayhan, W. G., Waltke, E. A., Fleckten, B., Thompson, R. W., & Baxter, B. T. (2002). Doxycycline in patients with abdominal aortic aneurysms and in mice: comparison of serum levels and effect on aneurysm growth in mice. *Journal of vascular surgery, 35*(5), 923-929.

Prasetyono, T. O. H., & Kreshanti, P. (2010). Efficacy of intra-lesional alcohol injection as alternative and/or complementary treatment of vascular malformations: A systematic review. *Journal of Plastic, Reconstructive & Aesthetic Surgery, 63*(7), 1071-1079.

Qiu, Y., & Park, K. (2001). Environment-sensitive hydrogels for drug delivery. *Advanced Drug Delivery Reviews, 53*(3), 321-339.

Ravi Kumar, M. N. (2000). A review of chitin and chitosan applications. *Reactive and functional polymers, 46*(1), 1-27.

Raymond, J., Guilbert, F., Metcalfe, A., Gévry, G., Salazkin, I., & Robledo, O. (2004). Role of the Endothelial Lining in Recurrences After Coil Embolization Prevention of Recanalization by Endothelial Denudation. *Stroke, 35*(6), 1471-1475.

Raymond, J., Sauvageau, E., Salazkin, I., Ribourtout, E., Gevry, G., & Desfaits, A.-C. (2002). Role of the endothelial lining in persistence of residual lesions and growth of recurrences after endovascular treatment of experimental aneurysms. *Stroke, 33*(3), 850-855.

Reis, R. L., Neves, N. M., Mano, J. F., Gomes, M. E., Marques, A. P., & Azevedo, H. S. (2008). *Natural-based polymers for biomedical applications*: Woodhead Pub.

Rosen, R. J., & Green, R. M. (2008). Endoleak management following endovascular aneurysm repair. *J Vasc Interv Radiol, 19*(6 Suppl), S37-43.

Rosiak, J. M., & Yoshii, F. (1999). Hydrogels and their medical applications. *Nuclear Instruments and Methods in Physics Research Section B: Beam Interactions with Materials and Atoms, 151*(1–4), 56-64.

Rowe, V. L., Stevens, S. L., Reddick, T. T., Freeman, M. B., Donnell, R., Carroll, R. C., & Goldman, M. H. (2000). Vascular smooth muscle cell apoptosis in aneurysmal, occlusive, and normal human aortas. *Journal of vascular surgery, 31*(3), 567-576.

Saeed Kilani, M., Izaaryene, J., Cohen, F., Varoquaux, A., Gaubert, J. Y., Louis, G., Vidal, V. (2015). Ethylene vinyl alcohol copolymer (Onyx(R)) in peripheral interventional radiology: indications, advantages and limitations. *Diagnostic and Interventional Imaging, 96*(4), 319-326.

Saeed Kilani, M., Zehtabi, F., Lerouge, S., Soulez, G., Bartoli, J. M., Vidal, V., & Badran, M. F. (2017). New Alcohol and Onyx Mixture for Embolization: Feasibility and Proof of Concept in Both In Vitro and In Vivo Models. *Cardiovasc Intervent Radiol, 40*(5), 735-743.

Sakalihasan, N., Limet, R., & Defawe, O. D. (2005). Abdominal aortic aneurysm. *Lancet, 365*(9470), 1577-1589.

Sarac, T. P., Gibbons, C., Vargas, L., Liu, J., Srivastava, S., Bena, J., Clair, D. (2012). Long-term follow-up of type II endoleak embolization reveals the need for close surveillance. *Journal of vascular surgery, 55*(1), 33-40.

Schermerhorn, M. (2009). A 66-year-old man with an abdominal aortic aneurysm: review of screening and treatment. *JAMA, 302*(18), 2015-2022.

Seriki, D. M., Ashleigh, R. J., Butterfield, J. S., England, A., McCollum, C. N., Akhtar, N., & Welch, M. (2006). Midterm follow-up of a single-center experience of endovascular repair of abdominal aortic aneurysms with use of the Talent stent-graft. *Journal of vascular and interventional radiology, 17*(6), 973-977.

Shanmuganathan, S., Shanumugasundaram, N., Adhirajan, N., Lakshmi, T. R., & Babu, M. (2008). Preparation and characterization of chitosan microspheres for doxycycline delivery. *Carbohydrate Polymers, 73*(2), 201-211.

Sheehan, M. K., Barbato, J., Compton, C. N., Zajko, A., Rhee, R., & Makaroun, M. S. (2004). Effectiveness of coiling in the treatment of endoleaks after endovascular repair. *J Vasc Surg, 40*(3), 430-434.

Sho, E., Chu, J., Sho, M., Fernandes, B., Judd, D., Ganesan, P., Dalman, R. L. (2004). Continuous periaortic infusion improves doxycycline efficacy in experimental aortic aneurysms. *Journal of vascular surgery, 39*(6), 1312-1321.

Sina, A., Proulx-Bonneau, S., Roy, A., Poliquin, L., Cao, J., & Annabi, B. (2010). The lectin concanavalin-A signals MT1-MMP catalytic independent induction of COX-2 through an IKKγ/NF-κB-dependent pathway. *Journal of Cell Communication and Signaling, 4*(1), 31-38.

Siracuse, J., Schermerhorn, M., Meltzer, A., Eslami, M., Kalish, J., Rybin, D., Farber, A. (2016a). Comparison of outcomes after endovascular and open repair of abdominal aortic aneurysms in low-risk patients. *British Journal of Surgery, 103*(8), 989-994.

Siracuse, J., Schermerhorn, M., Meltzer, A., Eslami, M., Kalish, J., Rybin, D., Farber, A. (2016b). Comparison of outcomes after endovascular and open repair of abdominal aortic aneurysms in low-risk patients. *British Journal of Surgery*.

Soulez, G., Lerouge, S., Darsaut, T., Salazkin, I., Oliva, V. L., & Raymond, J. (2008). Role of the endothelial lining in endoleak formation and persistence after endovascular repair of aneurysm. *Journal of vascular and interventional radiology, 19*(7), 1070-1078.

Soulez, G., Lerouge, S., Salazkin, I., Darsaut, T., Oliva, V. L., & Raymond, J. (2007). Type I and collateral flow in experimental aneurysm models treated with stent-grafts. *Journal of vascular and interventional radiology, 18*(2), 265-272.

Stavropoulos, Clark, T. W. I., Carpenter, J. P., Fairman, R. M., Litt, H., Velazquez, O. C., Baum, R. A. (2005). Use of CT Angiography to Classify Endoleaks after Endovascular Repair of Abdominal Aortic Aneurysms. *Journal of vascular and interventional radiology, 16*(5), 663-667.

Stavropoulos, Kim, H., Clark, T. W., Fairman, R. M., Velazquez, O., & Carpenter, J. P. (2005). Embolization of type 2 endoleaks after endovascular repair of abdominal aortic aneurysms with use of cyanoacrylate with or without coils. *Journal of vascular and interventional radiology, 16*(6), 857-861.

Stavropoulos, Park, J., Fairman, R., & Carpenter, J. (2009). Type 2 endoleak embolization comparison: translumbar embolization versus modified transarterial embolization. *Journal of vascular and interventional radiology, 20*(10), 1299-1302.

Stavropoulos, S. W., & Charagundla, S. R. (2007). Imaging techniques for detection and management of endoleaks after endovascular aortic aneurysm repair. *Radiology, 243*(3), 641-655.

Tamimi, F., Torres Garcia-Denche, J., Bettini, R., Ruggera, F., Rueda, C., López-Ponce, M., & López-Cabarcos, E. (2008). *Doxycycline sustained release from brushie cements for the treatment of periodontal diseases* (Vol. 85).

Thein-Han, W. W., & Kitiyanant, Y. (2007). Chitosan scaffolds for in vitro buffalo embryonic stem-like cell culture: An approach to tissue engineering. *Journal of Biomedical Materials Research Part B: Applied Biomaterials, 80*(1), 92-101.

Theocharis, A. D., Tsolakis, I., Tsegenidis, T., & Karamanos, N. K. (1999). Human abdominal aortic aneurysm is closely associated with compositional and specific structural modifications at the glycosaminoglycan level. *Atherosclerosis, 145*(2), 359-368.

Thompson, Ashton, H., Gao, L., Buxton, M., & Scott, R. (2012). Final follow-up of the Multicentre Aneurysm Screening Study (MASS) randomized trial of abdominal aortic aneurysm screening. *British Journal of Surgery, 99*(12), 1649-1656.

Thompson, R. W., & Baxter, B. T. (1999). MMP inhibition in abdominal aortic aneurysms: rationale for a prospective randomized clinical trial. *Annals of the New York Academy of Sciences, 878*(1), 159-178.

Tiwari, G., Tiwari, R., Sriwastawa, B., Bhati, L., Pandey, S., Pandey, P., & Bannerjee, S. K. (2012). Drug delivery systems: An updated review. *International Journal of Pharmaceutical Investigation, 2*(1), 2-11.

Vaidya, S., Tozer, K. R., & Chen, J. (2008). An Overview of Embolic Agents. *Seminars in Interventional Radiology, 25*(3), 204-215.

van Zeeland, M. L., & van der Laan, L. Late Complications Following Aortic Aneurysm Repair. *Infection, 1*, 3.

Vardulaki, K., Walker, N., Day, N., Duffy, S., Ashton, H., & Scott, R. (2000). Quantifying the risks of hypertension, age, sex and smoking in patients with abdominal aortic aneurysm. *British Journal of Surgery, 87*(2), 195-200.

Wang, Y., Xu, N., Luo, Q., Li, Y., Sun, L., Wang, H., Zhen, Y. (2011). In Vivo Assessment of Chitosan/ β-Glycerophosphate as a New Liquid Embolic Agent. *Interventional Neuroradiology, 17*(1), 87-92.

Wei, T., Zhang, H., Cetin, N., Miller, E., Moak, T., Suen, J. Y., & Richter, G. T. (2016). Elevated Expression of Matrix Metalloproteinase-9 not Matrix Metalloproteinase-2 Contributes to Progression of Extracranial Arteriovenous Malformation. *Scientific reports, 6*, 24378.

White, S. B., & Stavropoulos, S. W. (2009). Management of Endoleaks following Endovascular Aneurysm Repair. *Seminars in Interventional Radiology, 26*(1), 33-38.

Wiegand, S., Eivazi, B., Zimmermann, A. P., Sesterhenn, A. M., & Werner, J. A. (2011). Sclerotherapy of lymphangiomas of the head and neck. *Head & neck, 33*(11), 1649-1655.

Wills, A., Thompson, M., Crowther, M., Sayers, R., & Bell, P. (1996). Pathogenesis of abdominal aortic aneurysms—cellular and biochemical mechanisms. *European journal of vascular and endovascular surgery, 12*(4), 391-400.

Wu, P., Lucchesi, L., Guo, J., Prahl, S., & Gregory, K. (2005). *DEVELOPMENT OF IN-VITRO ADHESION TEST FOR CHITOSAN BANDAGES.* Paper presented at the Society for Biomaterials 30th annual meeting transactions.

Yakes, W., & Parker, S. (1992). Diagnosis and management of vascular anomalies. *Interventional radiology, 1*, 152-189.

Zehtabi, F., Dumont-Mackay, V., Fatimi, A., Bertrand-Grenier, A., Héon, H., Soulez, G., & Lerouge, S. (2017). Chitosan–sodium tetradecyl sulfate hydrogel: Characterization and preclinical evaluation of a novel sclerosing embolizing agent for the treatment of endoleaks. *CardioVascular and Interventional Radiology, 40*(4), 576-584.

Zehtabi, F., Ispas-Szabo, P., Djerir, D., Sivakumaran, L., Annabi, B., Soulez, G., Lerouge, S. (2017). Chitosan-doxycycline hydrogel: An MMP inhibitor/sclerosing embolizing agent as a new approach to endoleak prevention and treatment after endovascular aneurysm repair. *Acta Biomaterialia, 64*(Supplement C), 94-105.

Zhu, J., & Marchant, R. E. (2011). Design properties of hydrogel tissue-engineering scaffolds. *Expert Rev Med Devices, 8*(5), 607-626.

Ceccaldi, C., Strandman, S., Hui, E., Montagnon, E., Schmitt, C., Hadj Henni, A., Lerouge, S., (2017). Validation and application of a nondestructive and contactless method for rheological evaluation of biomaterials. *Journal of Biomedical Materials Research Part B: Applied Biomaterials,105(8), 2565-257.*